RELATIONSHIP BETWEEN THE MAGNETIC SUSCEPTIBILITY AND LITHOLOGICAL COMPOSITION IN SEDIMENT CORES FROM LAKES OF MATIȚA - MERHEI DEPRESSION (DANUBE DELTA, ROMANIA): TOWARDS A PROXY METHOD OF SEDIMENTOLOGICAL AND ENVIRONMENTAL FINGERPRINTING

Sorin - Corneliu RĂDAN[(1)], Silviu RĂDAN[(2)], Irina CATIANIS[(2)], Albert SCRIECIU[(2)]

[(1)]Geological Institute of Romania, 1 Caransebeș St., 012271 Bucharest, Romania
e-mail: sc.radan@yahoo.com
[(2)]National Institute of Marine Geology and Geo-Ecology (GeoEcoMar), 23-25 Dimitrie Onciul St., 024053 Bucharest, Romania
e-mail: radan@geoecomar.ro; irina.catianis@geoecomar.ro, albert.scrieciu@yahoo.com

Abstract. In the framework of the Danube Delta geosystem spatial evolution study, new results achieved for sediment cores – this time collected from the *Matița – Merhei Depression* lakes – are added up to the data which were previously published with regard to the *Meşteru – Fortuna Depression*. Actually, it is the second part of the series of papers dedicated to the magneto – lithological investigation of sediment columns, taken out from various aquatic environments, in both the *Fluvial* and *Marine Delta Plains*. Vertical profiles of magnetic susceptibility (**MS**) and contents of siliciclastic/minerogenic/detrital fraction (**SIL**), total organic matter (**TOM**) and carbonate (**CAR**) are carried out for 9 cores (not longer than 55.5 cm), collected from four lakes (*Babina*, *Matița*, *Polideanca* and *Bogdaproste*), a swamp (*Polideanca – Lopatna*) and a canal (*Lopatna – Polideanca*). These records are based on **MS** (**k**) measurements (with a Kappabridge KLY-2), and respectively, on lithological component contents analyses (by the "Loss on Ignition"/*LOI* method), performed on sediment samples obtained by core slicing, at 1-3 cm intervals. **MS**, **SIL**, **TOM** and **CAR** maps are carried out for surficial sediments, as well, in order to describe the magneto-lithological background which characterizes each of the lakes from where the short sediment cores were extracted. The **MS** calibration of the lake sediments (core and grab samples) is carried out by using a **k** scale with 5 classes. The correlation coefficient (**r**) is calculated for all 6 possible pairs of above specified parameters (**SIL** *vs*. **k**, **TOM** *vs*. **k**, **CAR** *vs*. **k**, **SIL** *vs*. **TOM**, **SIL** *vs*. **CAR** and **TOM** *vs*. **CAR**). To evaluate the correlation size, a scale with 6 steps is used. Positive/direct and negative/reversed correlations have always been obtained for **SIL** *vs*. **k**, and **TOM** *vs*. **k**, respectively. Therefore, new proofs are added to assign the magnetic parameter proxy quality as environmental and sedimentological fingerprinting tool. Another important result of the present study is the detection of some *marine clays* located very close below the water/sediment interface, intercepted, particularly, at the lower/basal part of two cores from the *Babina Lake*, two from *Matița Lake*, and another one from the *Lopatna – Polideanca Canal*. These *marine deposits* (with macroscopically identified specific fauna) are characterized by clearly different magnetic and lithological signatures (high **MS** values and **SIL** contents, low **TOM** contents), as compared with the fingerprints recovered from the overlying *muds* (sampled at the upper part of the cores). The presence of a *marine episode* revealed by some of the sediment cores collected from lakes of the *Matița – Merhei Depression*, which is a part of the *Fluvial Delta Plain*, is very interesting and can represent a contribution to the better knowledge of the deltaic system temporal and spatial evolution.

Key words: environmental magnetism, minerogenic/siliciclastic component, total organic matter component, carbonate component, lake sediments, marine clays.

1. INTRODUCTION – STUDY AREA

In a previous paper dedicated to the evaluation of relationship between the magnetic susceptibility and the lithological composition inferred from sediment cores (Rădan *et al*., 2013), the main lakes of *Meşteru – Fortuna Depression* (**I**, in Fig. 1) have been investigated. This depression is a deltaic unit placed in the western zone of the *Danube Delta* (*DD*) northern wing (which encompasses the area between *Chilia* and *Sulina* branches).

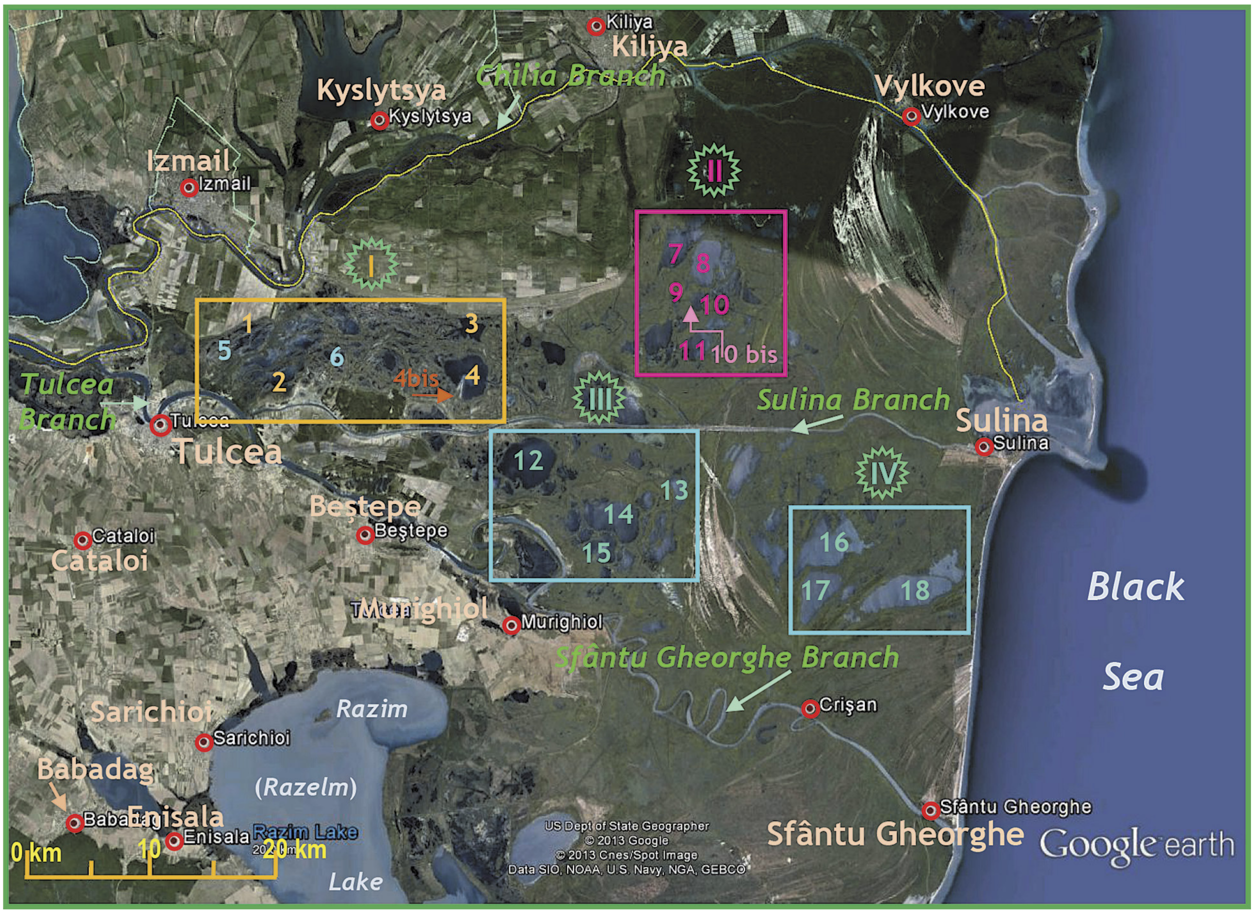

Fig. 1. Location of the lakes in the Danube Delta from where sediment cores were collected over the 2010 – 2014 period. **I. Meşteru – Fortuna Depression**: 1 – Cuteţchi Lake; 2 – Tătaru Lake; 3 – Băclăneşti Lake; 4 – Fortuna Lake; 4bis – Crânjală Canal; 5 – Trofilca Lake; 6 – Belâi Lake. **II. Matiţa – Merhei Depression:** 7 – Babina Lake; 8 - Matiţa Lake; 9 – Polideanca - Lopatna Swamp; 10 – Polideanca Lake; 11 – Bogdaproste Lake; 10bis – Lopatna - Polideanca Canal. **III. Gorgova – Uzlina Depression**: 12 – Gorgova Lake; 13 – Cuibeda Lake; 14 – Isacova Lake; 15 – Uzlina Lake. **IV. Lumina – Roşu Depression**: 16 – Lumina Lake; 17 – Puiu Lake; 18 – Roşu Lake. *Notes*: **I** – Area with published data (Rădan *et al*., 2013); 5, 6 – lakes from where 3 cores were collected in 2014, and consequently, are not included in the cited article; **II** – Area under attention in the present paper; **III**, **IV** – Deltaic areas from where the results are to be next published.

With a view to extending the analysis of results achieved from the integrated magneto-susceptibilimetric and lithological investigation of the cores taken out during the last five years (2010 – 2014) in the *Danube Delta*, the present paper focuses on the data obtained in the other depression situated in the northern wing, but in its central area, also in the *Fluvial Delta Plain*, *i.e.*, the *Matiţa – Merhei Depression* (**II**, in Fig. 1).

The results provided by 9 short cores, collected in the *Matiţa – Merhei Depression* from the *Babina*, *Matiţa*, *Polideanca* and *Bogdaproste lakes*, as well as from the *Polideanca – Lopatna Swamp* and the *Lopatna – Polideanca Canal* (Figs. 1 and 2), which are commented in the present paper, bring new arguments on the existing correlations between the geophysical/rock-magnetic parameter (**MS**) and the sedimentological/ **LITHO** ones. The vertical distribution of the magnetic susceptibility values, recorded for the sediment cores, reflects, accurately, the lithological variations, which, sometimes, are macroscopically less visible. Besides, the identification – during the process of core slicing and sediment description performed on the research vessel, right through the field trip – of some *marine deposits*, within several cores, is confirmed and "quantified" in laboratory; distinct **MS** and **LITHO** characteristics are decoded from the magneto-lithological signatures recovered from the sediment sample succession.

The data discussed in the paper represent a new contribution towards developing a proxy method of sedimentological and environmental fingerprinting in lake sediments, confirming the capability of the magnetic susceptibility record to be used as a proxy for the lithological composition characterization of the lake sediments.

2. LOGISTICS, MATERIALS AND METHODS

Essential data concerning the methods used to carry out an integrated magneto-lithological study of sediment cores were presented in the first paper (Rădan *et al*., 2013) of a series of 4 articles which are intended to be published related to the four main deltaic depressions (**I**, **II**, **III**, **IV**, in Fig. 1). Consequently, some significant (new) aspects only will be here mentioned.

The field works carried out by GeoEcoMar in the framework of the Core Program, Contract no. PN 09-41 03 04, aboard the fluvial vessel "*Istros*" in the *Danube Delta* lakes have gone on with the October 2013 expedition, and two other cruises, performed in April/May, and August 2014, respectively. The investigations were focused both on the direct observations related to the water and sediments and on collecting water and sediment samples/cores for analyses in specific laboratories. In the lakes where the water depth was lower than 1.50 m, a motor-boat ("*Măriuca*") was used. Several physico-chemical parameters have been investigated for the surface waters, and the study of the greenhouse gas emissions in different deltaic ecosystems was performed. The lithological and the magnetic susceptibility characterization of the lacustrine sediments represents an important objective of the respective multi-disciplinary campaigns. The detailed study of the relationship between these two distinct categories of parameters is just what this paper is dealing with.

As regards the *Matița – Merhei Depression*, under attention here, numerous samples from the surficial/bottom sediments have particularly been taken out (with the grab sampler) during 2010 – 2014; these gave information from the first ca. 20 cm beneath the water/sediment interface. Besides of the principal lakes of this aquatic area, *i.e. Merhei*, *Babina*, *Matița*, *Trei Ozere*, *Bogdaproste*, such samples have also come from several small lakes, *e.g*., *Ciorticuț* and *Corciovata* (situated north of *Babina L.*), *Polideanca – Lopatna Swamp* and *Polideanca L*. (south of *Matița L.*), and also *Covaliova L*. and *Căzănel L*. (located southwest and south, respectively, of *Trei Ozere L.*) (Fig. 2). Maps showing the areal distribution of the magnetic susceptibility, based on hundreds of sediment samples, taken out from all these lakes, during the above specified period, are also integrated in the paper.

The collection of 6 sediment cores (Fig. 2), extracted from the *Babina L*. (*cores DD 10-18*, *DD 10-106* and *DD 11-49*), *Matița L*. (*cores DD 10-01* and *DD 11-01*), and *Bogdaproste L*. (*core DD 13-104*), in the 2010 – 2013 period, has been completed – during the spring 2014 expedition – by taking a core (*DD 14-104*) from *Polideanca Lake*, another one (*core DD 14-113*) from *Polideanca – Lopatna Swamp*, and the *core DD14-112*, from the *Lopatna – Polideanca Canal* (Fig. 2).

Consequently, nine cores from the *Matița – Merhei Depression* (location in Figs. 1 and 2) have been available to be investigated for the vertical distribution of magnetic susceptibility and of three lithological components. The sediment columns (with lengths between 24 – 55.5 cm) were extracted with a Hydro-Bios type core sampler, with a transparent tube, and were sliced at 1 – 3 cm intervals, using an extruder, aboard the *R/V "Istros"*. Some details (photos included) can be found in a paper published by Rădan *et al*. (2013).

The magnetic susceptibility of the samples originating from different levels along each core was measured with a KLY-2 Kappabridge (*Instruction Manual for magnetic susceptibility bridge – KLY-2, Geofyzika n.p. Brno, Czechoslovakia, 1981*), in the laboratory of environmental magnetism of the Geological Institute of Romania (GIR). The **k** values were reported to the classes of a "magnetic susceptibility scale" (Fig. 3a; Rădan & Rădan, 2007), so that a **MS** calibration of the cores is feasible. In this connection, some information on the sediment quality, which is generally evaluated by means of the geochemical and ecological scales, is inferred from the **MS** records.

As regards the determination of lithological composition variation along the sediment cores, the *Loss on Ignition method* (*LOI*) (Dean, 1974; Catianis *et al*., 2013) was applied, in the specific laboratory of GeoEcoMar. Therefore, the contents of three lithological components, following the order **TOM** (**T**otal **O**rganic **M**atter), **CAR** (**CAR**bonates), and **SIL** (**SIL**iciclastic/minerogenic fraction) have been determined.

Based on the achieved **MS** and **LITHO** parameters, a series of magneto-lithological models associated with each sediment core are presented, analysed and discussed (see Chapter 3). To quantify and interpret the relationship between the magnetic susceptibility calibration of the sediment cores and their lithological composition, diagrams with the graphic correlation between the two categories of parameters (**MS** *versus* **LITHO**), but, also, between pairs of lithological components (**SIL** *vs*. **TOM**; **SIL** *vs*. **CAR**; **TOM** *vs*. **CAR**) are used. The resulted correlation coefficients (**r**) can be reported to a scale (Fig. 3b) which makes possible the correlation size evaluation related to the enviromagnetic parameter (**k**) and the **LITHO** components; six classes are nominated between **r** = 1 and **r** = –1, covering distinct stages between "strong positive correlation" and "strong negative correlation", passing, of course, through the "no correlation" *point* (**r** = 0) (Fig. 3b). In some cases, scatter-plots which demonstrate clustering of core sediments into distinct lithogenetic groups ("muds" and "marine clays") are also illustrated.

3. RESULTS AND DISCUSSION

The magnetic susceptibility records, together with the vertical distribution of the lithological components contents along the sediment cores, are discussed in this chapter. In its first part, the detailed study is following the order given by the sampling-site location, from northern lakes towards the southern ones, and, at the same time, within a lake, taking into consideration the temporal criterion related to the core extraction moment/year. Synoptic **MS** and **LITHO** images, and some applications and consequences inferred from them, are presented and commented in the second part of the chapter.

3.1. Magnetic susceptibility and lithological data

The results are analysed within four subchapters, devoted to the *Babina Lake*, *Mațița Lake*, *Lopatna Channel – Polideanca Lake area*, and, respectively, *Bogdaproste Lake* (Fig. 2).

3.1.1. Babina Lake (2010, 2011)

Three sediment cores were collected from the *Babina Lake*, during 3 expeditions, carried out by GeoEcoMar Institute, in the *Danube Delta*, in 2010 and 2011. Therefore, the *cores DD 10-18* and *DD 10-106* were taken out during the expeditions performed between 16 – 30 June 2010, and 8 – 18 October 2010, respectively, while the *core DD 11-49*, during the campaign organized in the period 29 April – 12 May 2011 (core location in Fig. 2).

a) Core DD 10-106

The macroscopic description of this core (44.5 cm length; location in Fig. 2) correlates very well with the magnetic susceptibility vertical variation, which shows continuously increasing values from the upper part towards the base (Fig. 4a); the **MS** successively passes through the **k** class **I** (43 %), **II** (33 %) and **III** (24 %) (Figs. 4a,c). First time, this **MS** profile was presented within a paper dedicated to a *brief overview of the recent sediments as enviromagnetic archives*, its short analysis being connected with a **MS** map based on the bottom sediments sampled from the *Babina Lake* (and *Mațița L.*), in 1978 (Rădan & Rădan, 2011). Now, the discussion related to the *core DD 10-106* is extended and diversified. Thus, the pie-chart, which synthetises the weights of the contents of **LITHO** components characterizing the core sediments, asserts the **MS** calibration: **SIL** (39 %), **TOM** (56 %), and **CAR** (5 %) (Fig. 4d). The **MS** record corresponds to the lithological composition regime: the *detrital/minerogenic* component (**SI**L) shows a trend of increasing content towards the core base, *i.e.*, from 15.38 % (0 – 1.5 cm) to (80.93 % – 88.09 %), within the 35 cm – 44.5 cm interval below the sediment - water interface (Fig. 4b); the richest in *organic substance* sediments are present in the first upper 35 cm, the **TOM** contens ranging between 79.66 % (for the first 1.5 cm of the sediment column) and 48.59 % (for the *mud* sequence base, *i.e.*, in the 33 – 35 cm depth interval; Fig. 4b). As regards the third lithological component, represented by *carbonates* (**CAR**), it is interesting to remark – even if their contents are very low – a similar vertical distribution trend with the **TOM** component, *i.e.*, higher contents in the 0 – 35 cm depth interval (4.96 % – 9.48 %; Fig. 4b), and lower contents within the bottom zone of sediment column (0.99 % – 2.53 %; Fig. 4b). Actually, when is quantified the relationship between these two lithological components, that is **TOM** *versus* **CAR**, the correlation coefficient (**r**) shows a strong positive correlation, *i.e.*, **r** = 0.81 (Fig. 4j). Instead, a strong negative correlation, as it is easily to be deduced from the previous comments, is revealed by the relathionship between the *silty fraction* and *carbonates* (**SIL** *vs*. **CAR**), namely **r** = – 0.84 (Fig. 4i). Surely, a (very) strong negative correlation is for **SIL** vs. **TOM**, with **r** = – 0.999 (Fig. 4h).

As regards the relationships between the lithological components and the magnetic parameter, the correlation coefficients indicate – as the previous comments are suggesting by now – strong correlations in all the cases, positive for **SIL** *vs*. **k** (**r** = 0.98; Fig. 4e), and negative for **TOM** *vs*. **k** (**r** = – 0.98; Fig. 4f), and **CAR** *vs*. **k** (**r** = – 0.79; Fig. 4g).

The above presented quantification supports the macroscopic observations made aboard the vessel, namely a rapid transition from a *silty*, *organic*, noncohesive *mud* – at the upper part, towards a progressively more compact *mud*, with darker colour, old bioturbations, silted up, and with a *Cardium* fragment, at base (42.5 – 44.5 cm depth), possibly a *marine clay* (Fig. 4).

The line-chart carried out for the vertical variation of the magnetic susceptibility **MS** (Fig. 5a) and the 2D area-chart for the lithological components **SIL**, **TOM** and **CAR**, particularly the first two (Fig. 5b), clearly illustrate the two distinct segments of the **k** and **LITHO** profiles recorded along the sediment core.

Starting from the general correlation diagrams concerning the *enviromagnetic parameter* **MS** *versus* the **LITHO** *components* (Figs. 4e,f,g, redrawn in Figs. 6a,d,g), we have analysed the same relationship type, but, separately, for the two parts in which the sediment column of the *core DD 10-106* was divided. The results are illustrated in Figs. 6b,e,h, for the correlations **SIL** *vs*. **k**, **TOM** *vs*. **k**, and **CAR** *vs*. **k**, related to the "*mud sequence*" (0 – 35 cm depth interval), and in Figs. 6c,f,i, with regard to the possibly intercepted *marine clay* sediment (35 – 44.5 cm). Strong correlations are indicated by the coefficient **r** for *muds*, in the case of **SIL** *vs*. **k** (positive **r**; Fig. 6b) and **TOM** *vs*. **k** (negative **r**; Fig. 6e), and also for **CAR** *vs* **k**, but concerning the *marine clay* horizon (positive **r**; Fig. 6i). Moderate correlations were obtained for the **SIL** *vs*. **k** case (positive **r**; Fig. 6c) and **TOM** *vs*. **k** (negative **r**; Fig. 6f), both relating to the *marine clay* horizon. The only case when a weak correlation (positive) was observed is for **CAR** *vs*. **k**, regarding the "*mud sequence*" (Fig. 6h). The scale used to evaluate the size of the correlation (**r**) between the lithological components **SIL**, **TOM**, **CAR** and the enviromagnetic parameter (**k**) was presented in previously published papers (*e.g.*, Rădan *et al*., 2013).

The magneto-lithological record recovered from the *core DD 10-106* is typical for a zone in which the episodic influences are attenuated by the distance to the banks and to the supply canal mouths.

b) Core DD 10-18

The magnetic susceptibility profile recorded along the *core DD 10-18* (location in Fig. 2) shows, in the first upper 18 cm (Fig. 7a), a vertical variation which is usually observed for the sediment cores collected from this type of lakes (protected from the direct fluvial influx), that is low values in the first centimeters, followed by an increasing trend towards the core base. This is the case of the previously analysed core from the *Babina Lake*, collected from its central part

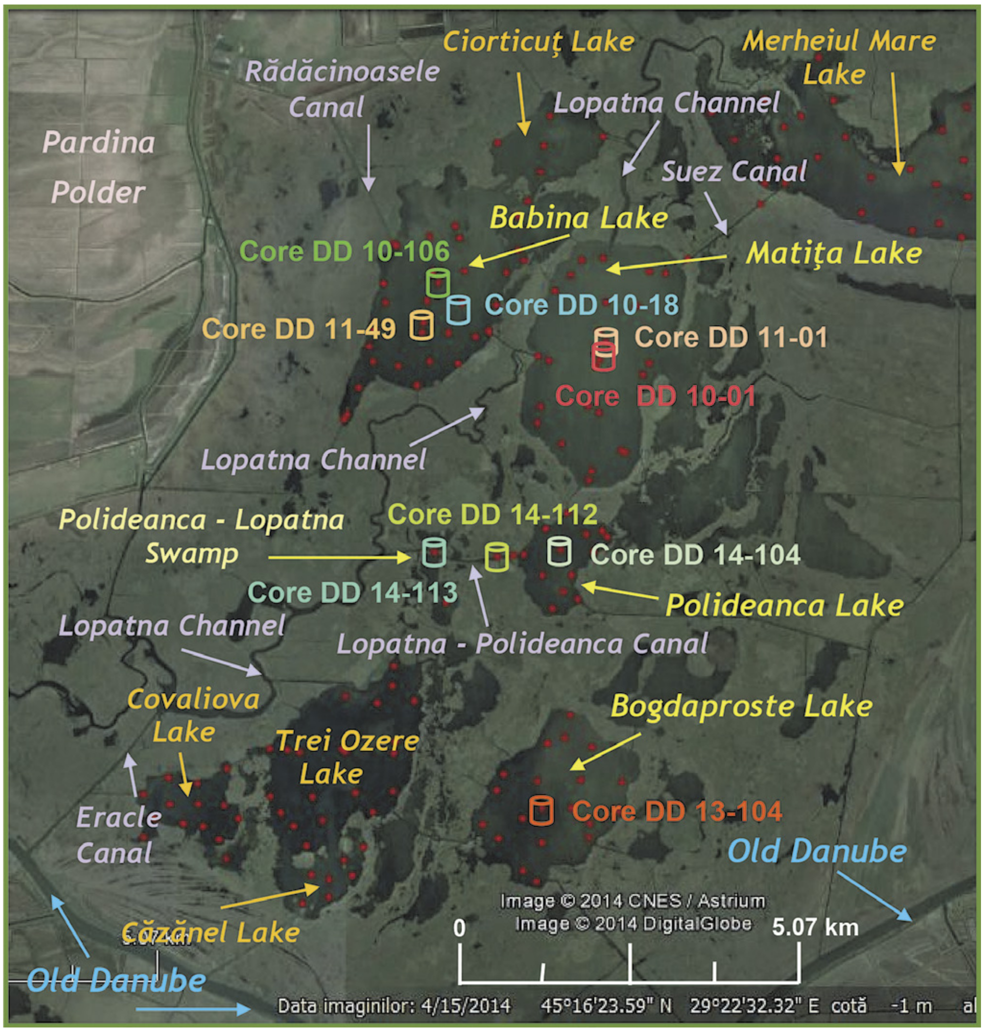

Fig. 2. Detailed map of the core locations in the Matiţa – Merhei Depression lakes.

Magnetic susceptibility (MS; k) scale		
Vd	> 1000	Coarse silts and sands
Vc	675 ÷ 1000	
Vb	575 ÷ 675	
Va	275 ÷ 575	
IV	175 ÷ 275	
III	75 ÷ 175	Clayey fine up to silty sediments
II	10 ÷ 75	Fine sediments, usually rich in organic matter and / or carbonates
I	< 10	(a)

Correlation coefficients (r)		
	0.65 ÷ 1.00	Strong positive correlation
	0.32 ÷ 0.64	Moderate positive correlation
	0.00 ÷ 0.31	No correlation – Weak positive correlation
	0.00 ÷ (- 0.31)	No correlation – Weak negative correlation
	(- 0.32) ÷ (- 0.64)	Moderate negative correlation
	(- 0.65) ÷ (- 1.00)	Strong negative correlation (b)

Fig. 3. Scales used in the magneto-lithological study of the sediment cores. **a)** Magnetic susceptibility (**MS**; **k**) scale used to calibrate the lake sediments and to correlate with their lithological characters. The **k** values defining the **MS** classes must be multiplied by (10 E-06) SI. **b)** Scale used to evaluate the size of the correlation (**r**) between the enviromagnetic parameter (**k**) and the lithological components (**SIL** – siliciclastic/minerogenic/detrital fraction; **TOM** – total organic matter fraction; **CAR** – carbonate fraction).

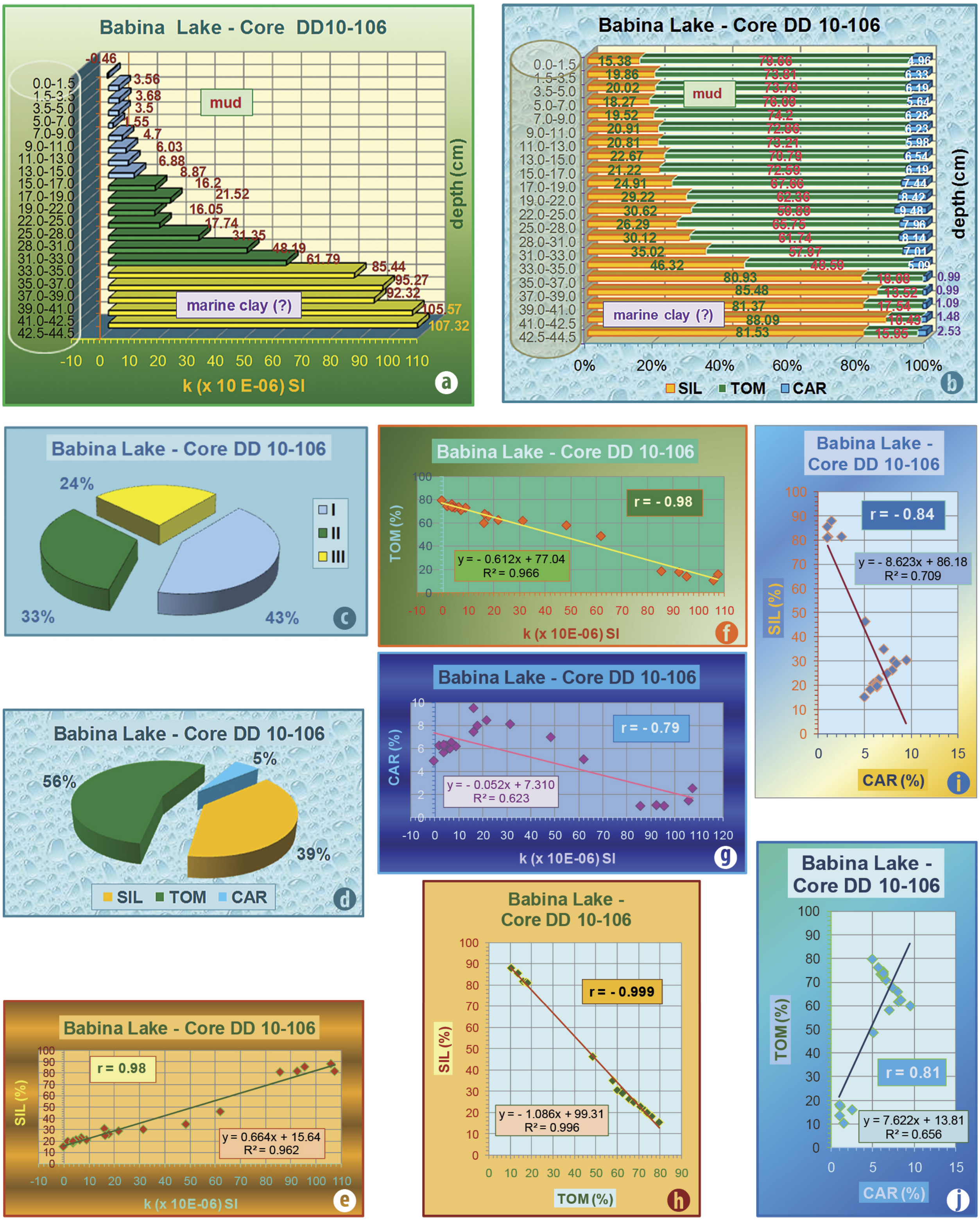

Fig. 4. Magneto-lithological model showing the vertical distribution of the enviromagnetic parameter (**MS**; **k**) and of the lithological components (**SIL**, **TOM**, **CAR**), along the core DD 10-106, collected from the Babina Lake (core location in Fig. 2). **a)** 3D bar-chart with the vertical distribution of the magnetic susceptibility; the bars are coloured according to the **k** scale classes (see Fig. 3a); **b)** 3D 100%-stacked bar-chart with the composite vertical distribution of the three main lithological components (**SIL**, **TOM**, **CAR**); **c)** 3D pie-chart showing the **MS** calibration of the core sediments, according to the **k** classes; **d)** 3D pie-chart showing the lithological composition of the core sediments, based on the **SIL**, **TOM** and **CAR** contents; **e)** Diagram showing the correlation **SIL** *versus* **MS** (**k**); **f)** diagram showing the correlation **TOM** *versus* **MS** (**k**); **g)** Diagram showing the correlation **CAR** *versus* **MS** (**k**); **h)** Diagram showing the correlation **SIL** *versus* **TOM**; **i)** Diagram showing the correlation **SIL** *versus* **CAR**; **j)** Diagram showing the correlation **TOM** *versus* **CAR**.

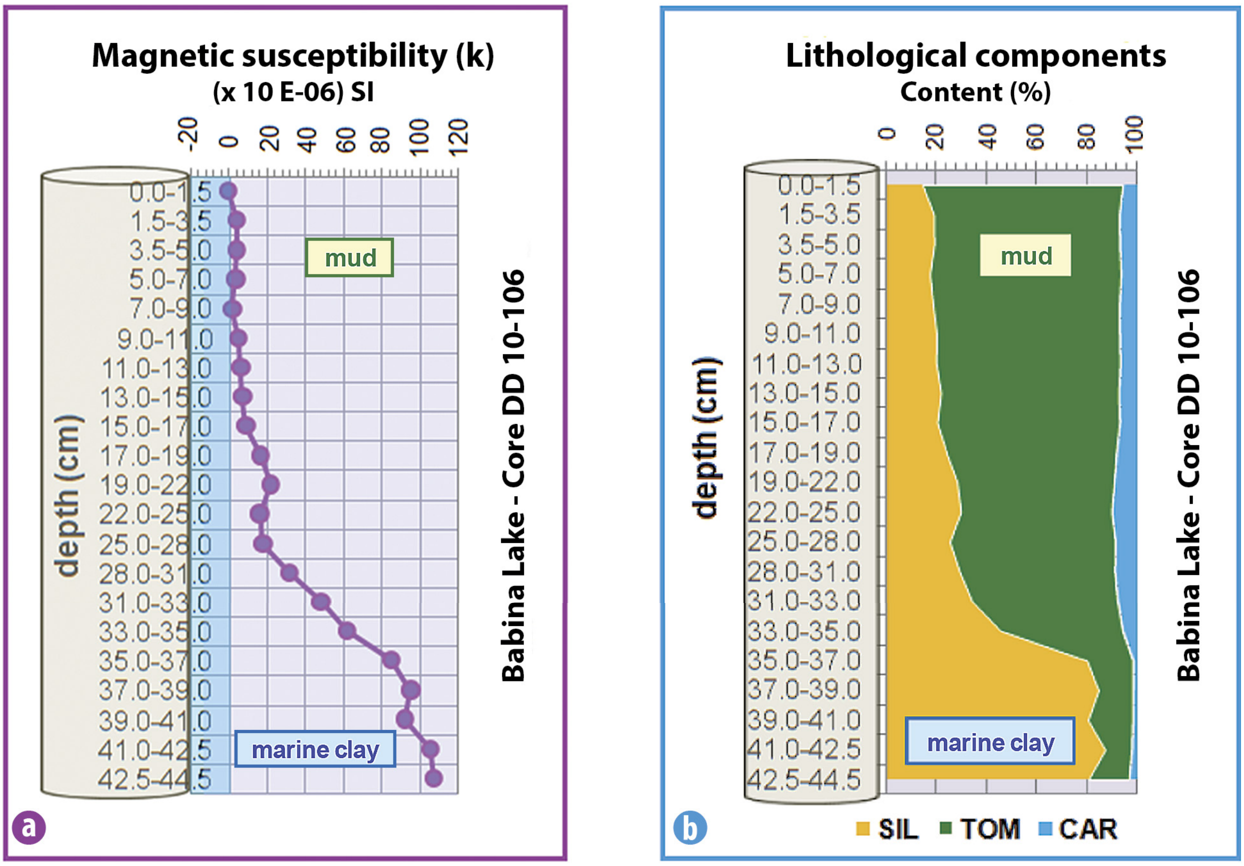

Fig. 5. Vertical distribution of the enviromagnetic parameter values (**k**) and of lithological component contents (**SIL**, **TOM**, **CAR**) along the sediment core DD 10-106, collected from the Babina Lake. **a)** Line-chart showing the magnetic susceptibility vertical profile. *Note*: in *blue*, is zone with negative **k** values; **b)** Area-chart with the distribution of **SIL**, **TOM** and **CAR** contents along the sediment core.

(*i.e.*, *DD 10-106*; Fig. 6a). Yet, the **k** profile of the *DD 10-18 core* is more complex, actually according with the vertical variation of the **SIL** and **TOM** lithological parameters (Figs. 7b,c). In Figs. 8a,b, the **MS**, **SIL**, **TOM** and **CAR** records, achieved for the sediment column of the core *DD 10-18*, are clearly illustrated. Its integrated magneto-lithological characterization is facilitated and argued by the strong direct and reversed correlations for **SIL** *vs*. **MS**, and **TOM** *vs*. **MS**, respectively (Figs. 7g,h). So, a large maximum zone is well defined by the **k** values recorded for the samples sliced from the median part of the core (with the highest **k** value of 102.69×10^{-6} SI; **k** class **III**), followed by a minimum zone, with its central axis (a **k** value of 18.5×10^{-6} SI; **k** class **II**) around the depth of 41 – 44 cm below the water/sediment interface (Fig. 7a). The 3D bar-charts with the vertical variations of the *siliciclastic/minerogenic fraction* (**SIL**; Fig. 7b) and the *total organic matter* (**TOM**; Fig. 7c) assert the magnetic susceptibility record along the *core DD 10-18*. In this context, the correlation diagrams from Figs. 7g,h reveal the strong positive/direct correlation for **SIL** *versus* **MS** (**r** = 0.93), and respectively, a strong reversed/negative correlation for **TOM** *versus* **MS** (**r** = – 0.86). As concerns the content of *carbonates* (**CAR**), this is very low (not higher than 9.9 %), with an exception, generated by the sample collected from the depth interval 41 – 44 cm (Fig. 7d), consisting of a hard and compact soil-like sediment, showing granular to columnar structure (31.41 % *carbonates*); the correlation **CAR** *versus* **MS** is a moderate negative one (**r** = – 0.47; Fig. 7i). When the lithological components **TOM** and **CAR** are considered together, the correlation coefficient for the relation (**TOM** + **CAR**) *versus* **MS** is increasing, becoming **r** = – 0.93 (Fig. 7j).

The magneto-lithological data assert the macroscopic observations performed aboard, during the core slicing procedure, pointing out a peculiar pattern. The first segment from 0 to 20 cm has a normal development, similar to that of other cores, starting with a grey-brownish, non-cohesive, fluffy organic *mud* (first 9 cm), which becomes more dense and hard in the lower part of the interval. This *mud* sequence is followed downwards by compact soil-looking clayey sediment, rich in plant debris, which explains some organic matter maxima (*e.g.*, 0 – 9 cm and 44 – 50 cm intervals; Fig. 7c) and the corresponding **MS** minima (Fig. 7a). This sediment could represent the partially emerged old substrate of a lake sector, close to the sea, taking into consideration the *Cardiidae* shells found in this deposit, atypical for the lakes included within the *fluvial delta plain* area. Its presence can acquire a great importance if absolute age determinations on shelly material of *marine* origin would be performed.

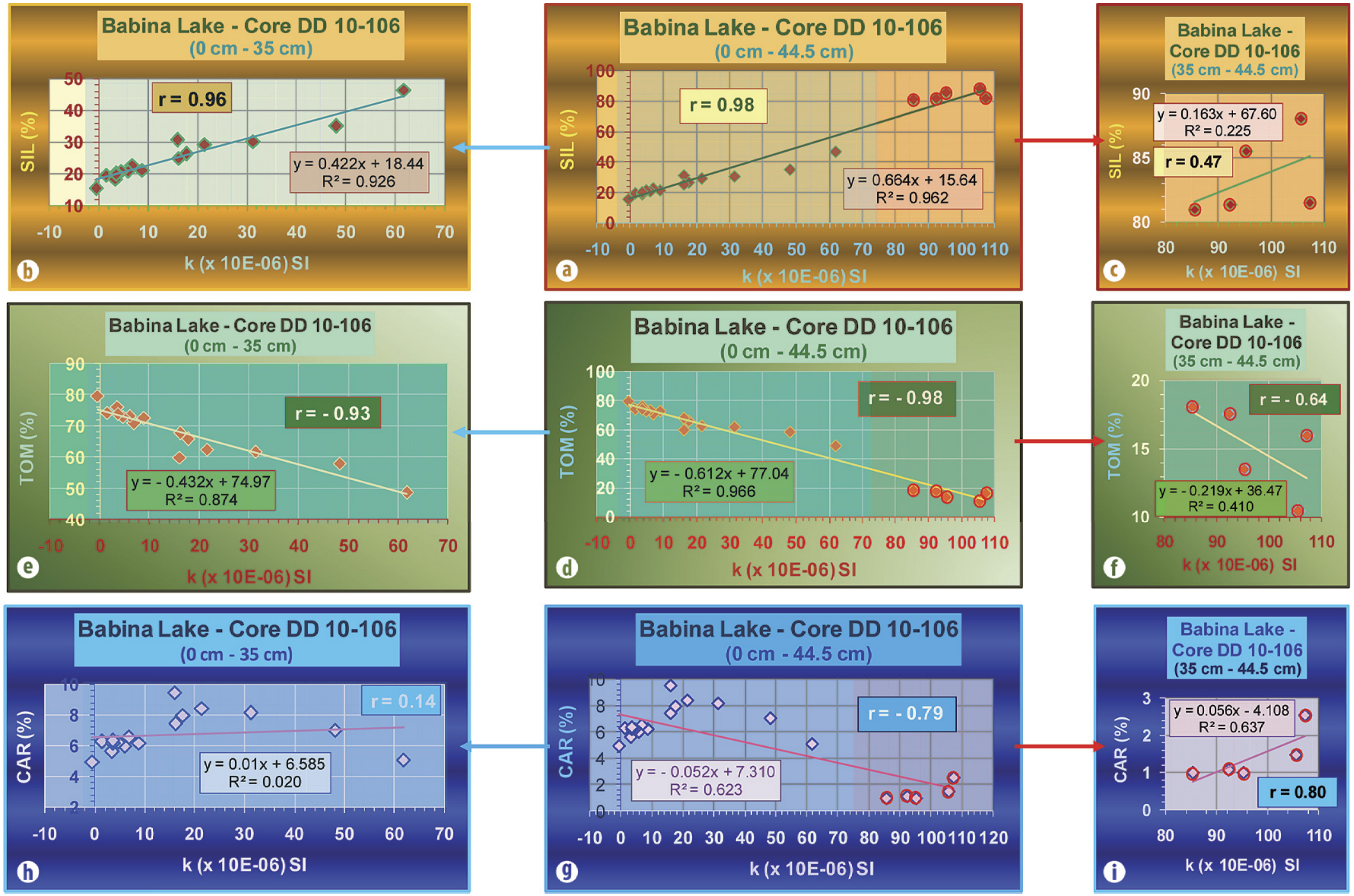

Fig. 6. Detail with the correlation of the enviromagnetic parameter (**MS**) with the lithological components (**SIL**, **TOM**, **CAR**), concerning the sediment core DD 10-106 (Babina Lake). **a)** Correlation **SIL** *versus* **k**, related to the entire core (0 – 44.5 cm); **b)** Correlation **SIL** *versus* **k**, related to the "mud sequence" (0 – 35 cm); **c)** Correlation **SIL** *versus* **k**, related to the intercepted "marine sediment" (35 – 44.5 cm); **d)** Correlation **TOM** *versus* **k**, related to the entire core (0 – 44.5 cm); **e)** Correlation **TOM** *versus* **k**, related to the "mud sequence" (0 – 35 cm); **f)** Correlation **TOM** *versus* **k**, related to the intercepted "marine sediment" (35 – 44.5 cm); **g)** Correlation **CAR** *versus* **k**, related to the entire core (0 – 44.5 cm); **h)** Correlation **CAR** *versus* **k**, related to the "mud sequence" (0 – 35 cm); **i)** Correlation **CAR** *versus* **k**, related to the intercepted "marine sediment" (35 – 44.5 cm).

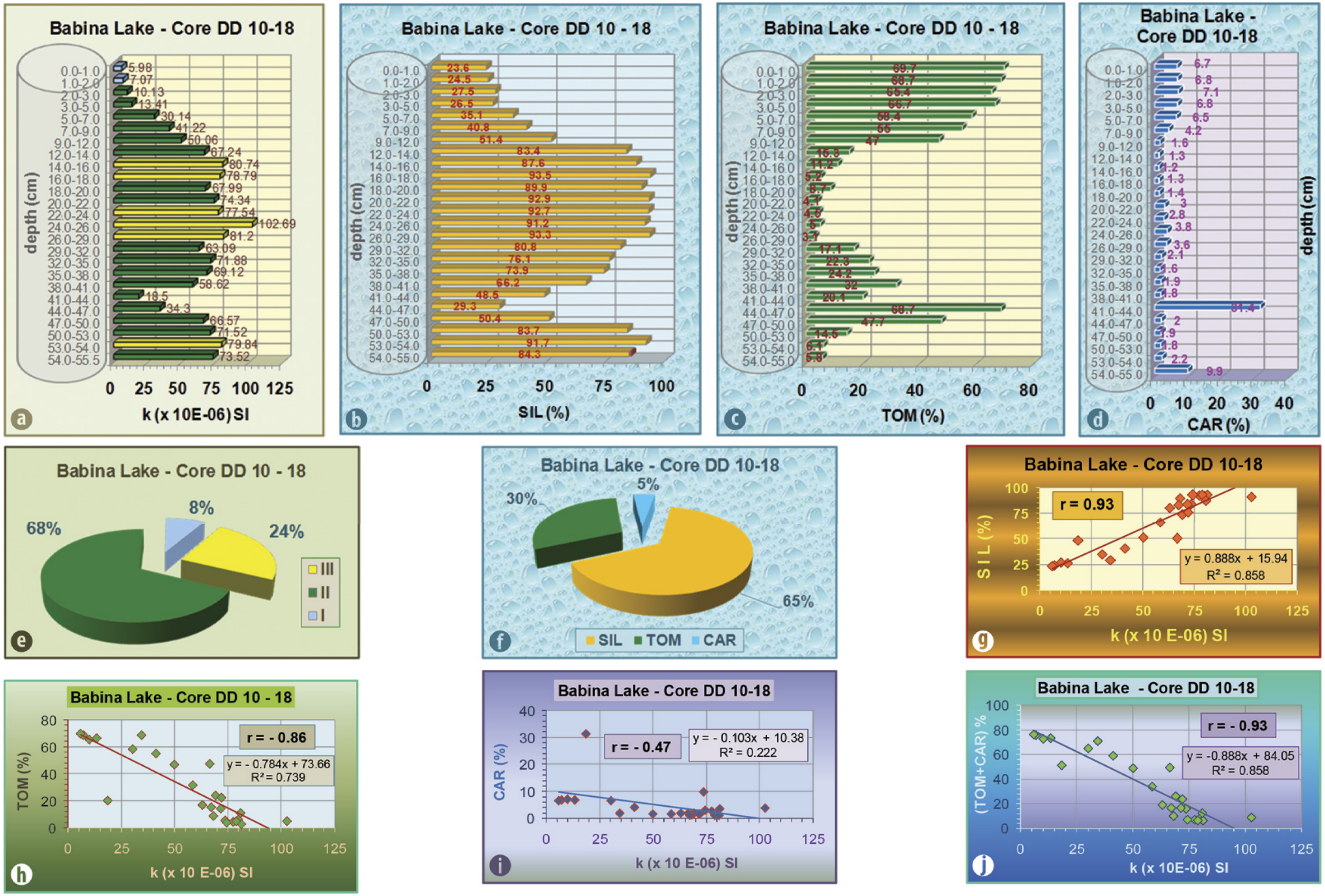

Fig. 7. Magneto-lithological model showing the vertical distribution of the enviromagnetic parameter (**MS**; **k**) and of the lithological components (**SIL**, **TOM**, **CAR**), along the core DD 10-18, collected from the Babina Lake (core location in Fig. 2). **a)** 3D bar-chart with the vertical distribution of the magnetic susceptibility; the bars are coloured according to the **k** scale classes (see Fig. 3a); **b)** 3D bar-chart with the vertical distribution of the siliciclastic/minerogenic component (**SIL**); **c)** 3D bar-chart with the vertical distribution of the total organic matter component (**TOM**); **d)** 3D bar-chart with the vertical distribution of the carbonate component (**CAR**); **e)** 3D pie-chart showing the **MS** calibration of the core sediments, according to the **k** classes; **f)** 3D pie-chart showing the lithological composition of the core sediments, based on the **SIL**, **TOM** and **CAR** contents; g) Diagram showing the correlation **SIL** *versus* **MS** (**k**); **f)** Diagram showing the correlation **TOM** *versus* **MS** (**k**); **g)** Diagram showing the correlation **CAR** *versus* **MS** (**k**); **h)** Diagram showing the correlation **SIL** *versus* **TOM**; **i)** Diagram showing the correlation **SIL** *versus* **CAR**; **j)** Diagram showing the correlation **TOM** *versus* **CAR**.

The clayey substrate, with an identified *marine* fauna, in the *Babina Lake*, at west of the initial palaeo-beach sand ridge, could be older or penecontemporaneous with its formation.

c) Core DD 11-49

This sediment core was taken from the southern-central part of the *Babina Lake* (location in Fig. 2), during the 2011 spring campaign. The crossed sequences make this sediment core very interesting, and some considerations are hereinafter given. The upper lacustrine *mud*, which is fluffy, non-cohesive, containing *Anodonta* shell fragments, is passing, after ca. 15 cm, to a more compact *mud*, with a granular aspect, and then, along the following 20 cm, it is getting to a *marine* grey *clay*, rich in *Cardiidae*. The lithological composition of the sediment column is synthesized and quantified in Fig. 9f by means of the three main components: **SIL** (*siliciclastic fraction*), **TOM** (*organic matter*) and **CAR** (*carbonates*); their weights are 59 %, 35 %, and 6 %, respectively. The downcore modification of the lithology is correspondingly recorded by the vertical variation of the **LITHO** components **SIL** and **TOM**, but also of the enviromagnetic parameter **MS** (Figs. 9b,c,a, respectively). The calibration of the core sediment to the **k** scale shows the predominance of the class **III** (64 %), followed by **k** class **I** (29 %), and class **II** (7 %) (Fig. 9e).This composite structure of the **k** classes assigned to the sediment samples extracted from the *core DD 11-49*, particularly classes (**I** + **II**) = 36 %, and class **III** = 64 %, is well correlated with the quantified lithological composition, particularly (**TOM** + **CAR**) = 41 %, and **SIL** content = 59 % (Fig. 9f). The integrated **MS** and **LITHO** characterization is well explained by the interception of a *marine clay* (Figs. 9a,b,c), which records higher magnetic susceptibility values, reaching 155.05×10^{-6} SI, assigned to **k** class **III** (Fig. 9a), and respectively, by the first sequence intercepted under the water/sediment interface, represented by fluffy *muds*, usually defined by low and very low **MS** values; in this case, for the first four samples, taken from the core top (0 – 11 cm), **k** values between 4.08×10^{-6} SI and 8.06×10^{-6} SI (attributed to class **I)** were measured, and for the following sample, a more compact *mud* (11 – 14 cm), a **k** value of 42.65×10^{-6} SI (assigned to class **II)** was determined (Fig. 9a). Accordingly, in the lower part of the *core DD 11-49*, higher contents of the *siliciclastic/minerogenic fraction* (up to 88.34%; Fig. 9b) were obtained, while higher *organic matter* contents (up to 83.07 %) were found in the core upper part (Fig. 9c). A parallel illustration of the 4 profiles recorded for the sediment core *DD 11-49* is given in Fig. 10a – related to the **MS** enviromagnetic parameter, and in Fig. 10b – for the **SIL**, **TOM** and **CAR** lithological components.

The scatter-plot analysis concerning the relationship between the magnetic susceptibility (**MS**; **k**) and each of the three main lithological components (**SIL**, **TOM**, **CAR**) (Figs. 9g,h,i) identified within the core sediments shows clustering into the two distinct lithogenetic groups: *muds* and *marine clays*. So, the *muds* are defined by lower **SIL**, and respectively, higher **TOM** contents, the **MS** recording low **k** values (Figs. 9g,h), as compared with the *marine clays*, which are characterized by higher **SIL**, and respectively lower **TOM** contents, the **MS** revealing high **k** values (Figs. 9g,h). As regards the scatter-plot of **CAR** *versus* **k** (Fig. 9i), the separation of the two distinct lithological categories is marked out by the magnetic parameter (**MS**) only, the **CAR** contents determined within the *muds* and *marine clays* being placed inside of a similar variation range, *i.e*., 4.2 % – 6.78 % (see also Fig. 9d). There is an exception, a higher **CAR** content (9.21 %), which was determined for the slice cut from the 20 – 23 cm depth interval, a lumashelic *grey clay*, very rich in *Cardiidae* fragments (and a few whole shells).

To interpret relative lake-level changes, Finkenbinder *et al*. (2014) use the scatter-plot analysis – related to the "organic matter content" *versus* "magnetic susceptibility" – for a composite sediment core from the *Harding Lake* (central Alaska, USA), in which case is also demonstrated clustering of some lithologic units into distinct groups.

As a concluding remark at the end of the study carried out for the sediment cores collected in the *Babina Lake* during the 2010 and 2011 campaigns, we can mention that to set off some *marine* deposits very close of the actual water/sediment interface is very important for the deltaic system evolution knowledge, taking into consideration that these are located behind of the initial *Jibrieni – Letea – Caraorman* sand ridge, and thence, older than this one.

3.1.2. Mațița Lake (2010, 2011)

Two cores were collected from the central zone of the *Mațița Lake*, in the years 2010 and 2011, particularly from the sampling stations *DD 10-01*, and *DD 11-01*, respectively (location in Fig. 2).

a) Core DD 10-01

This sediment core (location in Fig. 2) has provided an interesting magneto-lithological model. The first 20 cm from the upper part are constituted of a yellowish-brown, non-cohesive organic *mud*, fluffy on top and more compact towards the base, where a few gastropods and depigmented and loose *Dreissena* shells have been found; a H_2S-like smell is characteristic. These *muds* are defined by low magnetic susceptibilities, but with an increasing trend towards the lower part of the upper core interval (0 – 20 cm); **k** values between 0.26×10^{-6} – 49.35×10^{-6} SI were measured, that is the sediment is calibrated to **k** classes **I** and **II** (Fig. 11a). In fact, within these 20 centimeters, the total organic matter content (**TOM**) decreases from 55.6 % (the highest **TOM** content related to the entire core) up to 16.6 % (Fig. 11e), and correspondingly, the siliciclastic fraction content (**SIL**) increases from 34.5 % up to 70.8 % (Fig. 11b). In the following 11 centimeters (20 cm – 31 cm), where the *mud* becomes more compact, and the first *Cardium* shells (articulated valves included) occur, the **k** values measured on the core slices are increasing even more (79.82×10^{-6} – 219.63×10^{-6} SI), the sediment being calibrat-

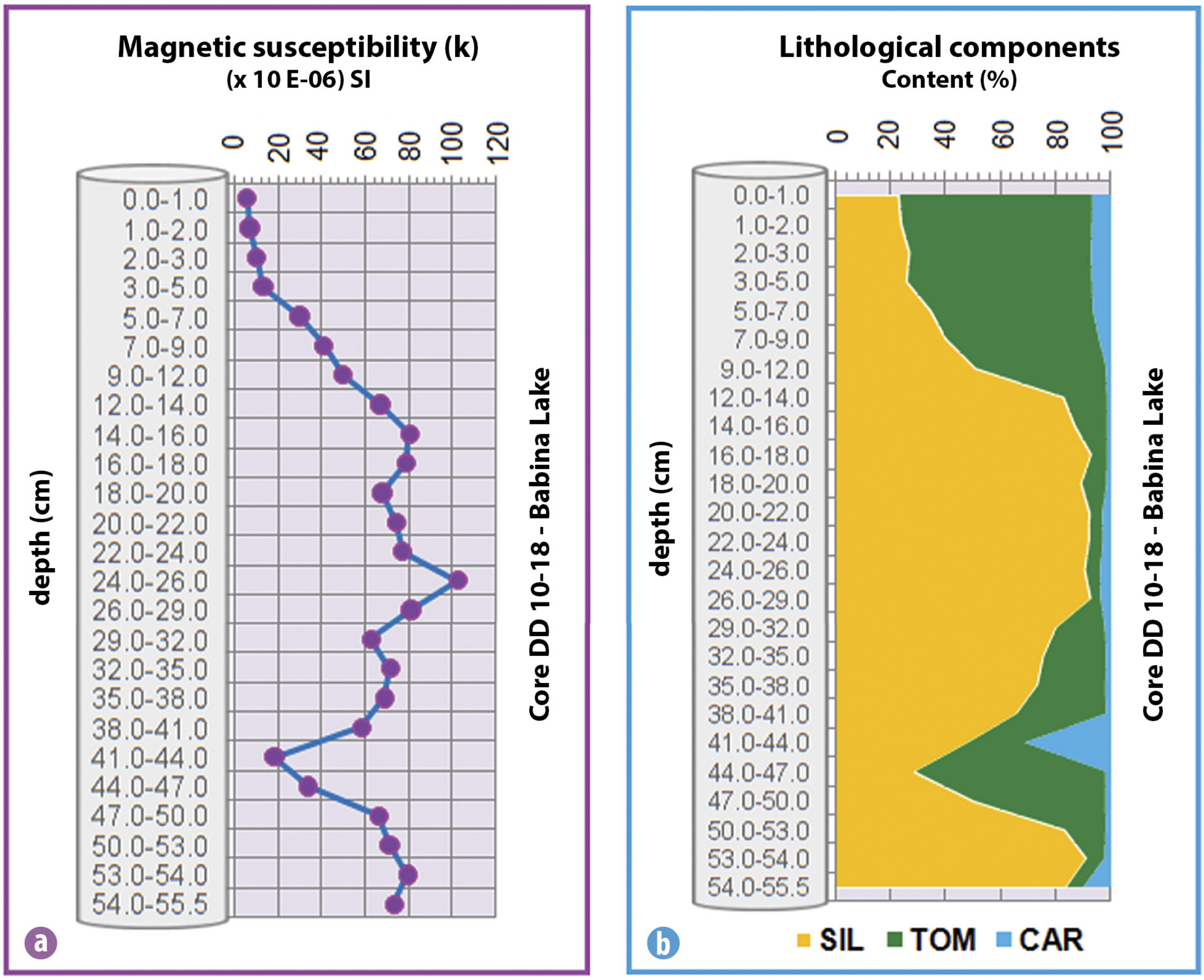

Fig. 8. Vertical distribution of the enviromagnetic parameter values (**k**) and of lithological component contents (**SIL**, **TOM**, **CAR**), along the sediment core DD 10-18, collected from the Babina Lake. **a)** Line-chart showing the magnetic susceptibility vertical profile; **b)** 100% stacked area-chart with the distribution of **SIL**, **TOM** and **CAR** contents along the sediment core.

ed to **k** classes **III** and **IV** (Fig. 11a). The lithological support related to the enviromagnetic parameter evolution is again evident: the minerogenic fraction (**SIL**) content increases from 75.5 % up to 84.8 % (Fig. 11b), and, correspondingly, the total organic matter (**TOM**) content decreases from 16.6 % up to 7.1 – 7.4 % (Fig. 11e). Further, in the following 25 centimeters, up to the core bottom, the sediments are defined by *marine* characteristics (light grey *clayey muds*, passing towards plastic *clays*, coarser at the core base, with *Cardiidae* inside). The magnetic susceptibility clearly records this lithological change, the **MS** measured on the sediment samples collected from this depth interval (31 – 55 cm) revealing high **k** values (230.32×10^{-6} – 285.44×10^{-6} SI), which are assigned to the classes **IV** and **Va** (Fig. 11a). On the other side, referring to this core lower half, the highest siliciclastic fraction (**SIL**) contents are ranging between 85.4 % – 90.0 % (Fig. 11b), with a mean value of 86.5%, while the lowest total organic matter (**TOM**) contents are defined between 4.6 % – 8.2 % (Fig. 11e), with a mean value of 6.95 %. So, the correlation of the enviromagnetic parameter with the main lithological characteristics, quantified by the (calculated) **r** coefficients (Figs. 11g,h), is suggested – even graphically only – by the corresponding 3D bar-charts (Fig. 11a, and Figs. 11b,e, respectively). A remark could be done on the relatively constant high and low contents determined for the **SIL** (Fig. 11b) and **TOM** (Fig. 11e) lithological components, respectively, along the specified depth interval (31 – 55 cm), where the *marine clay* horizon has been intercepted (Fig. 11a).The pie-charts from Figs. 11c,d help us to compare some synthesis magneto-susceptibilimetric and lithological data which characterize the *DD 10-01* core sediments, resulting from the **MS** *calibration*, based on **k** classes, and from the **LITHO** *composition analysis*, defined by the **SIL**, **TOM** and **CAR** components: classes **I** + **II** = 37 %, while the contents of **TOM** + **CAR** = 26 %; classes **III** + **IV** + **Va** = 63 %, while **SIL** content = 74 %.

The cause of the discussed evolution is a diminution of the detrital supplies, associated with an increase of the primary productivity and of the eutrophication, providing more and more organic material. This decrease of the *Danube*

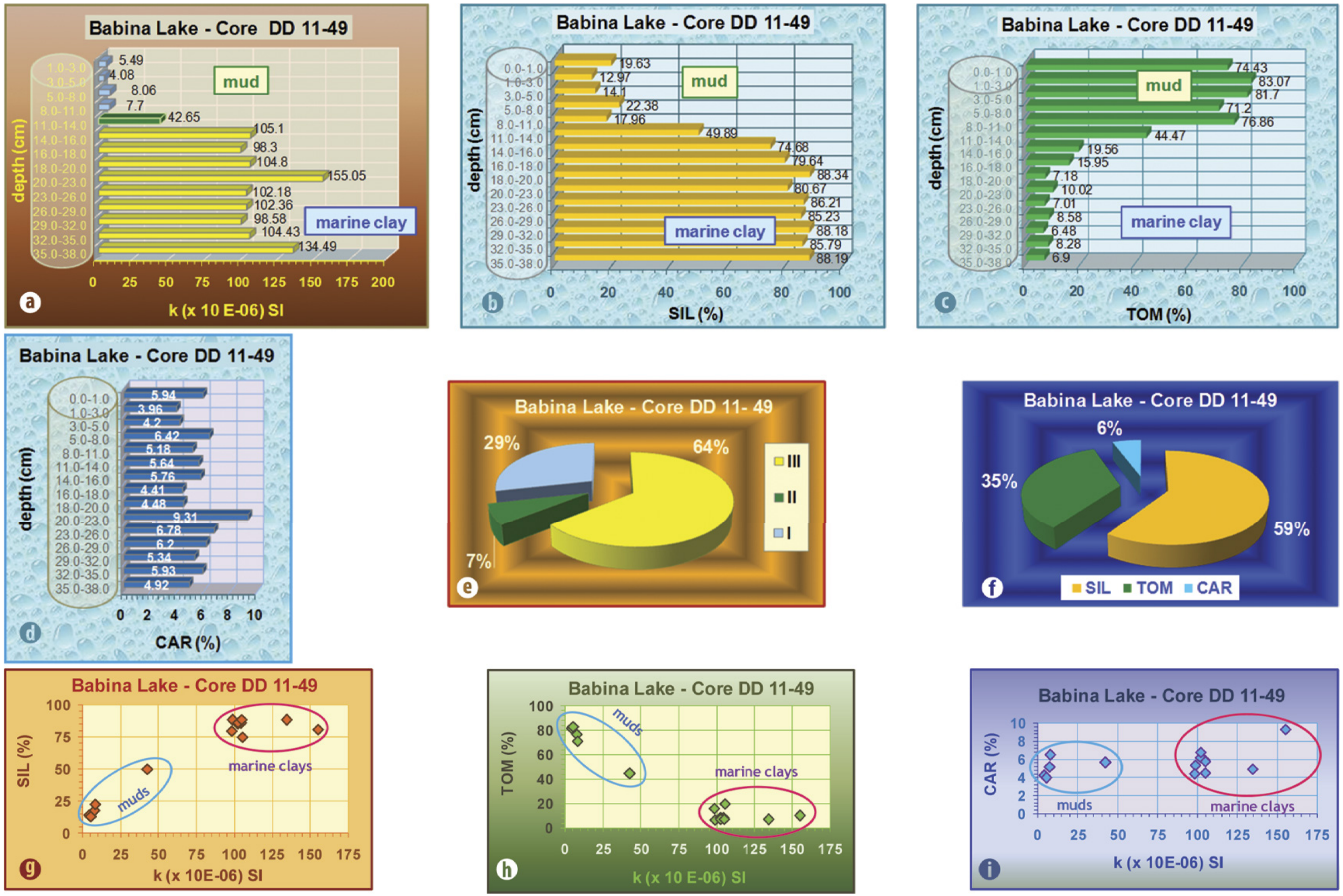

Fig. 9. Magneto-lithological model showing the vertical distribution of the enviromagnetic parameter (**MS**; **k**) and of the lithological components (**SIL**, **TOM**, **CAR**), along the core DD 11-49, collected from the Babina Lake (core location in Fig. 2). **a)** 3D bar-chart with the vertical distribution of the magnetic susceptibility; the bars are coloured according to the **k** scale classes (see Fig. 3a); **b)** 3D bar-chart with the vertical distribution of the siliciclastic/minerogenic component (**SIL**); **c)** 3D bar-chart with the vertical distribution of the total organic matter component (**TOM**); **d)** 3D bar-chart with the vertical distribution of the carbonate component (**CAR**); **e)** 3D pie-chart showing the **MS** calibration of the core sediments, according to the **k** classes; **f)** 3D pie-chart showing the lithological composition of the core sediments, based on the **SIL**, **TOM** and **CAR** contents; **g)** Scatter-chart of **SIL** *versus* **MS** (**k**), which shows clustering of the core sediments into two groups; **h)** Scatter-chart of **TOM** *versus* **MS** (**k**) (see text); **i)** Scatter-plot of **CAR** *versus* **MS** (**k**) (see text).

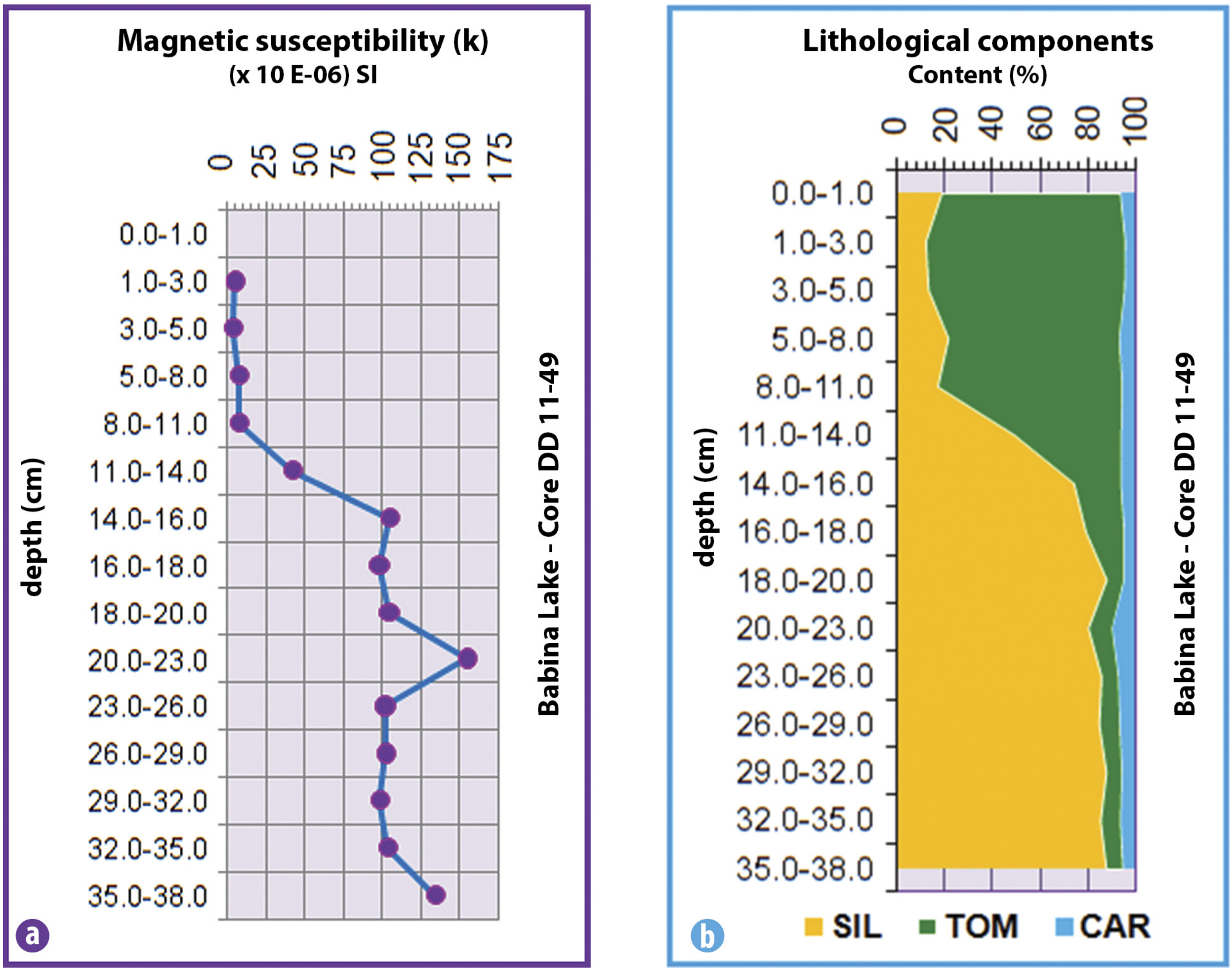

Fig. 10. Vertical distribution of the enviromagnetic parameter values (**k**) and of lithological components contents (**SIL**, **TOM**, **CAR**), along the sediment core DD 11-49, collected from the Babina Lake. **a)** Line-chart showing the magnetic susceptibility vertical profile; **b)** 100% stacked area-chart with the distribution of **SIL**, **TOM** and **CAR** contents along the sediment core.

influence has also been possible in the context of the silting up of the canal inputs, which were not dredged during the last decades. The mineralization and natural trend of the organic substance decay along with increasing of the depth beneath the water/sediment interface must not be neglected.

As regards the third lithological component – the *carbonates* (**CAR**), the evolution along the sediment core (Fig. 11f) shows a relatively constant content (5.3 % – 7.5 %, with a mean of 6.5 %), in the core lower half, as we mentioned for **SIL** and **TOM** components, as well; higher **CAR** contents were determined in the upper core half, with a second maximum zone around the depth of 24 – 28 cm (Fig. 11f), where the aboard macroscopic description has indicated a *mud* very rich in shells (*Cardium*, *Dreissena*, *Unio*).

The first samples were sliced at 1 cm intervals, so that it seems the resolution of the lithological analyses has been influenced along the respective depth interval (upper 4 centimeters) because of the small available material quantity.

The scatter-plot analysis concerning the relationship between the magnetic susceptibility (**MS**; **k**) and each of the three main lithological components (**SIL**, **TOM**, **CAR**) (Figs. 11g,h,i) reveals clustering of the core sediments into the two groups: *muds* and *marine clays*. A general remark concerns the broader ranges in which the lithological component contents (particularly, of **SIL** and **TOM**, but also of **CAR**) are defined for *muds*, as compared with the quasi-constant (narrow) ranges characterizing the **SIL** and **TOM** contents (anyway, less narrow for **CAR**, as well), determined for the *marine clays* (Figs. 11g,h,i). Yet, as in the case of the *core DD11-49* (*Babina Lake*; Ch. 3.1.1.c), the magnetic parameter (**MS**; **k**) gets on a better dissociation – inside of the scatter-plots – of core sediments into the two lithogenetic categories: the *muds*, defined by distinctly lower **k** values, comparing with the (high) magnetic susceptibilities which characterize the *marine clayey muds* and *clays* (Figs. 11g,h,i).

The area-chart from Fig. 12b shows the vertical distribution composite image of the lithological components **SIL**, **TOM** and **CAR** (Figs. 11b,e,f). As regards the line-chart

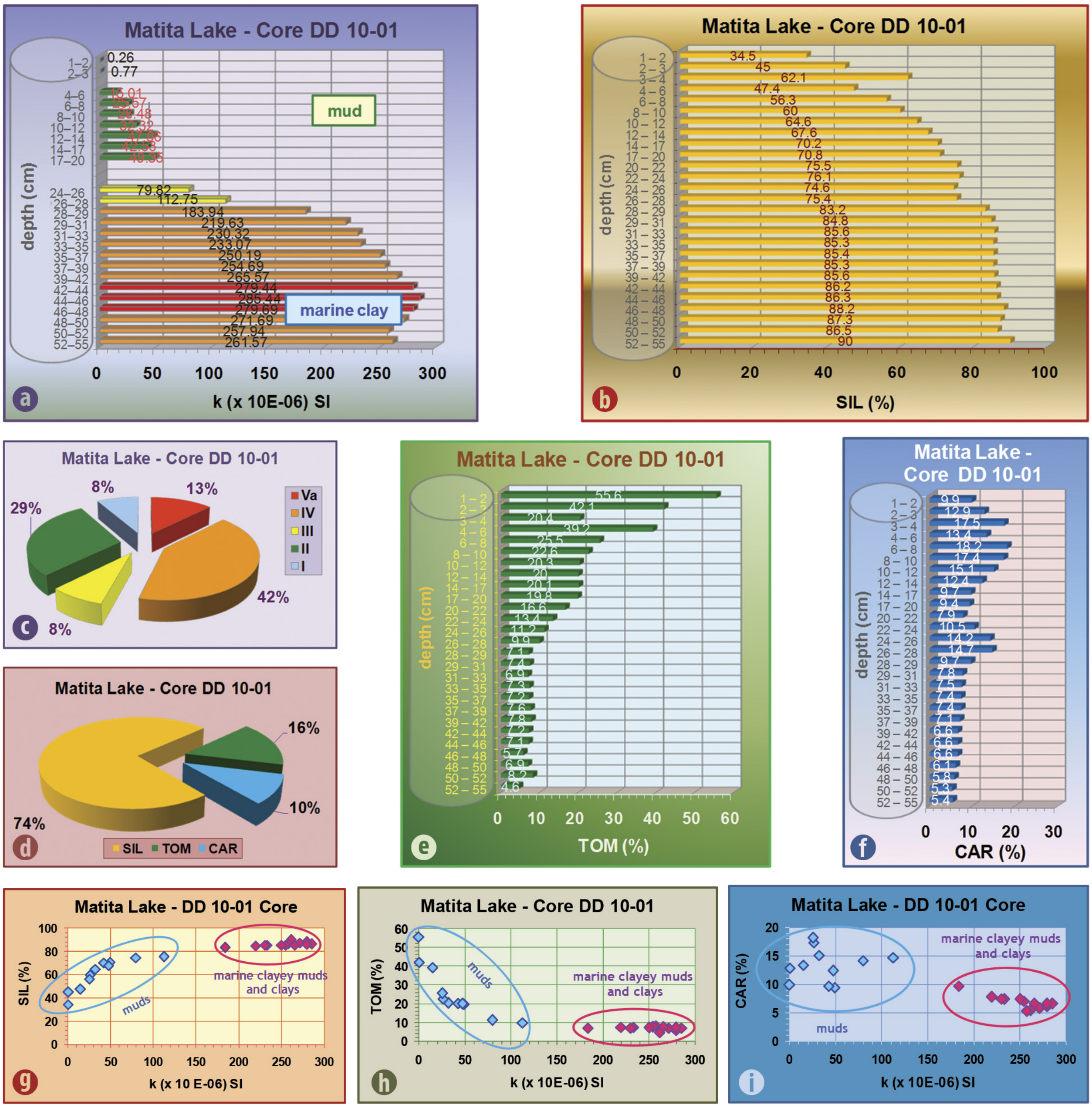

Fig. 11. Magneto-lithological model showing the vertical distribution of the enviromagnetic parameter (**MS**; **k**) and of the lithological components (**SIL**, **TOM**, **CAR**), along the core DD 10-01, collected from the Matița Lake (core location in Fig. 2). **a)** 3D-bar chart with the vertical distribution of the magnetic susceptibility; the bars are coloured according to the **k** scale classes (see Fig. 3a); **b)** 3D-bar chart with the vertical distribution of the siliciclastic/minerogenic component (**SIL**); **c)** 3D pie-chart showing the **MS** calibration of the core sediments, according to the **k** classes; **d)** 3D pie-chart showing the lithological composition of the core sediments, based on the **SIL**, **TOM** and **CAR** contents; **e)** 3D-bar chart with the vertical distribution of the total organic matter component (**TOM**); **f)** 3D-bar chart with the vertical distribution of the carbonate component (**CAR**); **g)** Scatter-plot of **SIL** *versus* **MS** (**k**), which shows clustering of the core sediments into two groups; **h)** Scatter-plot of **TOM** *versus* **MS** (**k**) (see text); **i)** Scatter-plot of **CAR** *versus* **MS** (**k**) (see text).

from Fig. 12a, carried out for the downcore variation of the magnetic susceptibility **MS** (Fig. 11a), this clearly illustrates – and asserts the above scatter-plot analysis – two distinct sequences recorded by the **k** profile: the upper, concerning the *muds*, within the first 20 cm beneath the water/sediment interface, and the lower, within the following 35 cm, up to the core base, related to the *marine clays*.

b) Core DD 11-01

The *Core DD 11-01* presents an interesting lithology, which starts with an organic, non-cohesive and fluffy *mud*, at the upper part, going towards the base to a darker, more compact sediment, rich in shells (*Dreissena*) and vegetal fragments, and passing, finally, to a grey *marine clay*, with *Car-*

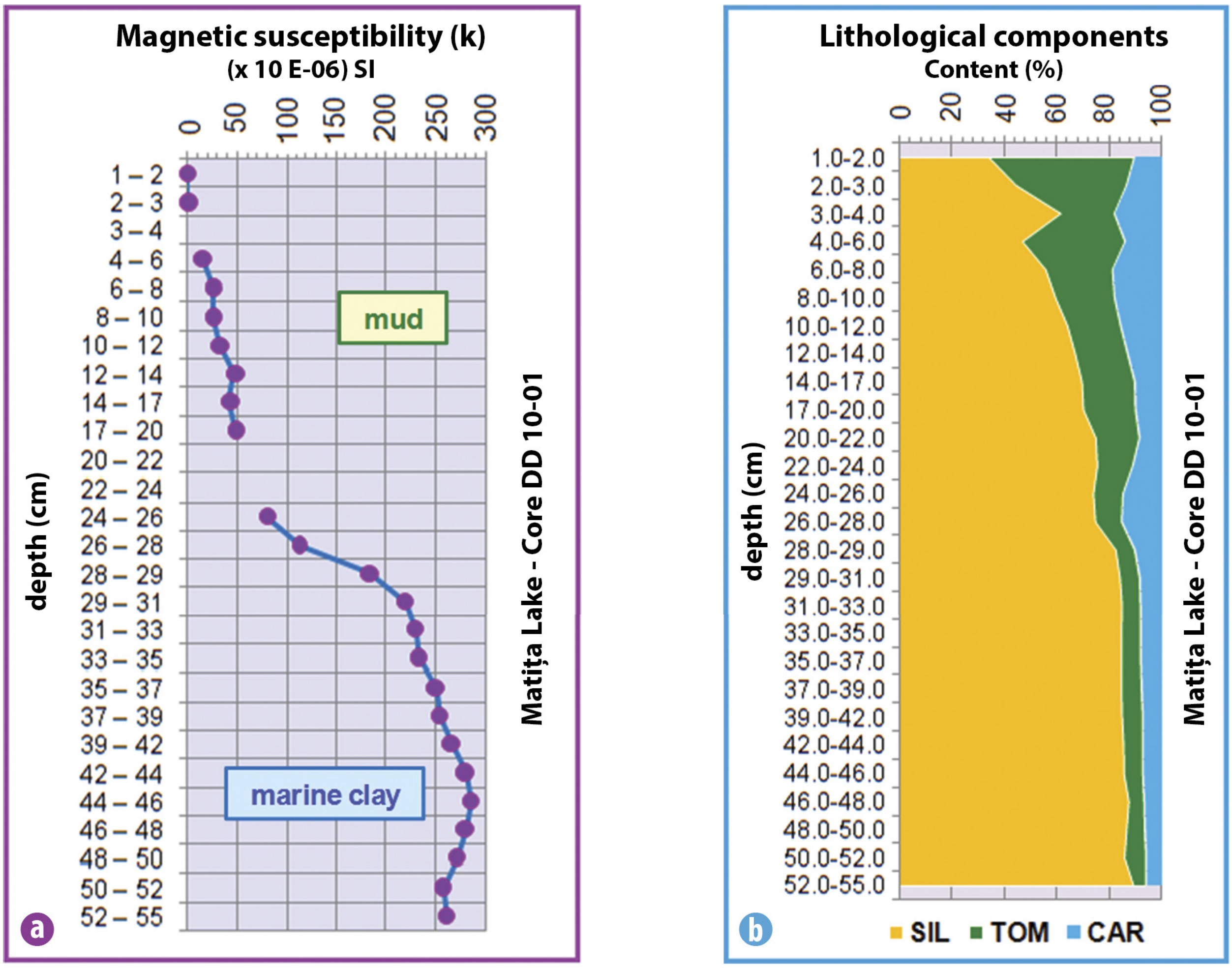

Fig. 12. Vertical distribution of the enviromagnetic parameter values (**k**) and of lithological components contents (**SIL**, **TOM**, **CAR**), along the sediment core DD 10-01, collected from the Matița Lake. **a)** Line-chart showing the magnetic susceptibility vertical profile; **b)** 100% stacked area-chart with the distribution of **SIL**, **TOM** and **CAR** contents along the sediment core.

diidae.The interception of the *marine clay* is clearly emphasised by all the parameters, both enviromagnetic (**MS**) and lithological ones (**SIL**, **TOM**); their vertical distribution along the sediment core is illustrated in Figs. 13a,b,c. The magnetic susceptibility (**MS**, **k**) record reflects, with a high accuracy, the lithological variations, data which become even more important when the respective changes are macroscopically less visible. The sediments are generally finer than those constituting the other core collected from the *Matița Lake* central area (*i.e.*, *DD 10-01*). The most samples (48 %) are calibrated to **k** class **II** (Figs. 13a,e), a rather significant weight comes to the **k** classes **I** (19 %) and **III** (19 %), the rest of 14 % being attributed to class **IV** (Figs. 13a,e).

The increasing trend of the magnetic susceptibility values along the *core DD 11-01*, from top downwards, is in agreement with the sediment lithology shown by the 23 slices (the first two samples extracted at intervals of 1 cm were not measured for **MS** because of the low available quantity of sediment). The organic *mud*, non-cohesive, fluffy, and presenting a H_2S smell, described along the first 10 cm of the core, is characterized by very low **k** values (0.31×10^{-6} – 2.41×10^{-6} SI), assigned to class **I** (Figs. 13a,e). The magnetic susceptibility is continuosly increasing along the following 30 cm, where a more and more compact *mud* (passing to a cohesive *mud*) was intercepted, but, anyway, keeping the measured **MS** values inside of the **k** class **II** (10.19×10^{-6} – 66.9×10^{-6} SI; Figs. 13a,e). Within the 40 – 47 cm depth interval, a lighter grey *mud* occurs, which contains shell fragments (*Cardiidae*, *Valvata*, *Dreissena*), and is characterized by higher **k** values (87.55×10^{-6} – 151.65×10^{-6} SI), assigned to class **III**. This horizon makes the transition to a grey-bluish plastic *clay*, with *Cardiidae*, which is atributed to a *marine clay*, and that is intercepted up to the core base, respectively 53 cm (Fig. 13a). This deposit is clearly remarked by the highest magnetic susceptibility measured for the *DD 11-01* core sediments, the **MS** values being assigned to the **k** class **IV** (195.3×10^{-6} – 219.86×10^{-6} SI; Figs.13a,e). It is worth mentioning that at the depth of 46 cm it was cut a sediment slice of 1 cm thickness only, the aboard macroscopic description pointing out a transition zone between the upper *mud*, and a light grey, plastic *clay* (actually, the *marine clay*).

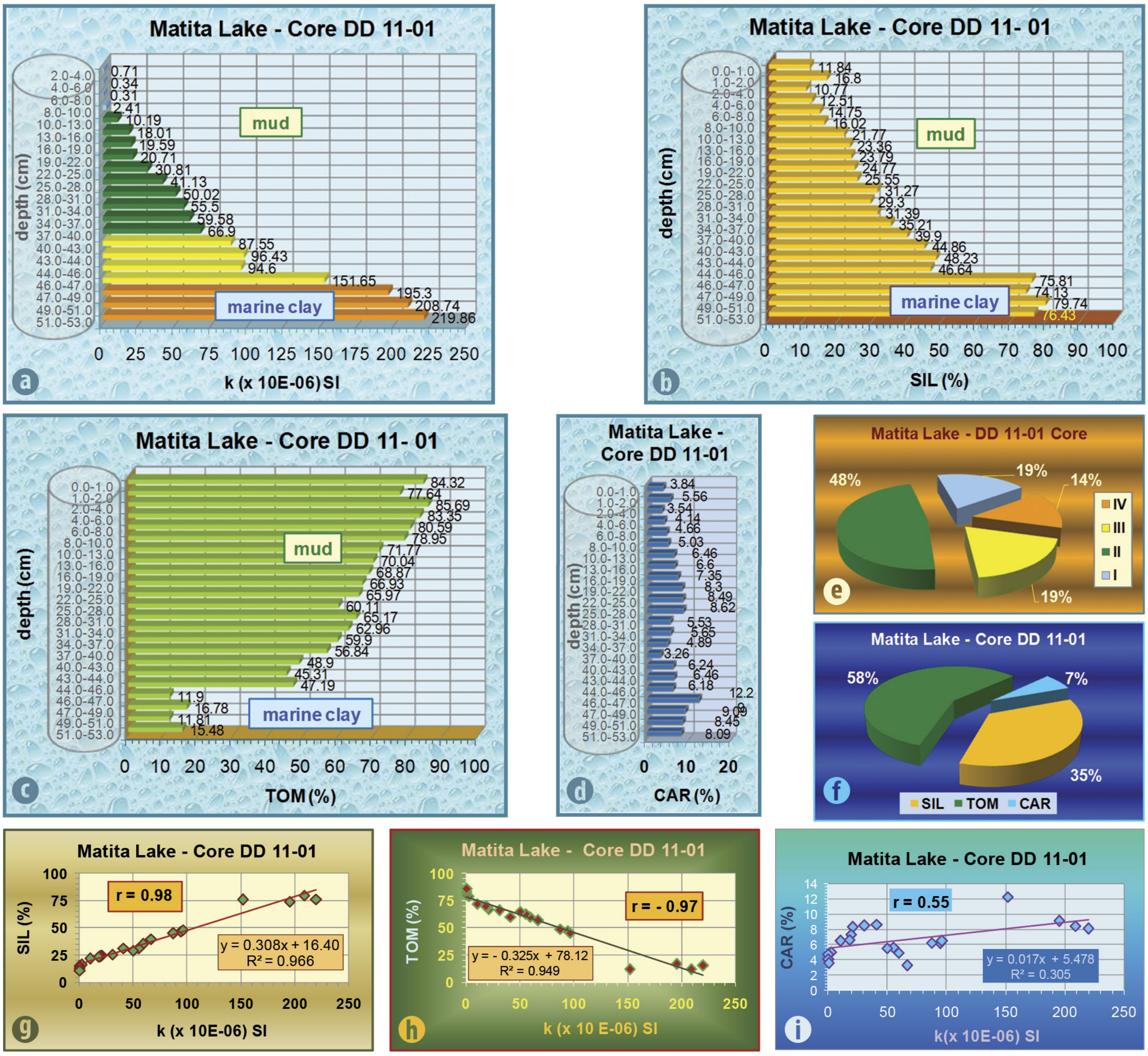

Fig. 13. Magneto-lithological model showing the vertical distribution of the enviromagnetic parameter (**MS**; **k**) and of the lithological components (**SIL**, **TOM**, **CAR**), along the core DD 11-01, collected from the Matița Lake (core location in Fig. 2). **a)** 3D bar-chart with the vertical distribution of the magnetic susceptibility; the bars are coloured according to the **k** scale classes (see Fig. 3a); **b)** 3D bar-chart with the vertical distribution of the siliciclastic/minerogenic component (**SIL**); **c)** 3D bar-chart with the vertical distribution of the total organic matter component (**TOM**); **d)** 3D bar-chart with the vertical distribution of the carbonate component (**CAR**); **e)** 3D pie-chart showing the **MS** calibration of the core sediments, according to the **k** classes; **f)** 3D pie-chart showing the lithological composition of the core sediments, based on the **SIL**, **TOM** and **CAR** contents; **g)** Diagram showing the correlation **SIL** *versus* **MS** (**k**); **h)** Diagram showing the correlation **TOM** *versus* **MS** (**k**); **i)** Diagram showing the correlation **CAR** *versus* **MS** (**k**).

The magnetic susceptibility measured on this sediment also shows a "transition value" (151.65×10^{-6} SI, assigned to class **III**; Figs. 13a,e), which is placed between the previous "**MS** level" ($87.55\times10^{-6} - 94.6\times10^{-6}$ SI; 40 – 46 cm depth interval; Fig. 13a) and the highest **k** values determined for the last 6 cm on the core bottom (Fig. 13a).

The vertical distribution of the lithological components, particularly concerning the *siliciclastic/mineral fraction* (**SIL**; Fig. 13b) and the *total organic matter* (**TOM**; Fig. 13c), asserts the integrated interpretation of the magnetic susceptibility core profile and of the macroscopic description. The highest **SIL** contents (74.13 % – 79.74 %; Fig. 13b), and, correspondingly, the lowest **TOM** contents (11.81 % – 16.78 %; Fig. 13c) were determined for the *marine clay*, while the lowest **SIL**, and the highest **TOM** contents were shown by the *muds* intercepted on core top (Figs. 13b,c). As regards the *carbonates* (**CAR**), the vertical distribution of their contents indicates two maximum zones (Fig. 13d), one with the apex around the 19

– 28 cm depth interval (with a maximum **CAR** content of 8.62 %), and the second, at the core lower part (with the highest **CAR** content of 12.29 % determined for the sample sliced at the 46 – 47 cm depth level). Inside of the depth intervals associated with the maximum **CAR** zones, the macroscopic description of the core has particularly indicated the presence of numerous shell fragments. The **MS** record, as well as the **SIL**, **TOM** and **CAR** profiles (represented by a unique area-chart) – illustrating the vertical variation of these magneto-lithological parameters along the *core DD 11-01* – are given in Figures 14a and 14b.

Taking into consideration the magneto-susceptibility and lithological data achieved for the entire sediment column (53 cm length), the general correlation diagrams performed for the «**MS** parameter *versus* **LITHO** components» illustrate and show a strong positive/direct correlation for **SIL** *vs.* **k** (**r** = 0.98; Fig. 15a), a strong negative/reversed one for **TOM** *vs.* **k** (**r** = – 0.97; Fig. 15d), and a moderate positive correlation for **CAR** *vs.* **k** (**r** = 0.55; Fig.15g). Starting from this information, we have analysed, separately, the previous relationships for each of the two parts in which the sediment column of the *core DD 11-01* was – lithologicaly – divided (*i.e.*, *muds* and *marine clay*, respectively). The results relating to the "*mud sequence*" (2 – 46 cm depth interval) are illustrated in Figs. 15b,e,h, for the correlations **SIL** *vs.* **k**, **TOM** *vs.* **k**, and **CAR** *vs.* **k**, respectively, while those regarding the *marine clay* deposit (intercepted between 46 – 53 cm) are given in Figs.15c,f,i. Strong correlations are indicated by the coefficient **r** for *muds*, in the **SIL** *vs.* **k** case (**r** = 0.98, *i.e.* a positive/direct correlation; Fig. 15b) and for **TOM** *vs.* **k** (**r** = – 0.96, *i.e.* a negative/indirect correlation; Fig. 15e), and also in the **CAR** *vs.* **k** case, but concerning the *marine clay* horizon (**r** = – 0.99, *i.e.* a negative/reversed correlation; Fig. 15i). Relating to this *marine* sequence, sampled along 7 cm, at the base of the *core DD 11-01*, moderate positive/direct correlations were obtained for both **SIL** *vs.* **k** (**r** = 0.34; Fig. 15c) and **TOM** *vs.* **k** (**r** = 0.43; Fig. 15f). As concerns the relationship **CAR** *vs.* **k**, yet evaluated for the *muds*, sampled from the core depth interval 2 – 46 cm, the coefficient **r** indicated a (very) weak positive correlation (**r** = 0.09; Fig. 15h).

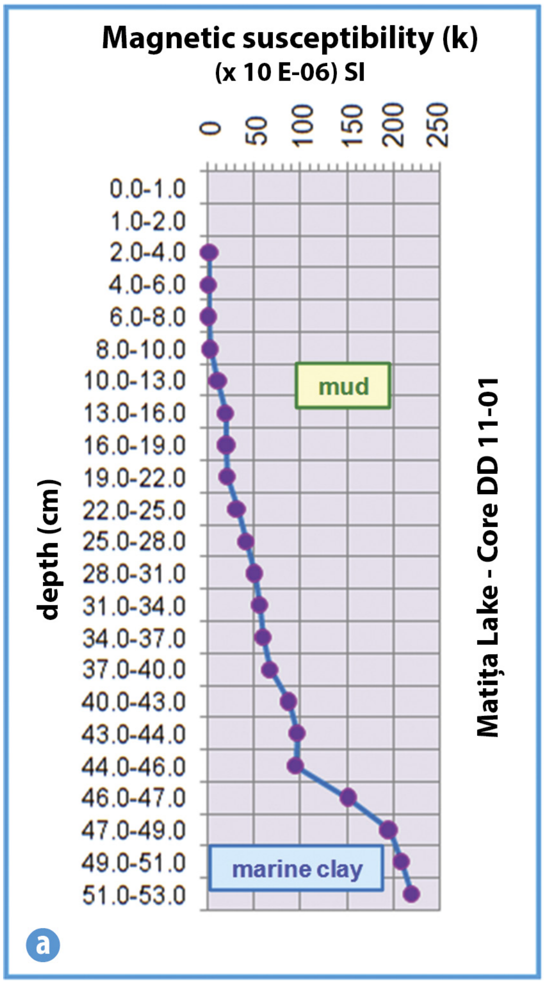

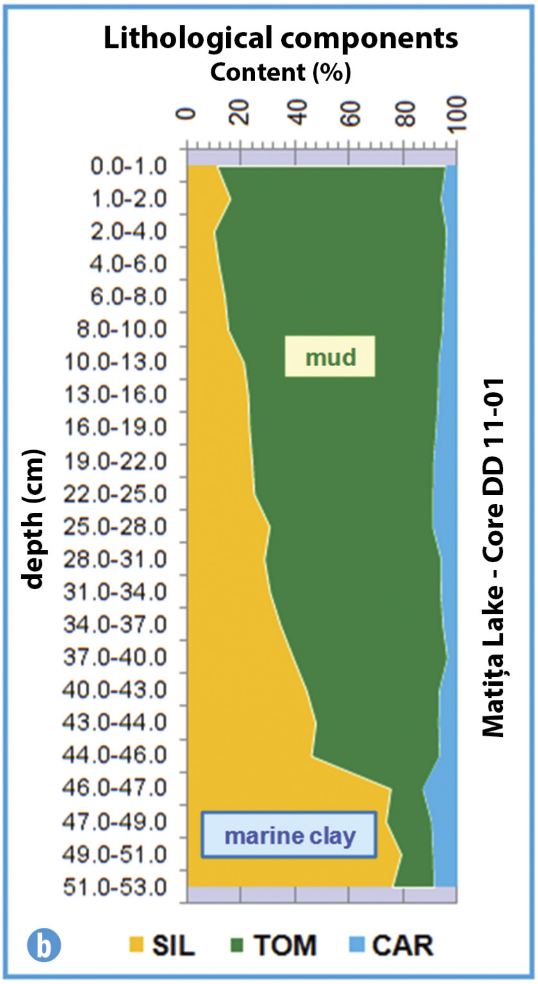

Fig. 14. Vertical distribution of the enviromagnetic parameter values (**k**) and of lithological components contents (**SIL**, **TOM**, **CAR**) along the sediment core DD 11-01, collected from the Matița Lake. **a)** Line-chart showing the magnetic susceptibility vertical profile; **b)** 100% stacked area-chart with the distribution of **SIL**, **TOM** and **CAR** contents along the sediment core.

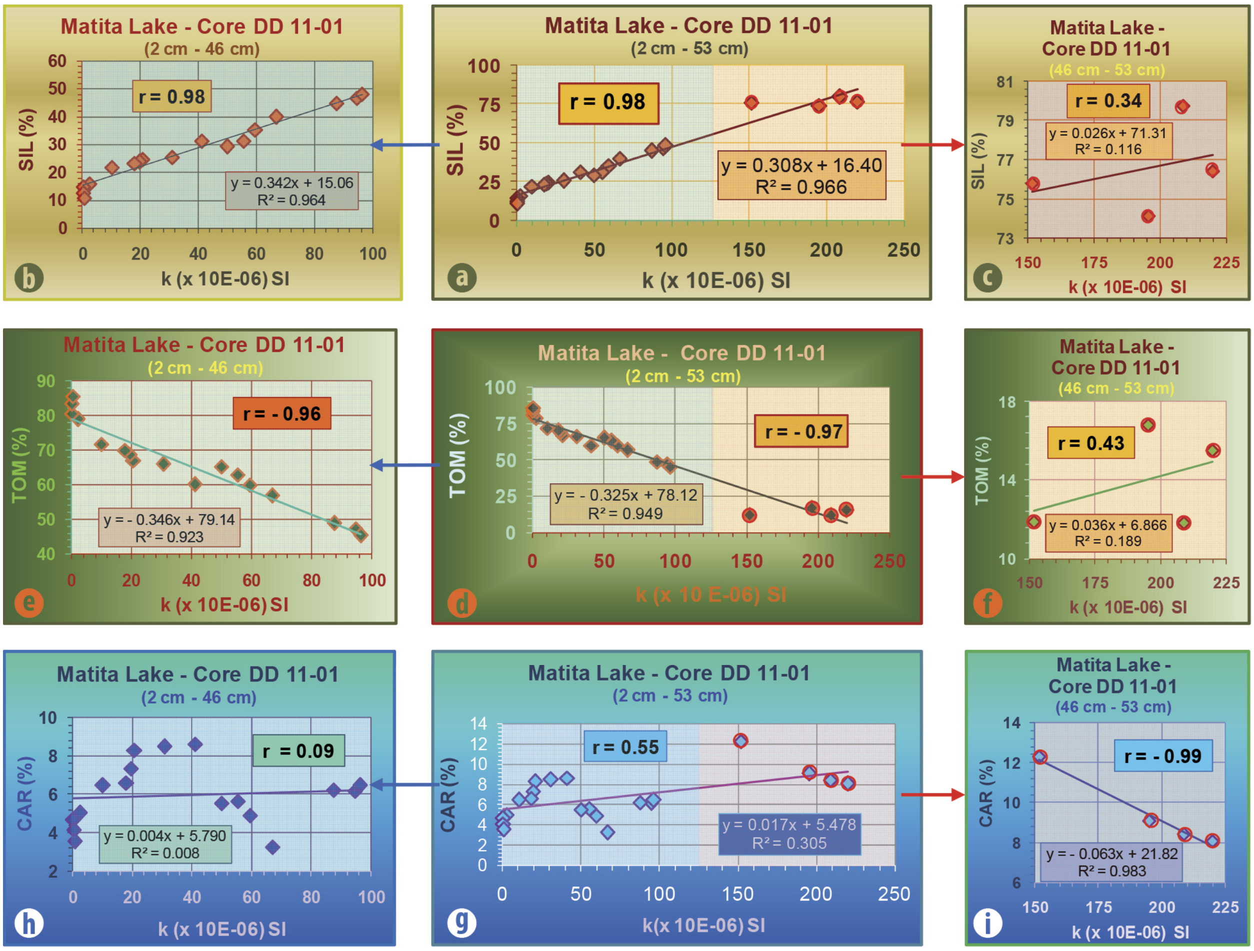

Fig. 15. Detail with the correlation of the enviromagnetic parameter (**MS**) with the lithological components (**SIL**, **TOM**, **CAR**), concerning the sediment core DD 11-01 (Matița Lake), in the context of the "marine clay" horizon interception at its basal part. **a)** Correlation **SIL** *versus* **k**, related to the entire investigated core (2 – 53 cm); **b)** Correlation **SIL** *versus* **k**, related to the "mud sequence" (2 – 46 cm); **c)** Correlation **SIL** *versus* **k**, related to the intercepted "marine clay sequence" (46 – 53 cm); **d)** Correlation **TOM** *versus* **k**, related to the entire investigated core (2 – 53 cm); **e)** Correlation **TOM** *versus* **k**, related to the "mud sequence" (2 – 46 cm); **f)** Correlation **TOM** *versus* **k**, related to the intercepted "marine clay sequence" (46 – 53 cm); **g)** Correlation **CAR** *versus* **k**, related to the entire investigated core (2 – 53 cm); **h)** Correlation **CAR** *versus* **k**, related to the "mud sequence" (2 – 46 cm); **i)** Correlation **CAR** *versus* **k**, related to the intercepted "marine clay sequence" (46 – 53 cm).

3.1.3. Lopatna Channel– Polideanca Lake Area (2014)

During the 2014 spring expedition (25 April – 7 May period), carried out in the *Danube Delta*, three sediment cores were collected from the *Lopatna Channel – Polideanca Lake* area (Fig. 2): *core DD 14-113* – from the *Polideanca – Lopatna Swamp*, *core DD 14-112* – from the canal which connects the *Lopatna Channel* with the *Polideanca L.*, and *core DD 14-104* – from the *Polideanca Lake* central zone. The magnetic susceptibility and lithological results are further analysed.

a) Core DD 14-113

This short core, of 24 cm length, collected from a swamp situated on the canal axis which makes the connection between *Lopatna Channel* and *Polideanca Lake* (Fig. 2), penetrated a dark grey *mud* sequence of 22 cm thickness, containing some vegetal material, intercepting then, at the 22 – 24 cm depth level, after a net boundary, a compact "*peaty*" *mud* – a dark grey *clayey-silty mud* (≈"*lacustrine clay*").

The magnetic susceptibility measurements confirm the presence of vegetal material within all the 12 sediment slices, the **MS** values being correlated with the **k** class **II** (Figs. 16a,c). The **MS** profile is defined by **k** values ranging between 24.51×10^{-6} – 59.47×10^{-6} (Fig.16a), the two extreme values being measured on the core top (0 – 2 cm) represented by a fluid *mud*, containing a coarser vegetal material and, respectively, at the core base (22 – 24 cm) – a compact *clayey-silty mud*, with rare vegetal remains.

The lithological composition of the *core DD 14-113* (Fig. 16b) supports the **MS** profile, particularly the above remarks. Thus, the contents of the *siliciclastic component* (**SIL**) determined for the 12 sediment samples are ranging between 15.23 % – 48.17 %, values provided by the first (top) and the last (bottom) core samples, respectively. Complementary, the highest *total organic matter* (**TOM**) content (84.11 %) was achieved for the top *mud* (0 – 2 cm), containing coarser vegetal material, while the lowest **TOM** content (49.74 %) was provided by the "*lacustrine clay*", with rare vegetal remains, intercepted at 22 – 24 cm depth. As regards the third lithological component – the *carbonates* (**CAR**), small contents (between 0.66 % – 2.1 %; Fig. 16b) characterize the core sediments; the ends of the **CAR** definition range were obtained for the samples collected from the same depth intervals as in the **SIL** and **TOM** component cases. The pie-chart from Fig. 16d quantifies the main characteristics of the lithological composition of the core sediments, and points out the highest content (73 %) of the **TOM** component, followed by the **SIL** (26 %) and **CAR** (1 %) components, respectively.

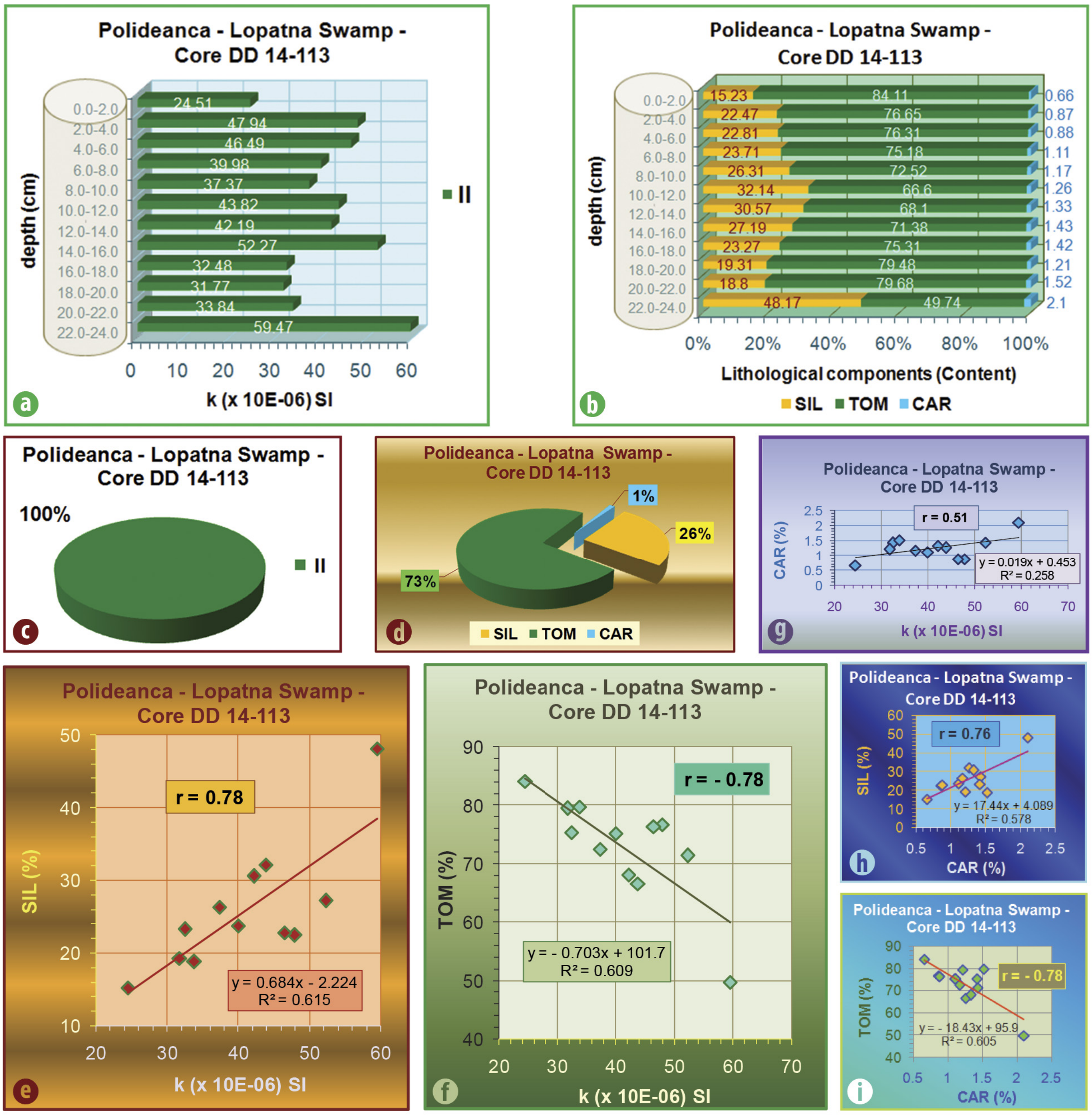

Fig. 16. Magneto-lithological model showing the vertical distribution of the enviromagnetic parameter (**MS**; **k**) and of the lithological components (**SIL**, **TOM**, **CAR**), along the core DD 14-113, collected from the Polideanca - Lopatna Swamp (core location in Fig. 2). **a)** 3D bar-chart with the vertical distribution of the magnetic susceptibility; the bars are coloured according to the **k** scale classes (see Fig. 3a); **b)** 100%-stacked bar-chart with the composite vertical distribution of the three main lithological components (**SIL**, **TOM**, **CAR**); **c)** 3D pie-chart showing the **MS** calibration of the core sediments, according to the **k** classes; **d)** 3D pie-chart showing the lithological composition of the core sediments, based on the **SIL**, **TOM** and **CAR** contents; **e)** Diagram showing the correlation **SIL** *versus* **MS** (**k**); **f)** Diagram showing the correlation **TOM** *versus* **MS** (**k**); **g)** Diagram showing the correlation **CAR** *versus* **MS** (**k**); **h)** Diagram showing the correlation **SIL** *versus* **CAR**; **i)** Diagram showing the correlation **TOM** *versus* **CAR**.

Actually, the correlation coefficients **r** (Figs. 16e,f,g,h,i) assert, quantitatively, the magnetic susceptibility and lithological characterization of the *core DD 14-113*. As concerns the relationships between the lithological components and the enviromagnetic parameter **MS**, we can remark the strong correlation for **SIL** *versus* **k** (Fig. 16e), and **TOM** *vs.* **k** (Fig. 16f), positive/direct (**r** = 0.78), and negative/reversed (**r** = – 0.78), respectively. A moderate positive correlation is shown by the **r** coefficient for **CAR** *vs.* **k** (**r** = 0.51; Fig. 16g). It is also interesting to mention the type/size of the relationships existing between the main two lithological components, **SIL** and **TOM**, and the carbonates (**CAR**). So, a strong direct correlation characterizes **SIL** *vs.* **CAR** (**r** = 0.76; Fig. 16h), and a strong reversed correlation is indicated by **TOM** *vs.* **CAR** (**r** = – 0.78; Fig. 16i).

Finally, the vertical variation of the magnetic susceptibility related to the *sediment core DD 14-113*, alongside of the vertical distribution of the contents of the three lithological components, are illustrated by the line-chart (Fig. 17a), and the 2D area-chart (Fig. 17b), respectively.

b) Core DD 14-112

Located between the *Polideanca – Lopatna Swamp* and the *Polideanca Lake*, on the connection canal with the *Lopatna Channel*, closer of its entry mouth into the *Polideanca L.* (Fig. 2), the *core DD 14-112* has a length of 44 cm (Fig. 18). The core sediment description made aboard the research vessel has revealed a sharp limit at cm 31 below the sediment/water interface, between an upper sequence (0 – 31 cm), consisting of blackish *mud*, and a lower one (31 – 44 cm), represented by a light grey *clay*. The *mud* which is rich in plant debris (fine roots, leaves and even reed fragments), non-cohesive at the upper part, becomes coarser and more cohesive at the base of the interval, and is characterized by a saprogenic or hydrogen sulfide smell. Some shells of freshwater molluscs (*Planorbis sp*., *Valvata sp*.) have been found within the 10 – 12 cm depth interval. The light grey *clay* is cohesive and softer in the upper few cms and becomes harder and more cohesive as depth increases, showing few vertical and horizontal bioturbations. Small shell fragments are present, including a *Cardium* valve, located at the sequence top, suggesting a *marine* origin of the *clay*.

The magnetic susceptibility, measured on 15 samples collected from the upper sequence (0 – 31 cm), is ranging between 3.67×10^{-6} – 43.56×10^{-6} SI, *i.e.* **MS** values assigned to **k** classes **I** and **II** (Fig. 18a). We must add to the above general description that these *muds* contain various quantities of vegetal material, in some of them being identified shell fragments, too, which influence the **MS** intensity, but within the above specified limits (**k** class **I** – **k** class **II**). An increasing trend is shown by the magnetic susceptibility of the sediment slices cut from the depth interval 18 – 31 cm (a dark grey *mud*), the *clayey mud* (*clay*) intercepted immediately after this level (*i.e.*, at 31 – 33 cm depth) providing a **MS** "jump" towards the **k** class **III**, namely to a value of 112.0×10^{-6} SI (Fig. 18a). The plastic *clay*, sampled up to the core bottom (a *marine clay*), keeps this **MS** regime defined by the **k** class **III**, the last/base

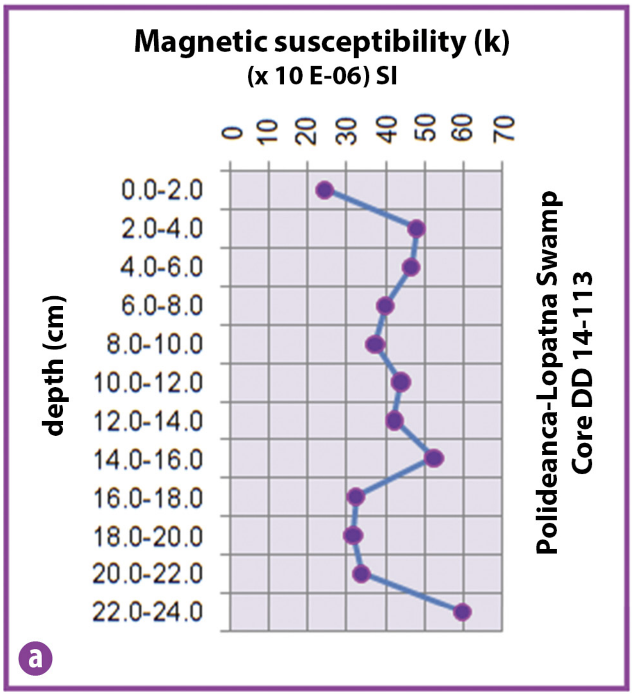

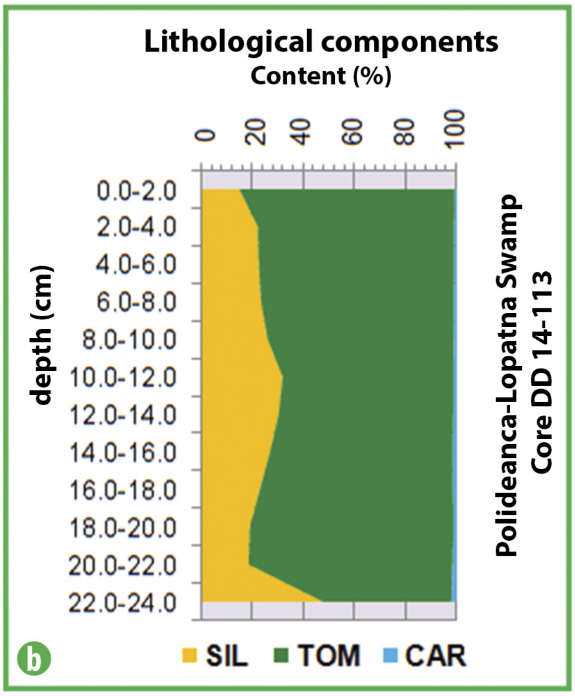

Fig. 17. Vertical distribution of the enviromagnetic parameter values (**k**) and of lithological components contents (**SIL**, **TOM**, **CAR**), along the sediment core DD 14-113, collected from the Polideanca - Lopatna Swamp. **a)** Line-chart showing the magnetic susceptibility vertical profile; **b)** 100% stacked area-chart with the distribution of **SIL**, **TOM** and **CAR** contents along the sediment core.

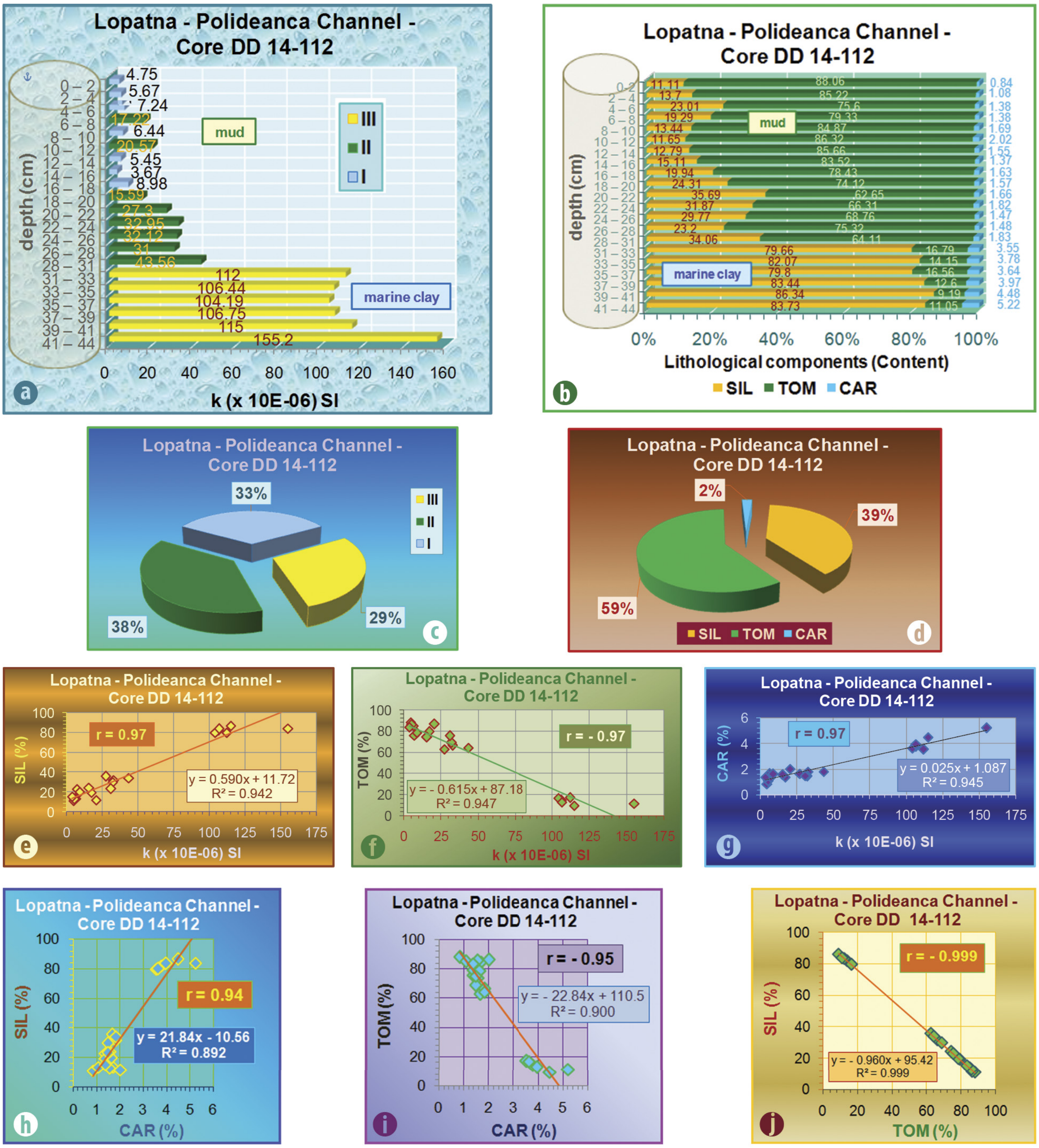

Fig. 18. Magneto-lithological model showing the vertical distribution of the enviromagnetic parameter (**MS**; **k**) and of the lithological components (**SIL**, **TOM**, **CAR**), along the core DD 14-112, collected from the Lopatna - Polideanca Canal (core location in Fig. 2). **a)** 3D bar-chart with the vertical distribution of the magnetic susceptibility; the bars are coloured according to the **k** scale classes (see Fig. 3a); **b)** 3D 100%-stacked bar-chart with the composite vertical distribution of the three main lithological components (**SIL**, **TOM**, **CAR**); **c)** 3D pie-chart showing the **MS** calibration of the core sediments, according to the **k** classes; **d)** 3D pie-chart showing the lithological composition of the core sediments, based on the **SIL**, **TOM** and **CAR** contents; **e)** Diagram showing the correlation **SIL** *versus* **MS** (**k**); **f)** Diagram showing the correlation **TOM** *versus* **MS** (**k**); **g)** Diagram showing the correlation **CAR** *versus* **MS** (**k**); **h)** Diagram showing the correlation **SIL** *versus* **CAR**; **i)** diagram showing the correlation **TOM** *versus* **CAR**; **j)** Diagram showing the correlation **SIL** *versus* **TOM**.

sediment sample reaching the highest **MS** value that was recorded along the whole core, namely 155.2×10^{-6} SI (Fig. 18a).

The lithological composition defined by the three main components **SIL**, **TOM** and **CAR** supports very well the magneto-susceptibilimetric characterization of the *core DD 14-112*, the distribution of their contents being illustrated by the 2D area-chart from Fig. 18b. It is easily to remark the "jump" of the *siliciclastic fraction*/**SIL** (towards much higher contents) and of the *total organic matter*/**TOM** (towards much lower contents), these sharp changes appearing at the same depth level as in the **MS** case, *i.e.* beginning with the 31 – 33 cm sediment slice (Fig. 18b). Thus, if in the first 31 cm, the **SIL** contents are ranging between 11.11 % – 35.69 %, and the **TOM** contents between 62.65 % – 88.06 %, then, in the following 13 cm (31 – 44 cm depth interval), where a *marine clay* was intercepted, the content ranges are defined by 79.66 % – 86.34 % for **SIL**, and by 9.19 % – 16.79 % for **TOM** (Fig. 18b). It is also interesting to remark the **CAR** profile, which in this case – even within low contents – shows similar main characteristics: lower contents for the *muds* described along the upper 31 cm of the core (0.84 % – 2.02 %), followed by a "jump" towards higher contents, ranging between 3.55 % – 5.22 %, related to the *marine clays*, from the core lower/basal part (Fig. 18b).

The synoptic illustration of the magnetic susceptibility and lithological characterization of the *core DD14-112* is given by the two pie-charts from Fig. 18c and Fig. 18d, respectively. The **MS** structure of the core reveals close percentages for the three **k** classes to which the sediments were calibrated, actually disposed along 9 percents, *i.e.*, ranging between 29 % – 38 % (Fig. 18c): **I** – 33 %; **II** – 38 %; **III** – 29 %. As regards the **LITHO** structure, the three main components are characterized by clearly different content distribution: **SIL** – 39 %; **TOM** – 59 %; **CAR** – 2 % (Fig. 18d). Yet, this observation is changing when we compare the two categories of parameters according with the lithological/sedimentological support of the **MS** scale (see Rădan & Rădan, 2007, 2013). Consequently, the **k** classes (**I** + **II**) show, together, 71 %, while the contents of (**TOM** + **CAR**), together, indicate 61 %; the **k** class **III** – defined by 29 %, and the **SIL** content – by 39 % also indicate closer amounts. This grouping is based by the "genuine" lithological support of the **MS** scale (Rădan & Rădan, 2011, 2013), so that the lower classes (**I** and **II**) correspond to *fine sediments*, usually rich in *organic material* and/or *carbonates*, while the intermediate class (**III**) is connected with the *fine clayey* to *silty sediments*. The macroscopic description of the *core DD 14-112* indicates a very good agreement with the lithological support of the **MS** scale. Moreover, the quantification of the relationships existing between the enviromagnetic parameter (**MS**) and the lithological components, illustrated in Figs. 18e,f,g, confirms the parallel observations which were above commented. There were calculated (very) strong correlation coefficients (**r**) in all the cases: **SIL** *versus* **k** (**r** = 0.97; Fig. 18e); **TOM** *vs*. **k** (**r** = – 0.97); **CAR** *vs*. **k** (**r** = 0.97). In all three cases, the **r** size is very close of the upper boundary (*i.e.*, 1.00) of the range within which the strong correlation is defined (see, *e.g*., Rădan & Rădan, 2013). We have to remark the result obtained for *carbonates*, which usually, in other cases of investigated cores/bottom sediments, showed reversed correlations with the **MS**. In our foregoing comment, it was revealed the similar behaviour and trends of the **SIL** and **CAR** components along the core, although these are distinctly defined, namely by high, and much lower contents, respectively (see Fig.18b). In fact, the correlation coefficient calculated for **SIL** *vs*. **CAR** confirms these remarks: **r** = 0.94 (Fig. 18h), that is a (very) strong positive/direct correlation. A similar result is obtained for **TOM** *vs*. **CAR**, but the correlation is a (very) strong negative/reversed one: **r** = – 0.95 (Fig. 18i). Certainly, for **SIL** *vs*. **TOM**, a very strong reversed correlation is shown by **r**, which is almost 1 (respectively, **r** = – 0.999; Fig. 18j).

Starting from the magneto-susceptibility and lithological data recorded for the entire sediment column (44 cm length), which were above discussed in detail, we analyse further, separately, the respective relationships for each of the two parts in which the sediment column of the *core DD 14-112* was lithologicaly divided: *muds*, and *marine clays* (a net boundary between them was identified). The general correlation diagrams, performed for the «**LITHO** components *versus* **MS** parameter» related to the entire core, are given again, in Figs. 19a,d,g, yet, with some additional elements, which regard the marking of the two zones associated with the two sediment categories composing the core. The results relating to the "*mud sequence*" (0 – 31 cm) are illustrated in Figs. 19b,e,h, for the correlations **SIL** *vs*. **k**, **TOM** *vs*. **k**, and **CAR** *vs*. **k**, respectively, and the data regarding the *marine clay* unit (31 – 44 cm) are represented in Figs.19c,f,i. As concerns the *muds*, the **r** coefficient indicates a strong positive/direct correlation in the case of **SIL** *vs*. **k** (**r** = 0.81; Fig. 19b), a strong negative/reversed one for **TOM** *vs*. **k** (**r** = – 0.81; Fig. 19e), and a moderate positive correlation for **CAR** *vs*. **k** (**r** = 0.53; Fig. 19h). In respect of the *marine clay* horizon, sampled along 13 cm, towards the base of the *core DD 14-112* (31 – 44 cm depth interval), moderate correlations were obtained for both **SIL** *vs*. **k** (**r** = 0.33; Fig. 19c), and **TOM** *vs*. **k** (**r** = – 0.47; Fig. 19f), positive/direct in the first mentioned case, and negative/reversed, in the second one. Related to the relationship **CAR** *vs*. **k**, analysed in the case of the *marine clay*, the **r** coefficient shows a strong positive/direct correlation (**r** = 0.90; Fig. 19i), a result which makes interesting, again, the discussion around the *carbonates* which are present inside of this core.

Finally, in Figs. 20a,b, the **MS**, **SIL**, **TOM** and **CAR** profiles are illustrated for the whole sediment *core DD 14-112*, by means of a line-chart, for the enviromagnetic parameter (**k**) vertical variation (Fig. 20a), and a 2D area-chart, for the simultaneous/composite illustration of the vertical distribution of the three lithological components (Fig. 20b).

c) Core DD 14-104

This core was collected from the central zone of the *Polideanca Lake* (Fig. 2) and points out an interesting vertical var-

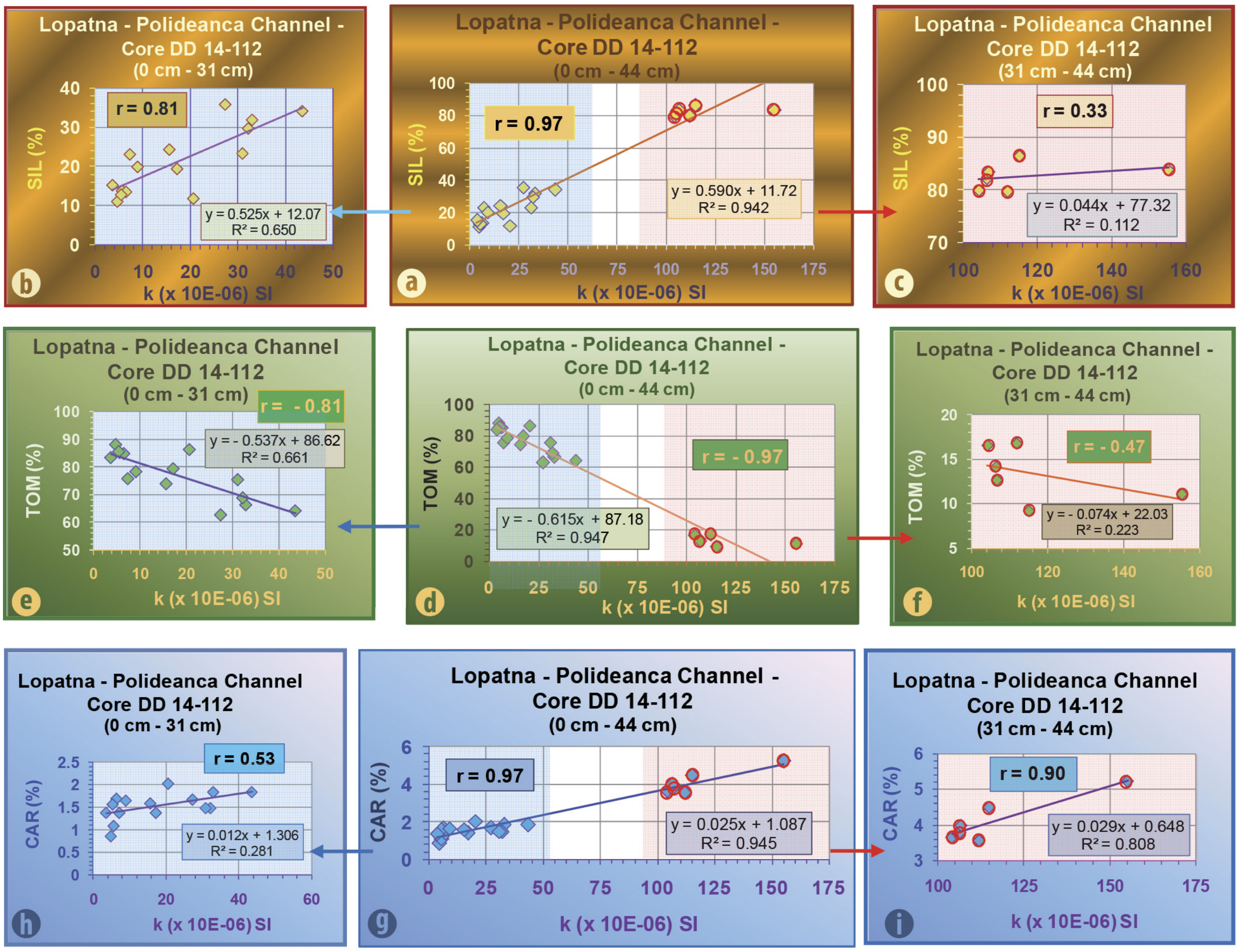

Fig. 19. Detail with the correlation of the enviromagnetic parameter (**MS**) with the lithological components (**SIL**, **TOM**, **CAR**), concerning the sediment core DD 14-112 (Lopatna - Polideanca Canal), in the context of the "marine clay" horizon interception at its basal part. **a)** Correlation **SIL** *versus* **k**, related to the entire core (0 – 44 cm); **b)** Correlation **SIL** *versus* **k**, related to the "mud sequence" (0 – 31 cm); **c)** Correlation **SIL** *versus* **k**, related to the intercepted "marine clay sequence" (31 – 44 cm); **d)** Correlation **TOM** *versus* **k**, related to the entire core (0 – 44 cm); **e)** Correlation **TOM** *versus* **k**, related to the "mud sequence" (0 – 31 cm); **f)** Correlation **TOM** *versus* **k**, related to the intercepted "marine clay sequence" (31 – 44 cm); **g)** Correlation **CAR** *versus* **k**, related to the entire core (0 – 44 cm); **h)** Correlation **CAR** *versus* **k**, related to the "mud sequence" (0 – 31 cm); **i)** Correlation **CAR** *versus* **k**, related to the intercepted "marine clay sequence" (31 – 44 cm).

iation of the sequences which were penetrated up to 44 cm below the water/sediment interface. The first 10 cm consist of typical *mud* for the *Polideanca Lake* (*i.e.*, a fluffy, non-cohesive sediment, with H_2S smell). The magnetic susceptibility measurements show low but positive **k** values (assigned to **k** class **I**), increasing from 0.07×10^{-6} SI for the core top (0 – 2 cm) up to 2.58×10^{-6} SI for the sample collected from the 8 – 10 cm depth level (Fig. 21a). The siliciclastic component (**SIL**) asserts this trend and its low definition range, showing contents of 9.70 % up to 13.99 % (Fig. 21b). Complementary, high contents were obtained for the organic matter (**TOM**), namely 88.49 % for the core top (Fig. 21b), decreasing then up to 83.43 % for the sample sliced at the depth interval 8 – 10 cm. Downwards, along the following 30 cm, the presence of the vegetal material – finely triturated, or as fragments – becomes more and more important, getting up to a *peat*-like sediment, very rich in organic material. The enviromagnetic parameter **MS** confirms this composition particularity of the sediment sequence, and records very low and negative **k** values (of course, attributed to **k** class **I**), ranging between (– 6.51)×10^{-6} SI and (– 0.05)×10^{-6} SI. The presence of some shell fragments, observed within this sediment sequence, could influence even more the very low level of the **MS** intensity. Further, it follows a stepwise transition towards a coarse *siliciclastic* sediment. Within the *peaty* horizon occurs a *clayey-silty* micaceous material, its presence increasing towards the core base. The magnetic susceptibility is fingerprinting this special composition of the sediment at the core bottom, and the **k** values measured on the last two sediment slices (40 – 44 cm) towards the base show the highest intensity recorded along the *core DD 14-104*, namely 6.99×10^{-6} SI (*i.e.*, **k** class **I**) and 12.40×10^{-6} SI (*i.e.*, **k** class **II**) (Fig. 21a). The *siliciclastic* and the *total organic material* components, **SIL** and **TOM**, respectively, support these **MS** fingerprints, indicating the highest

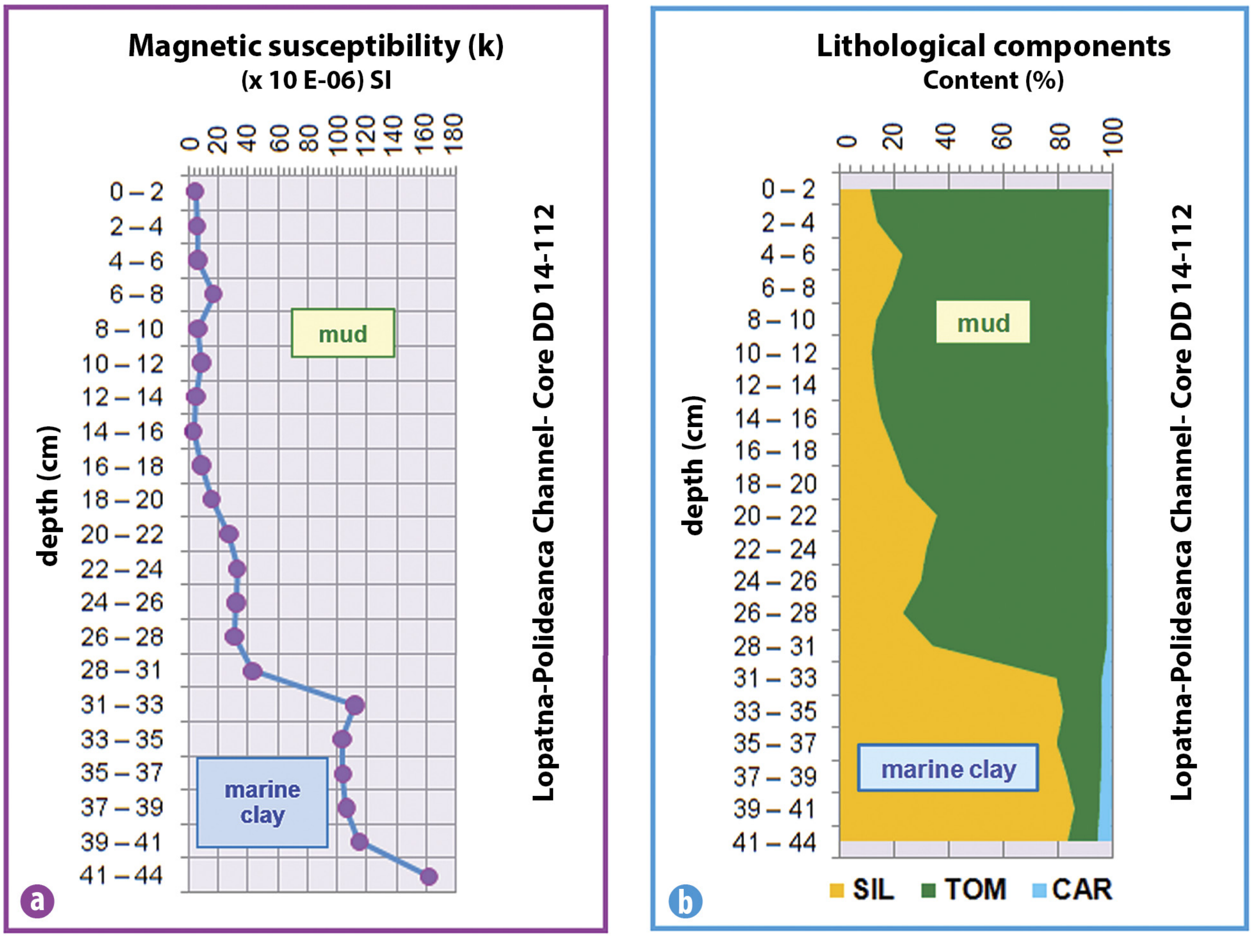

Fig. 20. Vertical distribution of the enviromagnetic parameter values (**k**) and of lithological components contents (**SIL**, **TOM**, **CAR**), along the sediment core DD 14-112, collected from the Lopatna - Polideanca Canal. **a)** Line-chart showing the magnetic susceptibility vertical profile; **b)** 100% stacked area-chart with the distribution of **SIL**, **TOM** and **CAR** contents along the sediment core.

contents (30.21 % and 33.3 %, for **SIL**), and, complementary, the lowest ones (63.85 % and 62.18 %, for **TOM**), respectively (Fig. 21b). As regards the third lithological component, the *carbonates* (**CAR**), the contents are ranging between 0.91 % – 5.93 % (Fig. 21b), the highest values being determined for the same two bottom slices, cut at the core base (40 – 44 cm depth interval beneath the water/sediment interface).

The **MS** and **LITHO** data, above commented, and illustrated in Figs. 21a,b, are synthetised by the pie-charts from Figs. 21c,d. Thus, concerning the enviromagnetic parameter **MS** (Fig. 21c), 5 % only are assigned to **k** class **II**, the remaining 95 % being attributed to class **I** (**k** values lower than 10×10^{-6} SI; see Rădan & Rădan, 2007, 2013). This magnetic characteristics is supported by the lithological composition of the core sediments, the synoptic image from Fig. 21d showing the highest average content is determined for the *total organic matter* component (85 %), to which there can be added 2 percents provided by *carbonates*. The *siliciclastic* component holds 13 % only within the core lithological composition (Fig. 21d), in agreement with the very low weight of the **k** class **II**, a **MS** range (10×10^{-6} SI – 75×10^{-6} SI; Rădan & Rădan, 2007, 2013) to which 5 % of samples only were calibrated (Fig. 21c).

The magneto-lithological data obtained for the *core DD 14-104* can be remarked for the very good correlations between the magneto-susceptibility and each of the three lithological components, as well as with regard to the correlations related to the pairs of **LITHO** components. So, the **r** coefficient calculated for **SIL** *versus* **k** is 0.83 (Fig. 21e), showing a strong positive correlation. Correspondingly, for **TOM** *vs*. **k** is indicated a negative correlation, also a strong one, as **r** = – 0.84 (Fig. 21f). Even for **CAR** *vs*. **k**, the **r** coefficient shows a strong correlation, a positive one (**r** = 0.80; Fig. 21g), as in the case of the *siliciclastic* component. Strong negative correlations define the cases **SIL** *vs*. **TOM** (**r** = – 0.996; Fig. 21h), and **TOM** *vs*. **CAR** (**r** = –0.86; Fig. 21i), while for **SIL** *vs*. **CAR**, a strong positive correlation (**r** = 0.81; Fig. 21j) is shown by the **r** coefficient.

A parallel view of the profiles recorded for the four parameters – **MS**, **SIL**, **TOM**, **CAR** – is offered by the line-chart from Fig. 22a, showing the downcore magneto-susceptibility vertical variation, and by Fig. 22b, in which the three profiles **SIL**, **TOM**, **CAR** are simultaneously drawn; the area-chart makes possible to display the parallel and therewith integrated vertical distribution of the lithological components, within

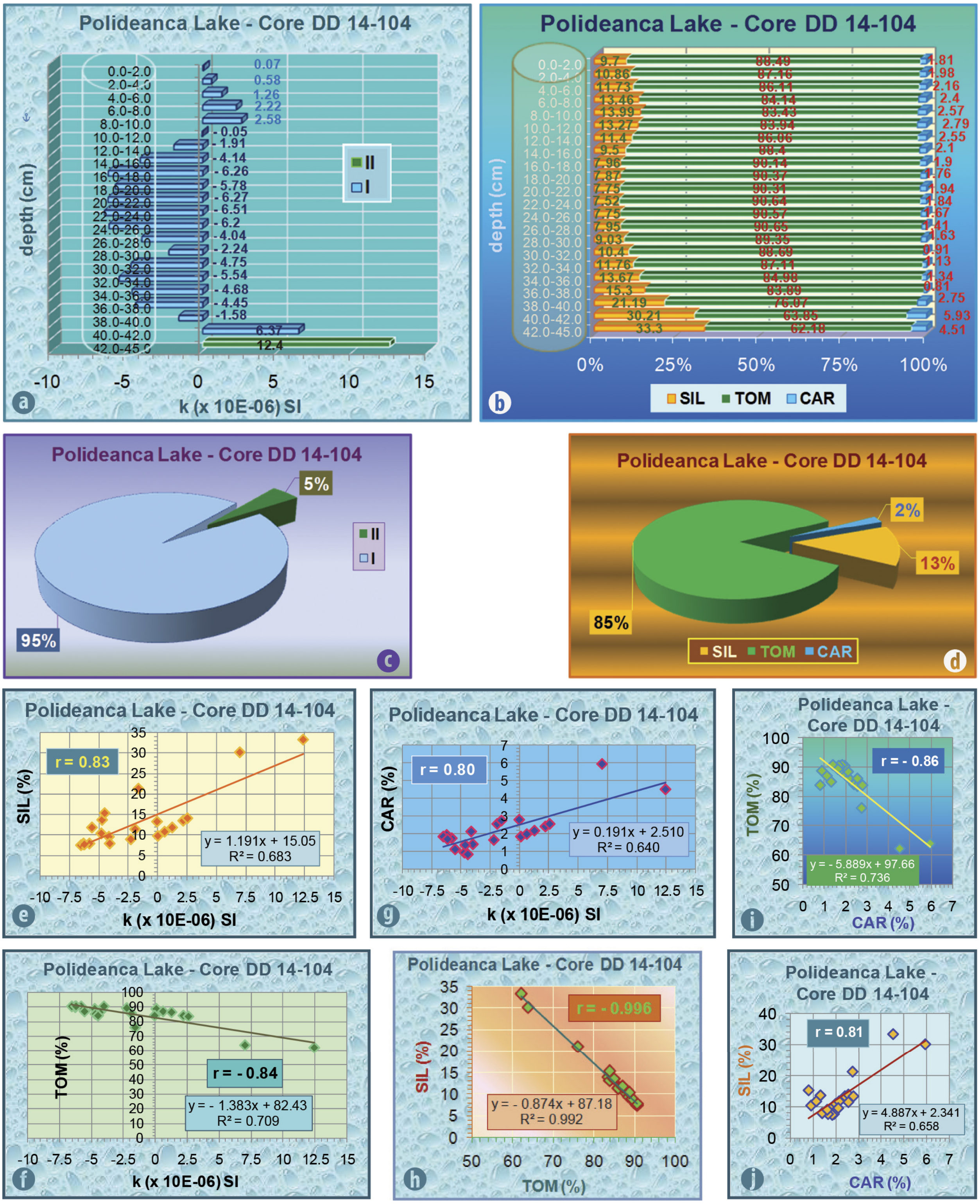

Fig. 21. Magneto-lithological model showing the vertical distribution of the enviromagnetic parameter (**MS**; **k**) and of the lithological components (**SIL**, **TOM**, **CAR**), along the core DD 14-104, collected from the Polideanca Lake (core location in Fig. 2). **a)** 3D bar-chart with the vertical distribution of the magnetic susceptibility; the bars are coloured according to the **k** scale classes (see Fig. 3a); **b)** 3D 100%-stacked bar-chart with the composite vertical distribution of the three main lithological components (**SIL**, **TOM**, **CAR**); **c)** 3D pie-chart showing the **MS** calibration of the core sediments, according to the **k** classes; **d)** 3D pie-chart showing the lithological composition of the core sediments, based on the **SIL**, **TOM** and **CAR** contents; **e)** Diagram showing the correlation **SIL** *versus* **MS** (**k**); **f)** Diagram showing the correlation **TOM** *versus* **MS** (**k**); **g)** Diagram showing the correlation **CAR** *versus* **MS** (**k**); **h)** Diagram showing the correlation **SIL** *versus* **TOM** **i)** diagram showing the correlation **TOM** *versus* **CAR**; **j)** Diagram showing the correlation **SIL** *versus* **CAR**.

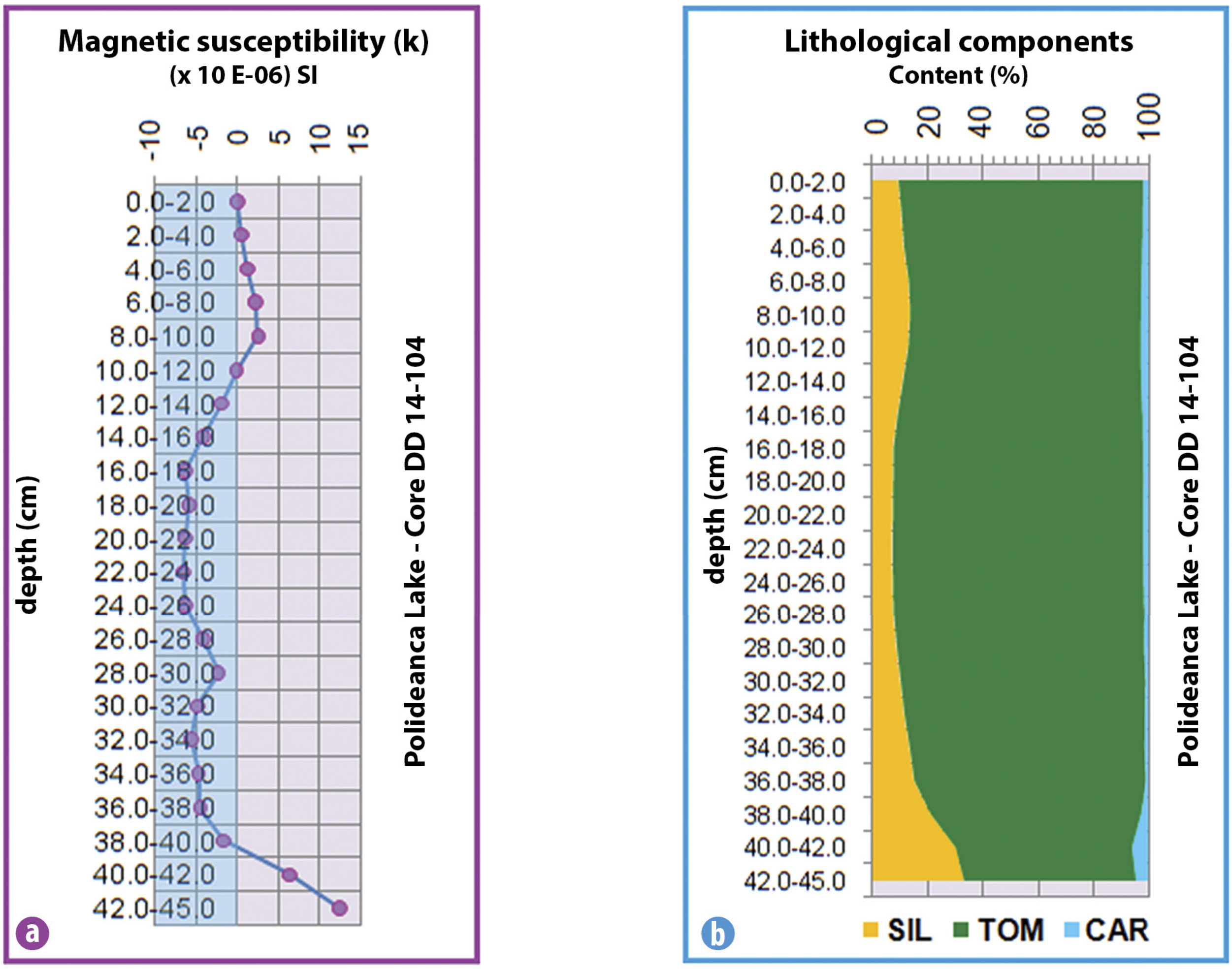

Fig. 22. Vertical distribution of the enviromagnetic parameter values (**k**) and of lithological components contents (**SIL**, **TOM**, **CAR**), along the sediment core DD 14-104, collected from the Polideanca Lake. **a)** Line-chart showing the magnetic susceptibility vertical profile. *Note*: in *blue*, is zone with negative **k** values; **b)** 100% stacked area-chart with the distribution of **SIL**, **TOM** and **CAR** contents along the sediment core.

a total area of 100 percents. This composite image could be seen as a corresponding **LITHO** background for the pie-chart from Fig. 21d, where the percentages of **SIL**, **TOM** and **CAR** contents are indicated, synoptically, for all the 22 samples sliced from the sediment column, which actually support the three **LITHO** profiles. The dominance of the *organic matter* is evident (85 %), followed by the *siliciclastic fraction*, but at a much lower level (13 %), and, finally, the *carbonates*, at an extremely low level (2 %). The macroscopic description of the core, particularly the complex analysis from the beginning of this section (3.1.3.c) – the presence of a *peaty* material within the core sediment being a significant element – is correspondingly asserted by the above remarks.

3.1.4. Bogdaproste Lake (2013)

Core DD 13-104

One sediment core only, namely *DD 13-104*, was collected from the *Bogdaproste Lake* (location in Fig. 2), during the 2013 spring expedition, carried out in the 16 – 29 April time interval.

The recovered sediment column, thick of 48 cm, includes three sequences, with a stepwise transition from a lithology to another (Fig. 23). The magneto-susceptibility and the lithological signature clearly reveal the gradual transition from the upper sequence (0 – 18 cm), consisting of dark grey to brown-greenish organic *muds*, loose, non-cohesive, rich in plant fragments and finely triturated vegetal material, with scarce small shell fragments, to a middle one (18 – 36 cm), represented by a dark brown, coarse *peat* deposit, containing rare shell fragments and minor but increasing downward amounts of coarse *silt* material that change the *peat* into a *peaty mud* which becomes more plastic and cohesive along the last 4 cm towards the base interval. The last unit (36 – 48 cm) starts with a grey, clayey, plastic, cohesive *mud*, with small fragments of reed and irregular enclaves of dark brown *muddy peat*, which changes to a more compact and coarse *mud*, with lower plasticity, containing small reed and peat fragments and quite frequent *marine* shells (*Cardiidae* and *Corbula*).

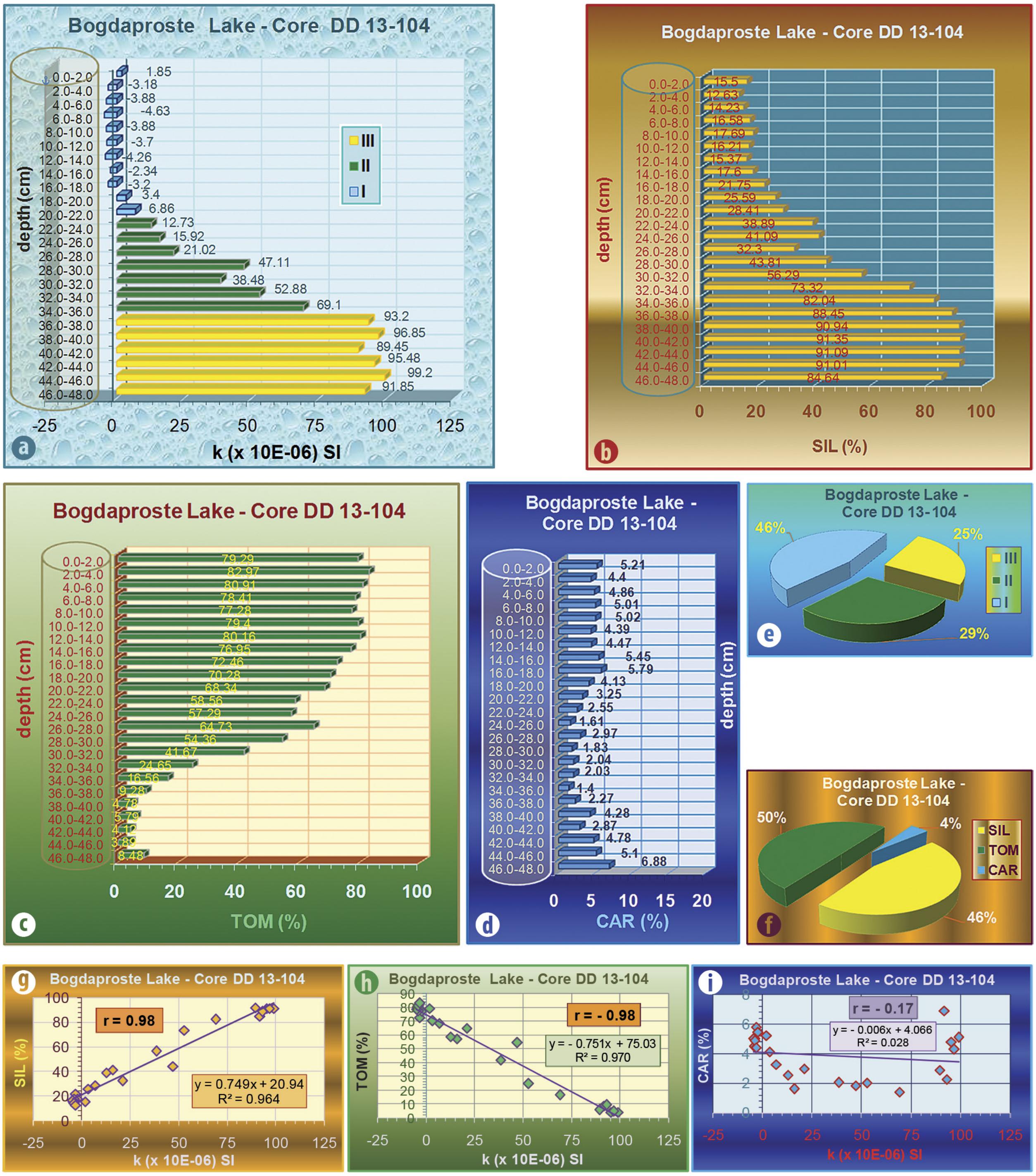

Fig. 23. Magneto-lithological model showing the vertical distribution of the enviromagnetic parameter (**MS**; **k**) and of the lithological components (**SIL**, **TOM**, **CAR**), along the core DD 13-104, collected from the Bogdaproste Lake (core location in Fig. 2). **a)** 3D bar-chart with the vertical distribution of the magnetic susceptibility; the bars are coloured according to the **k** scale classes (see Fig. 3a); **b)** 3D bar-chart with the vertical distribution of the siliciclastic/minerogenic component (**SIL**); **c)** 3D bar-chart with the vertical distribution of the total organic matter component (**TOM**); **d)** 3D bar-chart with the vertical distribution of the carbonate component (**CAR**); **e)** 3D pie-chart showing the **MS** calibration of the core sediments, according to the **k** classes; **f)** 3D pie-chart showing the lithological composition of the core sediments, based on the **SIL**, **TOM** and **CAR** contents; **g)** Diagram showing the correlation **SIL** *versus* **MS** (**k**); **h)** Diagram showing the correlation **TOM** *versus* **MS** (**k**); **i)** Diagram showing the correlation **CAR** *versus* **MS** (**k**).

The *upper* vegetal organic *mud sequence* (0 – 18 cm) is characterized by very low **MS** values, ranging from (– 4.63)$\times10^{-6}$ SI up to 1.85$\times10^{-6}$ SI, eight of nine values being negative (Fig. 23a); all are assigned to **k** class **I.** The *minerogenic/siliciclastic* component (**SIL**), and complementary, the *total organic matter* (**TOM**), support these magnetic fingerprints, the **SIL** and **TOM** contents ranging between 12.63 % – 21.65 % (Fig. 23b), and 72.46 % – 82.97 % (Fig. 23c), respectively. As regards the *carbonates* (**CAR**), they are present inside of these organic vegetal *muds* within a range with very close limits, *i.e.*, 4.39 % – 5.79 % (Fig. 23d); the shell fragments found within the samples collected from the sediment column along this depth interval (0 – 18 cm) could influence the level of the **CAR** contents.

Passing to the *middle sequence*, the dark-brown, non-cohesive coarse *peat*, which occurs downwards along the core up to the depth level 30 – 32 cm, where the *peat* becomes finer, the macroscopic description mentions some reed leafs inside, but also some *silty* to finely *sandy* grains. The magnetic susceptibility reflects very well the macroscopic lithological observations and records a continuous increasing, from the **k** value of 3.4$\times10^{-6}$ SI (class I), measured on the slice from 18 – 20 cm depth interval, up to 47.11$\times10^{-6}$ SI (**k** class **II**), on the sample sliced at 28 – 30 cm depth (Fig. 23a). The lithological analyses confirm the **MS** behaviour: the *siliciclastic* component (**SIL**) content increases from 25.59 % (for the 18 – 20 cm sample) up to 43.81 % (for the 28 – 30 cm sample) (Fig. 23b), while the *total organic matter* (**TOM**) content decreases from 70.28 % up to 54.36 % (Fig. 23c), along the respective depth interval (18 – 30 cm). The *transition zone* – it has already been revealed, at the beginning of this section, the existence of a stepwise passing from the middle sequence towards the lower one – is going on up to the depth interval 34 – 36 cm; the **MS** signature records an intensity which is increasing up to 69.1$\times10^{-6}$ SI (Fig. 23a). Along this depth interval (30 – 36 cm), the sediment becomes a *peaty mud*, more cohesive, containing some coarse *silt* or fine *sand*, but also some enclaves of compact *clayey mud* within the end sample of this sequence. The **SIL** contents are also increasing, ranging between 56.29 % – 82.84 % (Fig. 23b), and the **TOM** contents are decreasing, from 41.67 % up to 16.56 % (Fig. 23c).

The *lowest sequence*, which starts at the 36 cm depth, up to the base, the *clayey mud* being the main sediment core constituent, shows a different regime – comparing with the higher sequences – with regard to the **MS** and the main **LITHO** parameters. The **k** values "jump" to the class **III**, along the depth interval 36 – 48 cm (core bottom), the **MS** measurements showing a range with very close limits, namely 89.45$\times10^{-6}$ SI – 99.20$\times10^{-6}$ SI (Fig. 23a). The *siliciclastic component* asserts the **MS** signature, the **SIL** contents being placed within a very narrow interval, and defined by high value ends: 84.64 % – 91.35 % (Fig. 23b). Certainly, the *total organic matter* component (**TOM**) consolidates this distinct regime, revealing very low contents, placed between 3.89 % – 9.28 % (Fig. 23c). In this case, the range of values is very narrow, too, but opposite – as intensity – to those of the **MS** and **SIL** signatures. The **TOM** component records a very low level of contents, a situation which is in agreement with the macroscopic description of the samples sliced from the lowest part of the core. The highest **k** values and **SIL** contents – referring to the entire sediment column recovered from the *core DD 13-104* – were determined along this depth interval (36 – 48 cm), within which the **TOM** component has revealed the lowest contents (Figs. 23a,b,c).

In this context, referring to the sediment composition towards the core base, we must add the *clayey muds* become more *silty*, coarser, a lithological constitution which explains the **MS**, **SIL**, and oppositely, the **TOM** signatures.

As concerns the evolution of *carbonates* within the whole core, their contents are ranging between 1.4 % – 6.88 % (Fig. 23d). The **CAR** signature remarks a slightly constant level of the contents, and at the same time higher (4.39 % – 5.79 %), for the samples collected from the *upper sequence*, followed by a minimum anomaly (1.4 % – 2.27 %), which is defined within the *transition zone* and the *lower sequence*. The lowest **CAR** contents were recorded for samples collected from the *transition sediment sequence*, the minimum axis being located around the middle of the core. The *lower sequence* is defined by higher **CAR** contents (2.27 % – 6.88 %), placed on the lower increasing branch of the **CAR** minimum anomaly (Fig. 23d). As we mentioned before, several *Cardiidae* and *Corbula* shells and shell fragments have been observed along this interval.

The results of the magneto-lithological analysis of the sediment *core DD 13-104*, above discussed, are synthesised by means of the pie-charts from Fig. 23e – for the **MS** data, and in Fig. 23f – for the **LITHO** data. The structure of the **MS** pie-chart clearly reflects the core lithological constitution: an *upper sequence* (0 –18 cm) – with all 9 slices defined by negative values only, calibrated to **k** class **I**; a transition *sediment sequence*, of similar thickness (18 – 36 cm) – calibrated to **k** class **I** (first two samples), and to **k** class **II** (the following 7 slices; 29 %); a *lower sequence*, less thick (36 – 48 cm) – calibrated to **k** class **III** (25 %). As regards the **k** class **I**, to which 11 sediment slices are assigned, this holds 46 % of the pie-chart structure (Fig. 23e). The **LITHO** pie-chart (Fig. 23f) supports, in a great measure, the predominance of the lower **k** classes (**I** + **II**), *i.e.* 75 %, the **TOM** +**CAR** contents totalling 54 %; the remaining 46 % are covered by the **SIL** contents.

The relationships between the **MS** enviromagnetic parameter and the main lithological components **SIL** and **TOM** are illustrated in Figs. 23g,h. For both cases, *i.e.*, **SIL** *vs*. **k**, and **TOM** *vs*. **k**, the **r** coefficient shows strong correlations, positive/direct (**r** = 0.98; Fig. 23g), and negative/reversed (**r** = – 0.98; Fig. 23h), respectively. These results represent the quantification of the **MS** and **LITHO** characterization of the sediment column which has just been presented above. Instead, the **r** coefficient calculated for **CAR** *vs*. **k** shows a weak negative correlation (**r** = – 0.17; Fig. 23i; Table 1), indicating a low level of the connection of *carbonates* with the enviromagnetic parameter **MS** (if it is taken into consideration the whole sediment column). The diagram from Fig. 23i could suggest a composite trend line, which might be possible because of the different sediment sequences within the core constitution. A test regarding the calculation of the **r** coefficient related to the relationship **CAR** *vs*. **k**, analysed for each of the 3 parts (Table 1) in which the core was divided, as it has been above discussed, shows a moderate positive correlation in the case of the "upper sequence" (0 – 18 cm; **r** = 0.32), a strong negative correlation relating to the "transition sediment packet" (18 – 36 cm; **r** = – 0.75), and a weak positive correlation for the "lower sequence" (36 – 48 cm; **r** = 0.28). It is interesting to point out, the **r** coefficient for **SIL** *vs*. **CAR** also indicates (Table 1) a strong negative correlation (**r** = – 0.74) for the "transition zone" (as in the **CAR** *vs*. **k** case), so that it could be considered the *carbonates* are not connected with the *detrital fraction*. On the other side, for **TOM** *vs*. **CAR**, relating to the same "sediment sequence" (a coarse *peat* passing then into a *peaty mud*), a strong positive correlation is shown by the **r** coefficient (**r** = 0.72; Table 1), an argument for the

Lake/ Core code	Sediment column	Depth level (cm)	Correlation coefficient (r)		
			CAR *vs.* k	SIL *vs.* CAR	TOM *vs.* CAR
Bogdaproste Lake/ DD 13-104	Entire core	0 – 48	0.10	0.004	– 0.089
	Upper sequence	0 – 18	0.32	0.79	– 0.84
	Transition sediment packet	18 – 36	– 0.75	– 0.74	0.72
	Lower/basal sequence	36 – 48	0.28	– 0.51	– 0.13

Table 1. Detail with the correlation of the carbonate component (**CAR**) with the enviromagnetic parameter (**MS**; **k**) and the other two main lithological components (**SIL**, **TOM**), related to the principal sequences identified within the sediment core DD 13-104, collected from the Bogdaproste Lake. *Legend*: The circles are coloured according to the scale used to evaluate the size of the correlation (**r**) (see Fig. 3b).

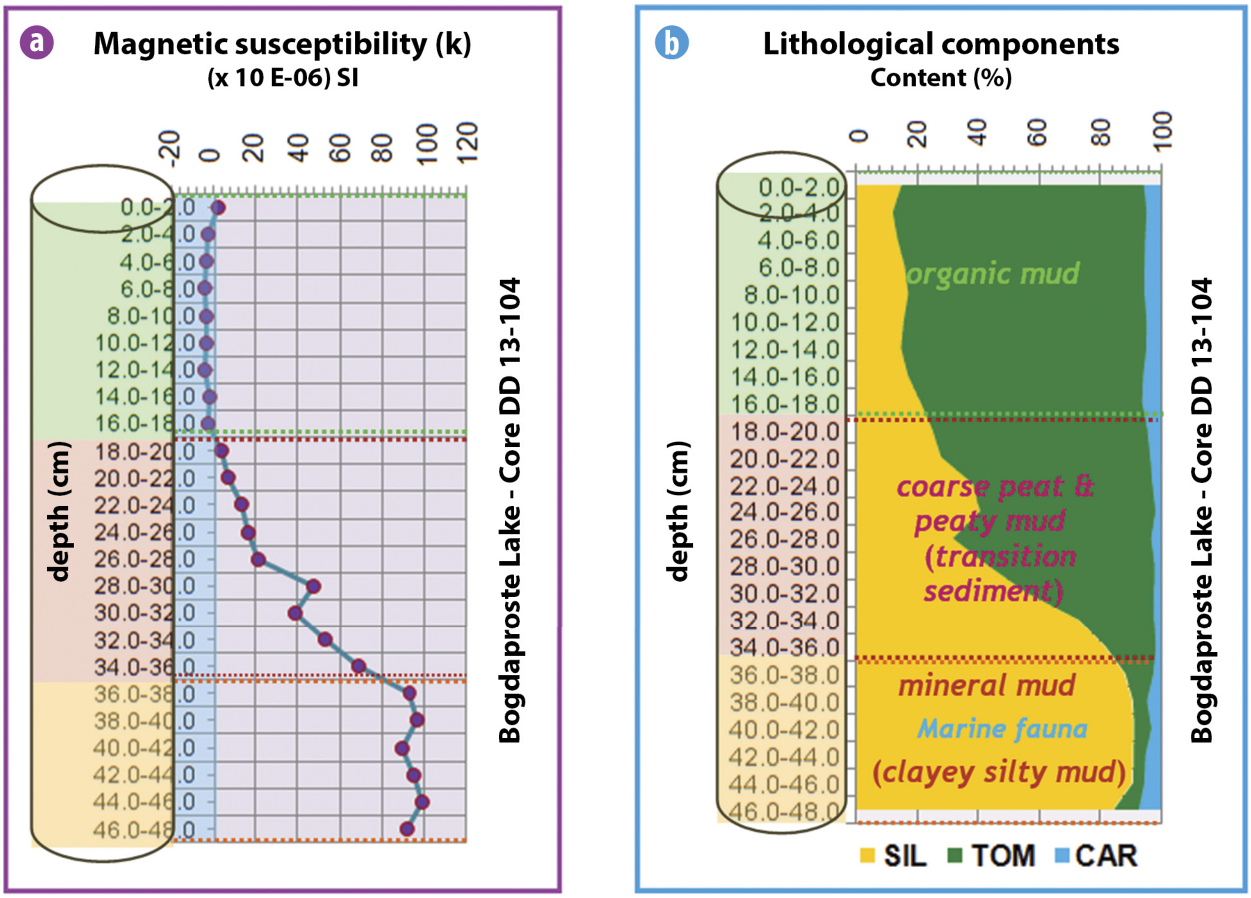

Fig. 24. Vertical distribution of the enviromagnetic parameter values (**k**) and of lithological components contents (**SIL**, **TOM**, **CAR**), along the sediment core DD 13-104, collected from the Bogdaproste Lake. **a)** Line-chart showing the magnetic susceptibility vertical profile; **b)** 100% stacked area-chart with the distribution of **SIL**, **TOM** and **CAR** contents along the sediment core.

direct connection of the *carbonates* with the *organic material*. Opposite data are obtained for the "upper sequence" of the core (Table 1), *i.e.*, a strong positive correlation for **SIL** *vs*. **CAR** (**r** = 0.79), and a strong negative correlation for **TOM** *vs*. **CAR** (**r** = – 0.84), results which could argue the detrital origin of the *carbonates* related to this sediment horizon. As regards the "lower sequence" (36 – 48 cm; a *clayey mud*, becoming more *silty* downwards the core bottom), a weak negative correlation is found for **TOM** *vs*. **CAR** (**r** = 0.13) (Table 1). As a moderate negative correlation defines **SIL** *vs*. **CAR** (**r** = – 0.51), it can be considered the *carbonates*, in the "lower sequence", generally, are bearing no relation to the *siliciclastic fraction* or to the *organic material*, the main lithological components.

The magnetic susceptibility (**MS**) vertical profile is illustrated in Fig. 24a, and next is given a composite image (Fig. 24b) for the vertical variation of the three lithological components – **SIL**, **TOM** and **CAR**. It can be easily remarked the similarity between the **MS** and **SIL** signatures, the **TOM** record representing a "negative/mirror counterpart" of the other two images. The core sediments are passing from the *organic vegetal muds* – at the upper part, towards the *mineral muds* – at the lower part.

The magneto-lithological parameters reflect these two opposite categories of *muds*, by distinct intensities:

- at the *upper part*: very low **k** values – an average of (– 3.02)×10^{-6} SI/**k** class **I**, confirmed by very low **SIL** contents – an average of 16.40 %, as a response to the very high **TOM** contents – an average of 78.65 %;
- at the *lower part*: higher **MS** values – an average of 94.34×10^{-6} SI/**k** class **III**, very high **SIL** contents – an average of 89.58 %, and, as a "negative/mirror counterpart", very low **TOM** contents – an average of 6.06 %.

It is also very interesting to observe that beginning with the depth level 38 cm, from where the sediment slice no. 20 was taken, therefore, within the "lower sequence", it has been identified a *marine fauna* (*e.g*., *Cardiidae*, *Corbula*), *in situ*, not-transported (*Corbula*, with both valves connected). This faunistic content of the *clayey muds* shows the existence of a *marine episode* at west of the *Letea – Caraorman initial spit*, in a zone, which, at present, is part of the *Fluvial Delta Plain*, suggesting an age corresponding to either an earlier period of the initial spit formation, or slightly afterwards, in an incipient phase, when the *Danube* bay blocking had not been settled into shape. Certainly, an absolute age analysis, supported by the fauna which was identified within this core, could help to clarify some aspects of the controversy relating to the age of the different events which led to the deltaic edifice building up.

3.2. Synopsis of magneto-susceptibility and lithological data provided by sediment core investigation

The nine cores analysed in the present paper were collected from an aquatic unit, which has been chosen – among others – as a representative monitoring area in the *Danube Delta*. So, in several expeditions carried out within the period under our attention (2010 – 2014), the bottom sediments of the *Matița – Merhei Depression* (M.– M. D.) lakes were investigated by different methods, in the field and in laboratory. The material needed for analyses has firstly been taken with "*Van Veen*" grab samplers; a number of cores were also extracted from a series of lakes.

3.2.1. A general magneto-lithological background, based on a short analysis of the MS and LITHO characteristics of the surficial sediments

As a magneto-lithological background, supported by several **MS** and **LITHO** maps and diagrams, general considerations on the surficial sediments from this deltaic area will be further presented.

Thus, in Fig. 25 and Fig. 26, the **MS** maps (a), as well as the **SIL** (b), **TOM** (c), and **CAR** (d) maps are illustrated for the bottom sediments sampled in the northern and southern halves of the *M.– M. D.*, respectively. Also, a synoptic image of the magnetic susceptibility calibration of these lake sediments is represented in Fig. 27, by using **MS** cubs which are coloured according to the **k** classes of the **MS** scale (Fig. 3a) and are located in the sampling stations from each lake/channel which were investigated during the last five years. A pie-chart, with the **k** classes to which the surficial sediments were calibrated, is associated to each lake investigated in the *M.– M. D.* (Fig. 27). As regards the lithological composition of the bottom sediments, a pie-chart with the content weights of the main **LITHO** components (*i.e*., **SIL**, **TOM** and **CAR**) is placed close to each **MS** pie-chart, and both of them are associated with each lake from this representative monitoring deltaic area (Fig. 27).

All these maps and diagrams show the most significant magneto-lithological characteristics of the *M.– M. D.* lacustrine sediments. It is easily to note their dominant feature, namely the calibration to the lowest **k** class (values under 10×10^{-6} SI, negative ones included), *i.e.* class **I** (Fig. 27), which, according to **MS** scale (Fig. 3a), is assigned to the "*fine sediments, rich in organic matter and/or carbonates*". The **MS** areal distribution provided by the **k** maps reflects the same particular remark, only at some of the entry mouths of the canals into the lakes being observed small **MS** anomalies (Fig. 25a and Fig. 26a). Therewith, in Fig. 27, these zones are marked out by the presence of some green cubs (**k** class **II**), or yellow cubs (**k** class **III**); the **k** class **II** is associated with the same sediment-type as the **k** class **I**, but with a slightly higher magnetic susceptibility (values ranging between 10×10^{-6} – 75×10^{-6} SI), while the class **III** (values which range between 75×10^{-6} – 175×10^{-6} SI) is assigned to "*clayey, fine up to silty sediments*" (Fig. 3a).

Related to the main 5 lakes of the *M.– M. D.*, *i.e*., *Merhei*, *Babina*, *Matița*, *Trei Ozere* and *Bogdaproste lakes*, the **k** class **I** percentages are ranging from 68 % – for *Babina Lake* surficial sediments up to 84 % – *Bogdaproste L*., 88% – *Matița L*., 95% – *Trei Ozere L*., and 96% – *Merhei L*. (Fig. 27).

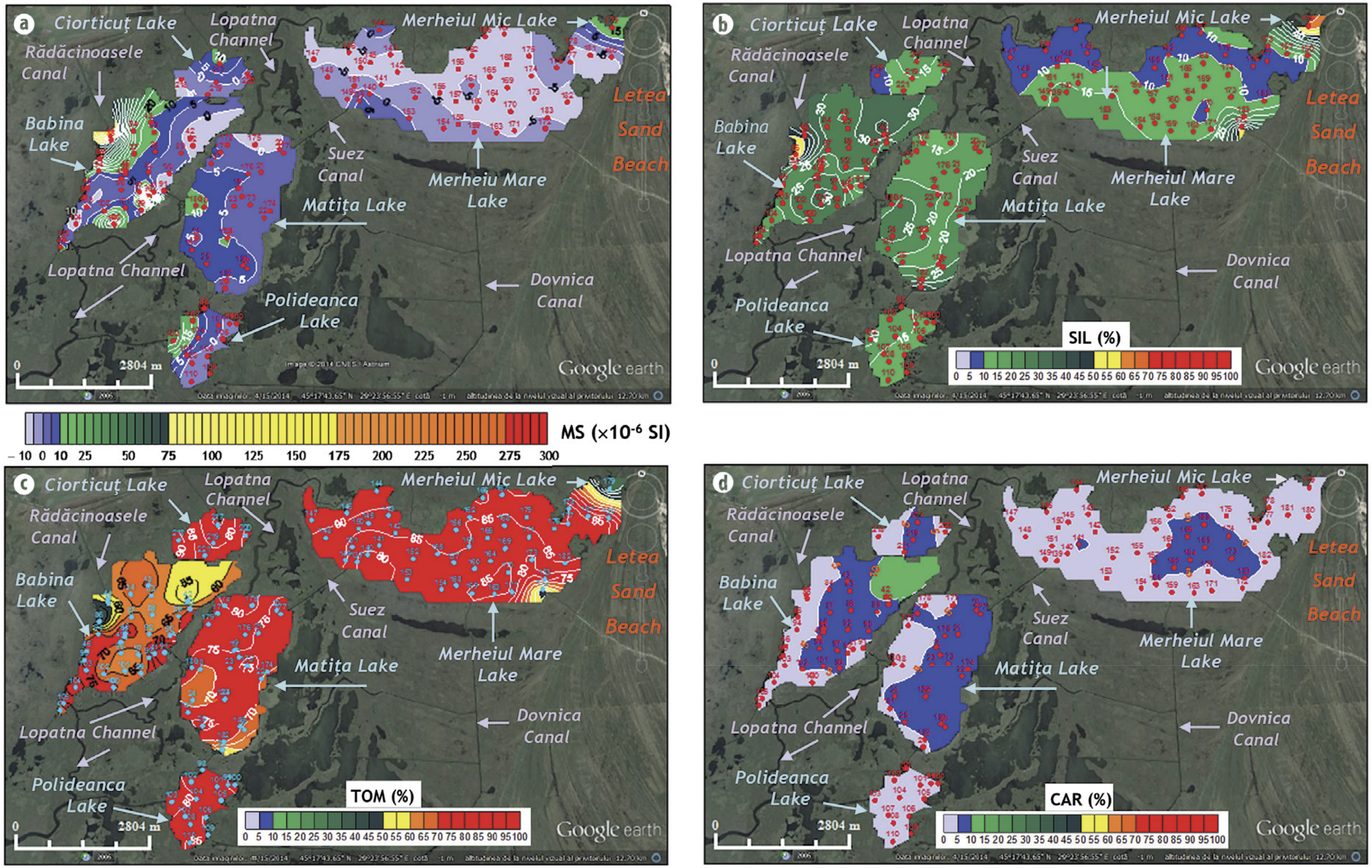

Fig. 25. Areal distribution of the enviromagnetic parameter (**MS**) values (**k**) and of the lithological component (**SIL**, **TOM**, **CAR**) contents, determined for the surficial sediments collected with a grab-sampler in the lakes from the northern half of Matiţa – Merhei Depression, over the period 2010 – 2014. **a)** Magnetic susceptibility (**MS**) maps. *Note*: The **k** (**MS**) contour lines are expressed in 10^{-6} SI and the coloured shading is according to the five classes of **MS** scale (see Fig. 3a); **b)** Siliciclastic/minerogenic/detrital component (**SIL**) maps; **c)** Total organic matter component (**TOM**) maps; **d)** Carbonate component (**CAR**) maps. *Note*: The **SIL**, **TOM** and **CAR** contour lines are expressed in percents (%).

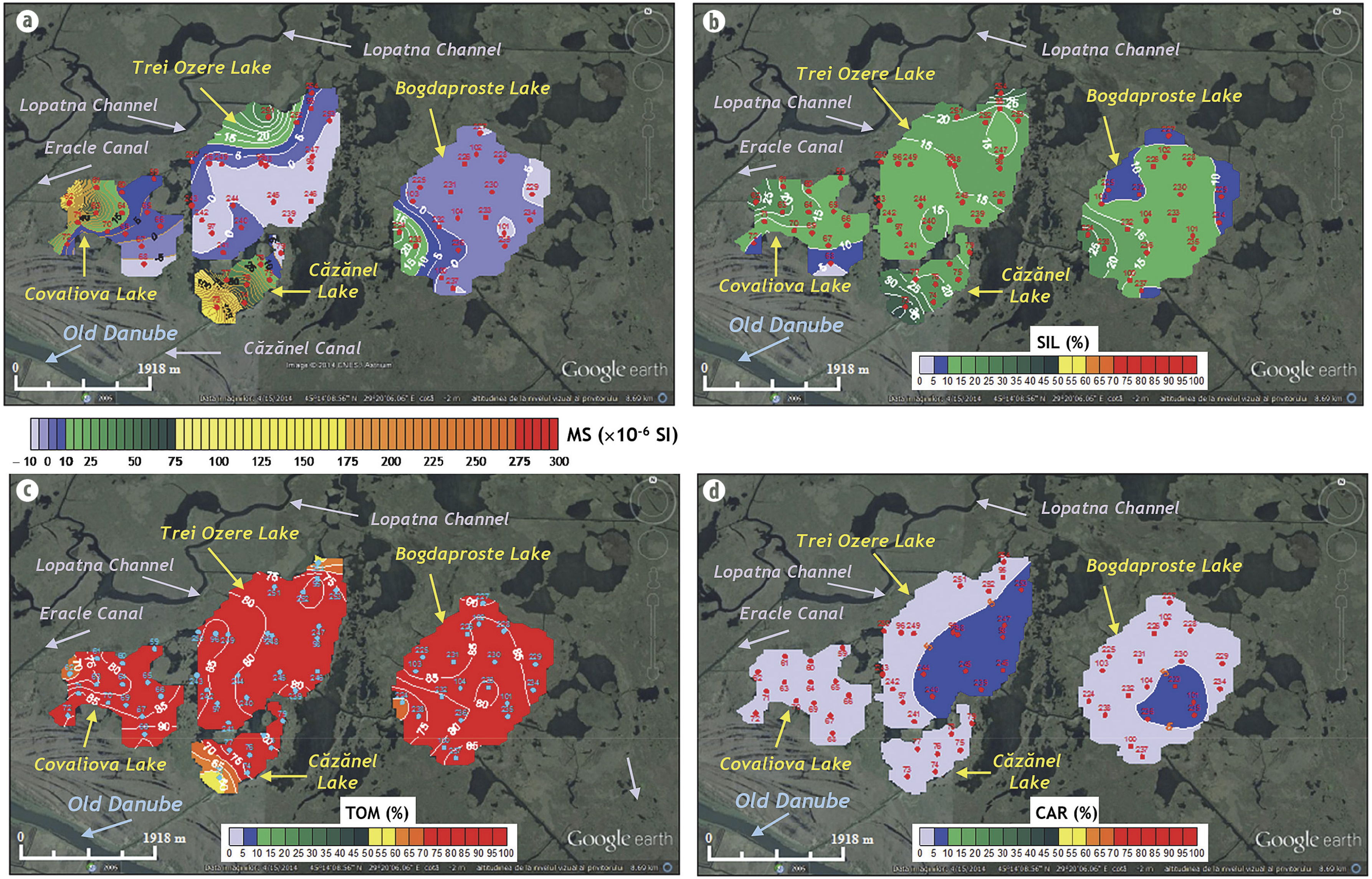

Fig. 26. Areal distribution of the enviromagnetic parameter (**MS**) values (**k**) and of the lithological component (**SIL**, **TOM**, **CAR**) contents, determined for the surficial sediments collected with a grab-sampler in the lakes from southern half of Matița – Merhei Depression, over the period 2010 – 2014. **a)** Magnetic susceptibility (**MS**) maps. *Note*: The **k** (**MS**) contour lines are expressed in 10^{-6} SI and the coloured shading is according to the five classes of **MS** scale (see Fig. 3a); **b)** Siliciclastic/minerogenic/detrital component (**SIL**) maps; **c)** Total organic matter component (**TOM**) maps; **d)** Carbonate component (**CAR**) maps. *Note*: The **SIL**, **TOM** and **CAR** contour lines are expressed in percents (%).

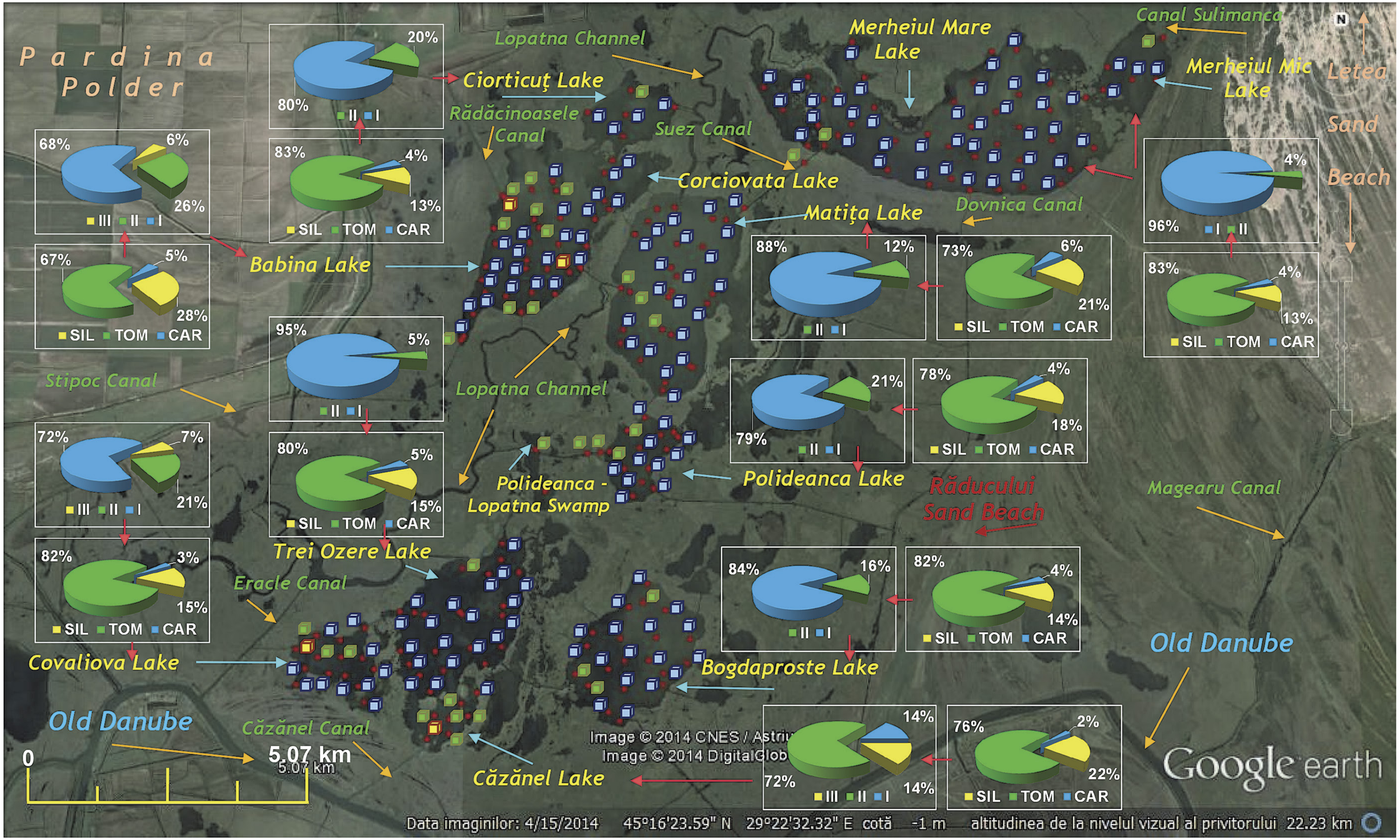

Fig. 27. Synoptic image with the 3D pie-charts showing the **MS** calibration (by using the **k** scale classes) and the lithological composition (based on the contents of **SIL**, **TOM** and **CAR** components) of the surficial sediments sampled in the lakes, some swamps and canals from the Matiţa – Merhei Depression, over the period 2010 – 2014.

Correspondingly, the total organic matter (**TOM**) contents record very high percentages, ranging from 67 % – in the *Babina L.* up to 83 % – in the *Merhei L.* (Fig. 27). The **MS**, **SIL**, **TOM** and **CAR** maps (Fig. 25, Fig. 26) confirm these remarks. Therefore, these maps point out – by the areal distribution of the magnetic (a) and lithological (b,c,d) parameters, respectively – low **k** value contours (Fig. 25a, Fig. 26a), connected to the lowest **MS** scale part (*i.e.*, associated with the *blue* colour; Fig. 3a), and, respectively, high **TOM** content contours (connected with the upper **LITHO** scale part, *i.e.* associated with the *red* colour) (Fig. 25c, Fig. 26c). Complementary, the characteristics of the **TOM** maps are presented "*in mirror counterpart*" by the **SIL** maps (Fig. 25b, Fig. 26b), which suggest comparative features with the **MS** maps.

All these data reflect the affluence of the organic matter of autochthonous origin within the surficial sediments of the main *M.– M. D.* lakes, which is mainly generated by the decay of phytoplankton, zooplankton and macrophyte vegetation, as a consequence of the protection conditions characterizing these lakes in relation to the direct fluvial supplies. In the *Merhei L.*, where the lowest **k** values (most of them, negative; Fig. 25a), the highest **TOM** contents (Fig. 25c), and, complementary, the lowest **SIL** contents (Fig. 25b, Fig. 27) were determined, the great majority of the sediments are placed inside of the *organic muds* category. A small **k** and **SIL** maximum anomaly, and a **TOM** minimum one, respectively, can be observed in the northeastern part of the *Merheiul Mic Lake,* at the entry mouth zone of the *Sulimanca Canal* (Figs. 25a,b,c), where *mineral-organic muds* were sampled; this canal is flowing close along the *Letea Sand Beach ridges*, from where some siliciclastic (sandy and silty) material could be washed-out. Small anomalies are also illustrated by the **MS**, **SIL** and **TOM** maps in the other four *M.– M. D.* main lakes (Figs. 25a,b,c, Figs. 26a,b,c), located at the entry mouths of some canals, as well. Yet, slightly more extended anomaly zones are illustrated by the **MS** maps carried out for the *Babina L.* (at the entry mouth area of the *Rădăcinoasele Canal*; Fig. 25a), *Trei Ozere* (at the mouth of a short canal coming from the *Lopatna Channel*, and extended, possibly due to some emerged zones, in the northern lake area; Fig. 26a), and *Bogdaproste L.* (in southwest, at the mouth of the connection canal with the *Trei Ozere L.*; Fig. 26a).

As regards the *carbonates*, they do not have an important contribution to the lithological composition of the surficial sediments; excepting the **CAR** content (higher than 10 %) provided by a sample taken from the northeastern *Babina Lake*, the *carbonates* present within the sediments from the 5 main lakes record lower contents, all the maps showing **CAR** content contours not higher than 5 % (Fig. 25d, Fig. 26d). They generally have a biochemical origin, with a few exceptions, probably explained by a local contribution of a finely triturated – by fragmentation and leaching – shelly material.

Passing now to the other (smaller) lakes of the *Mațița – Merhei Depression*, *i.e. Polideanca*, *Covaliova* and *Căzănel*, which actually have recently been investigated (during the 2014 spring expedition), we mention a general characteristic, namely the bottom sediments are calibrated to the same three **k** classes, **I**, **II** and **III**, but with some differences related to the size of their percentages (Fig. 27).

The lower **k** classes **I** and **II** define, particularly, the bottom sediments of *Polideanca* and *Covaliova lakes*; the predominance of the lowest **k** class **I** is clearly observed (79 %, and 72 %, respectively), 21 % belonging to **k** class **II** in both lakes. This **MS** calibration (Fig. 27), as well as the **TOM** and **SIL** average contents, defined by 78 % and 18 %, respectively, in the *Polideanca L.* case (Fig. 27), and by 82 % and 15 %, respectively, in the *Covaliova L.* case (Fig. 27), indicate the prevalence of the *organic matter* within the bottom sediments, as it has previously been revealed with regard to the 5 main lakes of the deltaic area under attention. The sediments are mainly placed within the category of *organic* and *organic-mineral muds*, the *mineral-organic* ones being subordinated to them.

Yet, a **MS** anomaly is observed at the mouth of the canal which makes the connection of the *Polideanca L.* with the *Lopatna Channel* (Fig. 25a), where sediments with a higher *minerogenic* material content are transported from this canal, which was dredged some time ago. In the **SIL** and **TOM** maps, this zone is also evident, but the anomalies, of maximum (Fig. 25b) and minimum (Fig. 25c), respectively, are less strongly marked out by content contour lines. Besides, it is worth to remark the presence of a *marine fauna* (*e.g.*, *Cardiidae*, *Corbula*) within the sediments sampled in the lake western extremity (at the *Lopatna – Polideanca Canal* mouth), probably reworked from the underlying horizon, as a consequence of digging works necessary to the canal deepening. Moreover, we remember the *core DD 14-112* (see Ch. 3.1.3.b), extracted from the above mentioned canal, just before entering into the *Polideanca L.* (Fig. 2), and the *marine clay horizon* intercepted within the 31 – 44 cm depth interval. The magneto-lithological characteristics of this sediment sequence were presented and analysed in the cited chapter.

In addition, in the *Covaliova Lake*, in its western extremity, just at the mouth of the canal which makes the connection with the *Oracle Can*. (Fig. 26a), the **MS** map remarks a **k** anomaly, mainly generated by the sample of coarse mud with some fine sand traces (station *DD 14-62*), which provides the highest magnetic susceptibility (*i.e.*, 139.45×10^{-6} SI, correlated with the **MS** *class* **III**). This is supported by some **k** values associated with the *class* **II,** recorded in the neighbouring stations, so that a **MS** positive anomaly is clearly evidenced in the lake western area (Fig. 26a). Correspondingly, there can be observed a (maximum) **SIL** anomaly around the same sampling station (Fig. 26b), where the highest minerogenic material content (*i.e.*, 33.24 %) – related to the sediments of this lake – was determined, and, respectively, a (minimum) **TOM** anomaly (Fig. 26c), mainly defined by the lowest organic substance content (*i.e.*, 64.14 %) recorded in the above nominated station (*DD 14-62*).

Fig. 28. Synoptic image with the magnetic susceptibility (**MS**) records obtained for five sediment cores collected from the Babina and Matiţa lakes, in 2010 and 2011. *Legend*. The red points located on the map within the lakes and along some canals indicate the grab sampling stations (over the period 2010 – 2014). The coloured cylinders mark the collecting sites for the sediment cores.

As regards the third small lake, *i.e*. *Căzănel*, investigated in the southern extremity of the *Matița – Merhei Depression*, situated closely south of *Trei Ozere Lake* (Fig. 2, Fig. 26), the surficial sediments are a bit more various, due to the *Căzănel Canal* intervention in the southern area.

Consequently, the areal distribution of the *enviromagnetic parameter* (**MS**) measured on the collected samples (Fig. 26a) reveals the influence of the mentioned canal, which makes the connection with the *Old Danube Branch*, and contributes with an important *siliciclastic fraction* (**SIL**) to the lithological composition of the lake sediments. This minerogenic contribution is gradually diminished from the canal entry mouth towards the northern lake extremity, the **SIL** contents decreasing along this direction, from 41.04 %, in station *DD 14-73*, to 13.02 %, in station *DD 14-79* (Fig. 26b). This trend is even better reflected by the **MS** contour lines (Fig. 26a), the **k** map showing the decreasing gradient from the **k** class **III** (a value of 164.04×10^{-6} SI, in the station *DD 14-73*), to which the *coarse silty* (possibly a bit *sandy*) *muds*, from the canal mouth, are calibrated, passing then through the class **II** (**k** values of maximum 57.03×10^{-6} SI, measured on the muds from the central lake zone), and reaching the class **I**, in the station *DD 14-79*, in the northern lake extremity, where for the sampled fluffy, non-cohesive muds a **k** value of 2.47×10^{-6} SI, only, was recorded. This variation of the lithological characteristics of the bottom sediments, from the entry mouth canal (placed in south) up to the *Căzănel Lake* northern extremity, is also well reflected by the **TOM** contour lines of the *organic matter* content map (Fig. 26c). Therefore, the **TOM** contents are gradually increasing from 55.97 % (in south) up to 83.72 % (in north), *i.e*. from the **TOM** contour line of 60 % up to the **TOM** contour line of 80 % (Fig. 26c).

The distribution of the magnetic susceptibility classes to which the bottom sediments of the *Căzănel Lake* are calibrated, *i.e.* the significant majority is defined by the **k** classes **I** and **II** (14% + 72%), which are specific to the organic sediments, is well reflected by the lithological model, which shows the highest weight (76 %) for the **TOM** component, to which an average content of 2 % is added by the *carbonate* component (**CAR**) (Fig. 27). The remaining 22 % are allocated to the *detrital/siliciclastic fraction* (**SIL**), a level comparable with the percentage determined for the **k** class **III** (14 %) (Fig. 27), a situation in agreement with the magneto-lithological scale (Fig. 3a). Actually, the **r** coefficients calculated for **SIL** *vs*. **k**, and **TOM** *vs*. **k**, related to the *surficial sediments* sampled in the *Căzănel L*., show (very) strong correlations (see the scale in Fig. 3b), positive, and negative, respectively: **r** = 0.99, **r** = – 0.98. This asserts, again, the quality of *proxy parameter* of the magnetic susceptibility for the lithological characterization of the lake sediments.

As concerns the other **LITHO** component – the *carbonates* –, the **CAR** contents are lower than 5 % for the sediments investigated in all these three small lakes (Fig. 25d, Fig. 26d), namely *Polideanca* (4 %), *Covaliova* (3 %) and *Căzănel* (4 %) (Fig. 27).

3.2.2. Synoptic images of the MS and LITHO signatures recovered from sediment cores in the Matița – Merhei Depression

A magneto-lithological data base is now constituted by integrating the **MS** and **LITHO** signatures recovered from nine cores collected from the lacustrine sediments of five lakes from the *Matița – Mehei Depression* (Fig. 1, Fig. 2). To illustrate together the recorded vertical *magnetic susceptibility* profiles, we formally divided the *M.– M. D.* area into the northern and southern halves. Therefore, relating to the first, the three cores from the *Babina Lake* (*i.e*., *DD 10-106*, *DD 10-18*, *DD 11-49*) and the two cores from the *Matița Lake* (*i.e*., *DD 10-01*, *DD 11-01*) have provided the **MS** records from Fig. 28. As regards the second zone, the southern half, in Fig. 30 are redrawn the **MS** records for the three cores collected along a West – East profile, starting from the *Lopatna – Polideanca Swamp* (*DD 14-113*), continuing the canal course which connects the *Lopatna Channel* with the *Polideanca L.* (*core DD 14-112*), and finally entering into the central area of this lake (*core DD 14-104*). Besides, in this synoptic image, is illustrated the **MS** profile carried out for the *core DD 13-104*, collected from the *Bogdaproste Lake* central zone. Following the same *scenario*, the associated *lithological signatures*, expressed by composite images which integrate the three main **LITHO** components (**SIL**, **TOM**, **CAR**), are also illustrated for the sediment cores taken from the *M.– M. D.* northern and southern halves, in Fig. 29 and Fig. 31, respectively.

Details, supported by various diagrams and extended analyses and comments, were presented in the subchapters 3.1.1 ÷ 3.1.4. Some general observations, based on these synoptic images, are feasible. They can be applied in the future – together with new data – to approach various stratigraphic, sedimentogenetic, mineralogical and ecological studies within the *Danube Delta*. As concerns the use of the downcore **MS** records in lacustrine stratigraphy, we mention, *e.g*., Trodahl (2010), who emphasizes the necessity of additional information – provided by grain size and charcoal analyses, as well as radiocarbon dating – to get clarification with regard to the ambiguity associated with matching magnetic susceptibility peaks identified in the **MS** profiles along two sediment cores extracted from the *Lake Wairarapa* (New Zealand).

The connections between the magnetic susceptibility *proxy* parameter and the lithological composition of the lake sediments from the *Danube Delta* have proved to be of great interest. In Table 2, the **r** coefficients calculated for four cores are synthesized (the five cores in which *marine deposits* were detected are not included in the Table 2), assessing all the possible correlations related to the four (magnetic and lithological) parameters (**MS**, **SIL**, **TOM** and **CAR**). Firstly, we remark 3 pairs of parameters for which the **r** coefficient shows strong correlations in all these cases: **SIL** *vs*. **k** (positive;

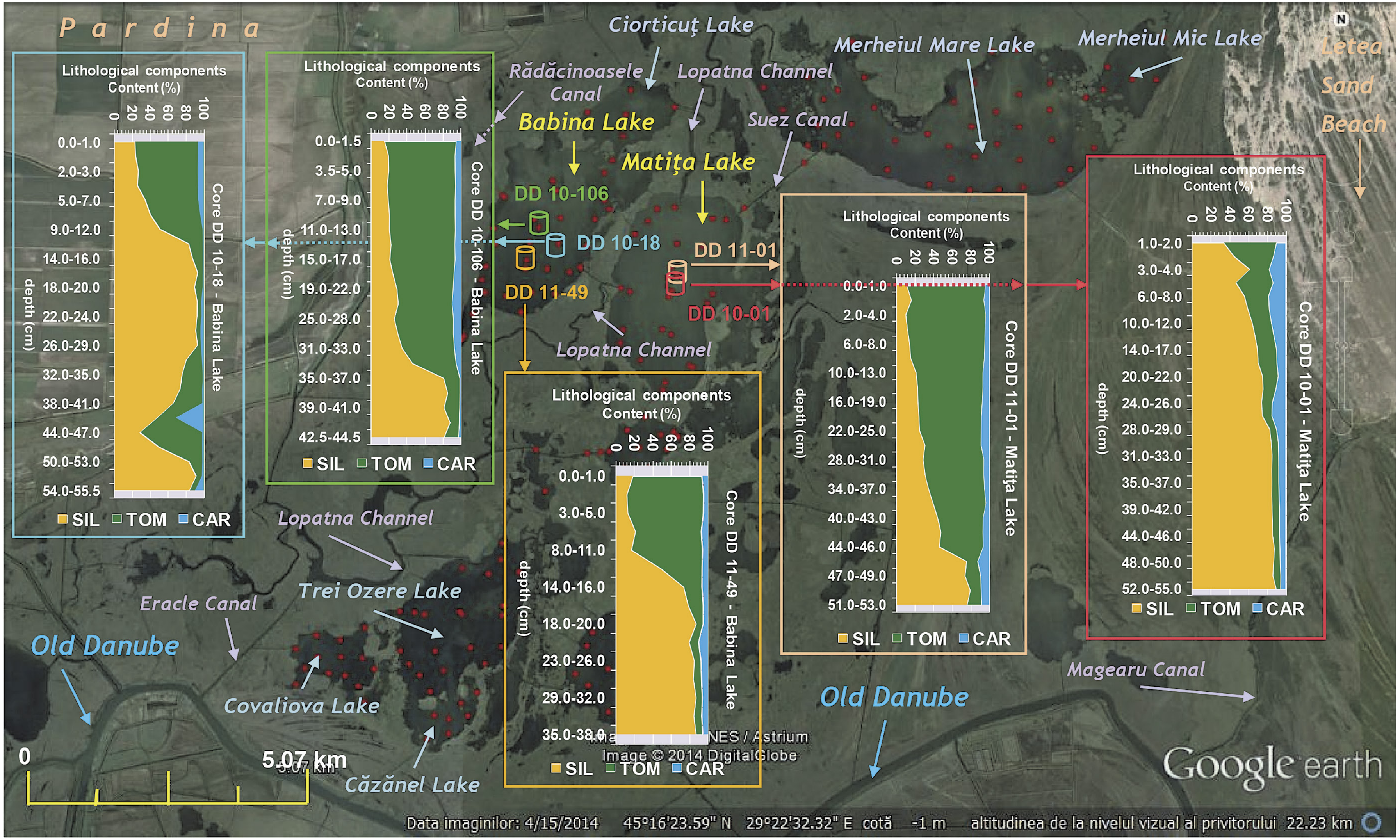

Fig. 29. Synoptic image with the composite lithological (**SIL**, **TOM**, **CAR**) records obtained for five sediment cores collected from the Babina and Matiţa lakes, in 2010 and 2011. *Legend*. The red points located on the map within the lakes and along some canals indicate the grab sampling stations (over the period 2010 – 2014). The coloured cylinders mark the collecting sites for the sediment cores.

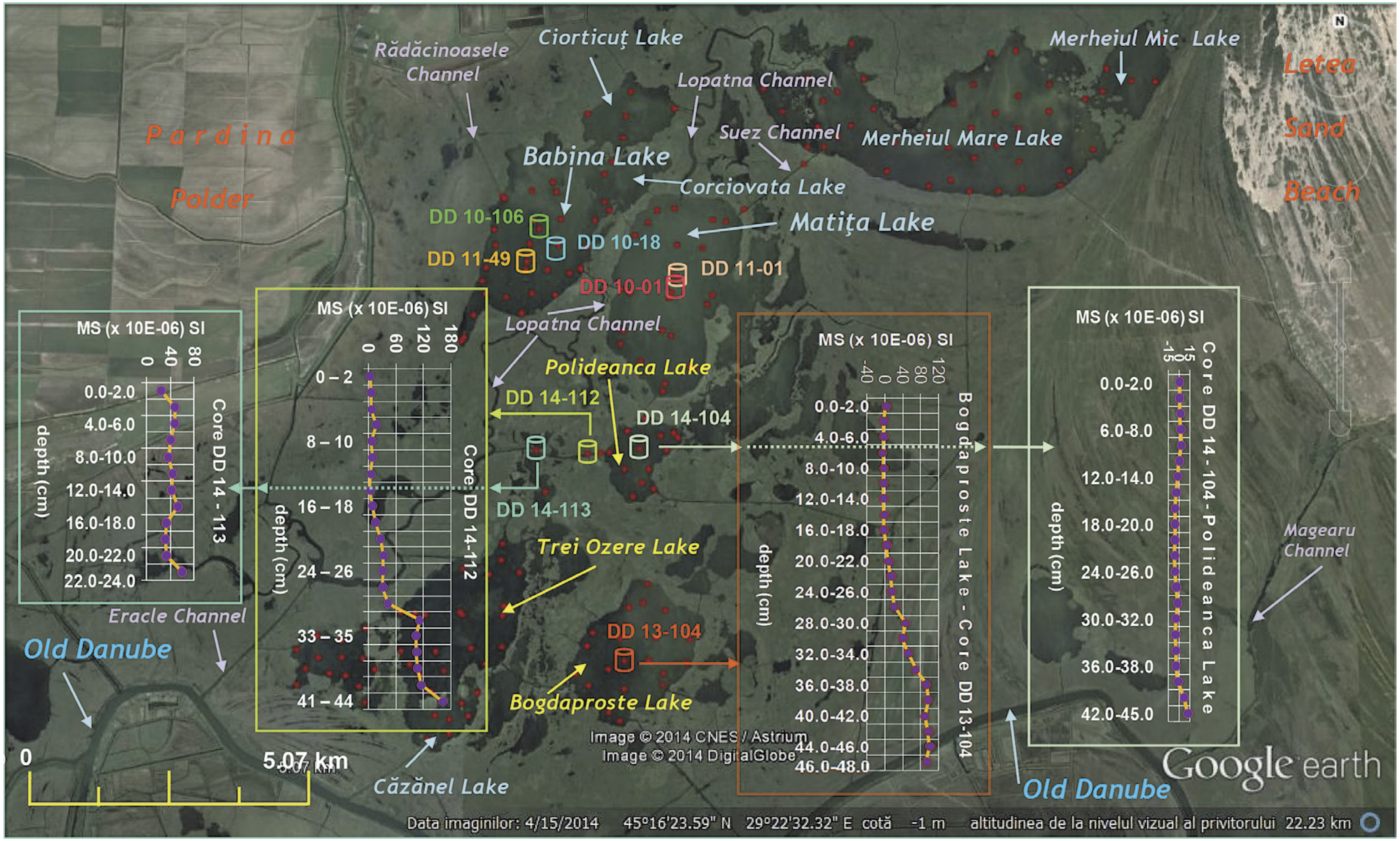

Fig. 30. Synoptic image with the magnetic susceptibility (**MS**) records obtained for four sediment cores collected from the Polideanca and Bogdaproste lakes, the Polideanca - Lopatna swamp, and the Lopatna - Polideanca canal, in 2013 and 2014. *Legend*. The red points located on the map within the lakes and along some canals indicate the grab sampling stations (over the period 2010 – 2014). The coloured cylinders mark the collecting sites for the sediment cores.

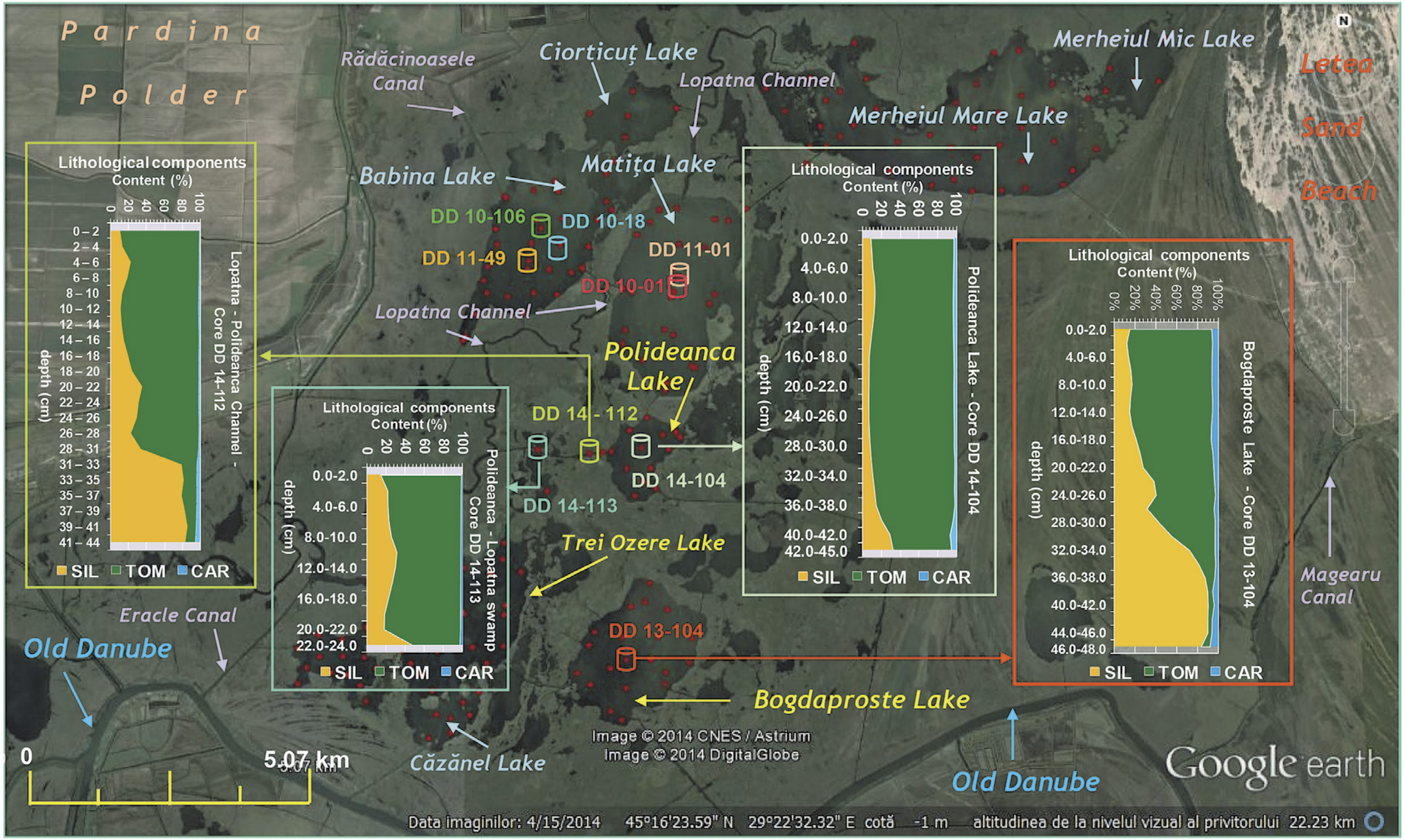

Fig. 31. Synoptic image with the composite lithological (**SIL**, **TOM**, **CAR**) records obtained for four sediment cores collected from the Polideanca and Bogdaproste lakes, the Polideanca - Lopatna swamp, and the Lopatna - Polideanca canal, in 2013 and 2014. *Legend*. The red points located on the map within the lakes and along some canals indicate the grab sampling stations (over the period 2010 – 2014). The coloured cylinders mark the collecting sites for the sediment cores.

Table 2. Synoptic table with the correlation coefficients (**r**) calculated for all possible pairs of parameters [magnetic susceptibility (**MS**; **k**) and three main lithological components (**SIL**, **TOM**, **CAR**)], related to four sediment cores, collected from the Matița – Merhei Depression, over the period 2010 – 2014. *Note*: The five cores in which *marine deposits* were detected are not included in the table (see text). *Legend*: The circles are coloured according to the scale used to evaluate the size of the correlation (**r**) (see Fig. 3b).

Lake/ Swamp	Core code	Correlation coefficient (r)					
		SIL *vs.* k	TOM *vs.* k	CAR *vs.* k	SIL *vs.* TOM	SIL *vs.* CAR	TOM *vs.* CAR
Babina Lake	*DD 10-18*	0.93	– 0.86	– 0.47	– 0.97	– 0.32	0.095
Lopatna – Polideanca Swamp	*DD 14-113*	0.78	– 0.78	0.51	– 0.999	0.76	– 0.78
Polideanca Lake	*DD 14-104*	0.83	– 0.84	0.80	– 0.996	0.81	– 0.86
Bogdaproste Lake	*DD 13-104*	0.98	– 0.98	0.10	– 0.996	0.004	– 0.089

0.78 < **r** < 0.98), **TOM** *vs.* **k** (negative; – 0.78 < **r** < – 0.98), and **SIL** *vs.* **TOM** (negative; – 0.97 < **r** < – 0.999). The *proxy* quality of the *magnetic susceptibility* related to the main lithological components of sediments is thence quantified. As regards the relationships in which the **CAR** component is involved, taking into consideration the possible generating alternatives for *carbonates* within the sediments, the **r** coefficient is correspondingly showing various correlation types (*positive* or *negative*) and *intensities* ("weak", "moderate" and "strong", according to the scale from Fig. 3b). Referring to the relationship **SIL** *vs.* **CAR**, it is worth to note the total parallelism of its correlation type (*positive* or *negative*), and the general similarity or so of the range sizes with that of the **CAR** *vs.* **k**, even in the case of the weak correlation which was determined for the sediments sampled from the *core DD 13-104* (Table 2). This example could be a very good argument towards consolidating the quality of *proxy* parameter of the *magnetic susceptibility* with regard to the lithological composition evaluation of lake sediments. Following a similar approach in the **TOM** *vs.* **CAR** case, and comparing the **r** coefficients with those calculated for **CAR** *vs.* **k** (Table 2), we remark, this time, a perfect antagonism between them, in what it concerns the correlation type, *i.e.*, *positive* or *negative*. Again, there are examples, in which even if the **r** coefficient, in this case, for **TOM** *vs.* **CAR**, is very low [≈ 0.1, for the *core DD 10-18*, and respectively (≈ – 0.1), for the *core DD 13-104*; Table 2], the correlation type which is suggested by each of them looks opposite to that defined for **CAR** *vs.* **k**, correspondingly, in each of the two specified cores (**r** = – 0.47, and **r** = 0.10, respectively; Table 2). Of course, this observation could be added to that above mentioned, concerning the quality of *proxy* lithological indicator of the *enviromagnetic parameter* **MS** (in use, in our studies on the recent sediments from the *Danube Delta* and *Razelm/Razim–Sinoie Lagoon Complex*, since 1977).

Anyway, these problems must be analysed in detail, an example being given in the previous subchapter (Ch. 3.1.4), just concerning the *core DD 13-104* (*Bogdaproste Lake*), which was in our attention above, and in which case the sediment column begins with *organic muds*, continues downwards with a sequence of *coarse peat* and *peaty muds*, to finish at its base within a horizon of *mineral muds* (*clayey-silty muds*) with a *marine fauna*. The data commented in the mentioned chapter remark the possible complex character of such an integrated approach, and the necessity to investigate the lithological, faunistic and enviromagnetic particularities of each of the distinct sediment sequences crossed even by the short cores.

4. CONCLUSIONS

In the context of the study of *Danube Delta* geosystem spatial evolution, the present paper continues the work dedicated to the data base achievement, involving magneto-lithological models carried out for sediment cores collected from lakes, swamps and canals in various sedimentary environments. Consequently, the results analysed in the previous chapters for the cores taken out from 4 lakes, a swamp and a canal in the *Matița – Merhei Depression* are to add up the data which were published for the cores collected from 4 lakes and a channel of the *Meşteru – Fortuna Depression* (Rădan *et al*., 2013), also situated in the *Fluvial Delta Plain*, in the Danube Delta northern wing (but in its western area). This succession of the studied deltaic areas, from north southwards and from west eastwards, brings very interesting data; the *Meşteru – Fortuna Depression* lakes are directly influenced by the *Danube* supplies (particularly, through the *Mila 36* and *Crânjală canals*), while the *Matița – Merhei Depression* lakes are located far from the main *Danube Delta distributaries*, and are protected from the direct fluvial influx, and, therefore, they are not significantly affected by the riverine inputs. Yet, a parallel analysis of the magneto-lithological models associated with the cores collected from these two depressions with distinctly different characteristics will be performed when the study will be finished, that is the results achieved for the cores extracted in the other two main *Delta depressions* (*Gorgova – Uzlina* and *Lumina – Roşu*) will be published, as well.

In these circumstances, the principal aspects resulting from the investigation of the short cores collected from the *Matița – Mehei Depression* sedimentary environments are further synthesized.

The lithological data reflect the important supply of organic matter of autochthonous origin within the surficial sediments of the principal *Matița – Merhei Depression* lakes, mainly generated by phytoplankton, zooplankton and macrophyte vegetation decay as a consequence of the confined conditions characterizing this deltaic area in relation to the direct fluvial influxes. *Magnetic susceptibility* (**MS**) maps, as well as *siliciclastic/minerogenic* (**SIL**), *total organic matter* (**TOM**), and *carbonate* (**CAR**) *component* maps were carried out for the surficial sediments, in order to describe the magneto-lithological background which characterizes each of the investigated lakes. The dominant feature was the calibration of the bottom sediments to the lowest **k** class (**I**, *i.e.*, values under 10×10^{-6} SI, negative ones included), and **II** (**k** values ranging between $10\times10^{-6} \div 75\times10^{-6}$ SI), to which the "*fine sediments, rich in organic matter and/or carbonates*", are usually included. Only at some of the entry mouths of the canals into the lakes were observed small **MS** anomalies (some of them reaching the **k** class **III**, *i.e.*, **MS** values within $75\times10^{-6} \div 175\times10^{-6}$ SI interval), assigned to "*clayey, fine up to silty sediments*". The **SIL** and **TOM** maps offer a coincident support to the **MS** areal distribution analysed in the lakes**.** The first lithological component follows the same variation type/intensity (defined by the **SIL** content contour lines, *i.e.*, gradient, maximum/minimum anomalies) with the **MS** magnetic parameter, while the second **LITHO** component (**TOM**) follows, precisely, the **SIL** (and **MS**) areal variation pattern, but as seen "*in mirror*", as regards the anomaly/gradient "trend sign". These clearly opposite "images" which concern **SIL** *vs*. **MS** related to **TOM** *vs*. **MS** (and **SIL** *vs*. **TOM**) are confirmed by the magneto-lithological models carried out for all the sediment cores investigated; the relationships are quantified by the **r** coefficients which were calculated for all possible correlations between the four investigated parameters (the third analysed lithological parameter is added, *i.e.*, the *carbonates*/**CAR**). The surficial sediments showed low **CAR** contents (lower than 10 %, with an exception only, given by a sample from the *Babina L.*), the 5 % content contour lines being the highest ones within the **CAR** maps.

The sedimentation environments from the *Matița – Merhei Depression* are well characterized by specific magnetic susceptibility (**MS**) fingerprints, recovered from the sediments of the investigated lakes. The cores, even their lengths did not exceed 55.5 cm (*Core DD 10-18*, *Babina Lake*), the shortest being of 24 cm (*Core DD 14-113*, *Lopatna – Polideanca Swamp*), have offered interesting specific **MS**, **SIL**, **TOM** and **CAR** signatures, associated with the crossed sediment sequences. The vertical distribution of the **k** values reflects, accurately, the lithological variations, in some cases being revealed details which sometimes are macroscopically less visible.

The *proxy* quality of *lithological index* assigned to the *magnetic susceptibility*, which was discussed in the paper devoted to the *Meşteru – Fortuna Depression* (Rădan *et al*., 2013), is again demonstrated, this time by the **MS** – **LITHO** models carried out for the cores collected in the *Matița– Merhei Depression*. The **r** correlation coefficients, calculated for all 6 possible combinations related to the **MS**, **SIL**, **TOM**, and **CAR** parameters, quantitatively argue the availability shown by the **MS** enviromagnetic quantity as a *proxy* lithological indicator. Not lastly, they attest the reliability of the "Magneto-Susceptibilimetric technique" and "Loss on Ignition method", which were applied in the specialized laboratories from *GIR* and *GeoEcoMar*, respectively. In some cases, the deviation from the correlation lines (shown, especially, by the scatter-plots **SIL** *vs*. **MS** and **TOM** *vs*. **MS**) imposed the reanalysis of certain samples, and higher **r** coefficients resulted, being confirmed the benefit of this methodology. An improvement of the correlations related to the lithological components (**SIL** *vs.* **TOM**, **SIL** *vs*. **CAR,** and **TOM** *vs*. **CAR**) has been recorded, as well.

This integrated magneto-lithological study, carried out on sediment cores taken during the last five years from the *Matița – Merhei Depression*, has also resulted in the detection of some *marine deposits* located very close to the water/sediment interface. Particularly, two cores from the *Babina Lake*, two from *Matița Lake*, and another one from the *Lopatna – Polideanca Canal* crossed *marine clays*. The intensity of the **MS** fingerprint associated with the *marine clays* is clearly higher than that of the *muds* which occur in the upper part of these cores. So, if the *muds* are correlated with the **k** class **I,** possibly with the class **II** (*i.e*., **MS** values not higher than 75×10^{-6} SI)**,** the *marine deposits* are calibrated to **k** class **III**, and sometimes to class **IV** (*e.g*., the case of the *core DD 11-01*, collected from the *Matița Lake*, for which **k** values of 195.3×10^{-6} – 219.86×10^{-6} SI were recorded). The *siliciclastic/minerogenic* (**SIL**) component supports this distinct magnetic characteristics, showing high **SIL** contents, as well (ranging between 74.13 % – 88.34 %); complementary, the organic fraction is defined by low **TOM** contents (within the range 6.48 % – 19.56 %). A detailed analysis of the **MS** and **LITHO** data, associated with these five cores in which some *marine clays* were intercepted, has been performed, by dividing the respective extracted sediment columns into two main parts: upper (and median/central) – the *muds*, and lower – the *marine clays*. In three of these cases, the correlation coefficients (*e.g*., related to **SIL** *vs*. **k** and **TOM** *vs*. **k**) were calculated for each of their distinct lithological parts; for the other two cores, a scatter-plot analysis was carried out, which indicated clustering of the core sediments into two groups, assigned to *muds*, and *marine clayey muds/clays*, respectively. This approach will be further applied to similar cases from lakes investigated in the other *Danube Delta* depressions, and some more conclusions will be drawn at the end.

Anyway, we can mention that the identification within the *Fluvial Delta Plain* of some *marine deposits* very close to the actual water/sediment interface is very important for the deltaic system evolution knowledge, taking into consideration that these are located behind of the initial *Jibrieni – Letea – Caraorman* sand ridge, and thence older than this one. The presence of the *marine fauna* (*e.g*., *Cardiidae*) inside of certain studied cores, at a low depth, corresponds either the former period of the initial belt, or slightly afterwards, related to an incipient phase, when the *Danube bay* blocking had not been settled into shape.

Certainly, an absolute age analysis, supported by the identified fauna within the respective cores, could help to clarify some aspects of the controversy relating to the development in time of the different events which led to the deltaic edifice building up.

Another important new direction – possibly to be initiated by the synoptic images which present together the profiles with the vertical distribution of the magnetic susceptibility recorded along each sediment core – is the *stratigraphy* of the recent sediment sequences. Even the studied cores are short, being not longer than 55.5 cm, some distinct features are seen in the most of them. The 2D area-charts with the vertical distribution of the three main lithological components, particularly the **SIL** and **TOM** diagrams, analysed in detail, but in the same time in connection with the **MS** profiles and other known parameters, are of use in testing the capabilities of the investigated cores for stratigraphic applications in deltaic environments. The multi-proxy study, supported by the lithological, sedimentological, mineralogical, faunistic data, as well as grain size analyses, radiocarbon dating, and other complementary information, could generate interesting applications in the future, particularly in a stratigraphic context.

Besides, the high correlation coefficients which characterize the relationships concerning the *susceptibility* **(MS)** and the *siliciclastic/detrital material* (**SIL**), which is present, in more or less quantity, within the sediment core composition, can constitute arguments towards the *proxy* quality assignment of the *magnetic* parameter as *sedimentological* and *environmental fingerprinting tool*, one of the main objectives towards which the paper has been directed just from beginning.

REFERENCES

Catianis, I., Rădan, S., Grosu, D. (2013). Distribution of lithological components of recent sediments from some lakes in the Danube Delta; environmental significance, *Carpath. J. of Earth Environ. Sci*., **8**, *2*, 55-68.

Dean, W.E. (1974). Determination of carbonate and organic matter in calcareous sediments and sedimentary rocks by loss on ignition: comparison with other methods, *Journal of Sedimentary Petrology*, **44**, 242-248.

Finkenbinder, M.S., Abbot, M.B., Edwards, M.E., Langdon, C.T., Steinmand, B.A., Finney, B.P. (2014). A 31,000 year record of paleoenvironmental and lake-level change from Harding Lake, Alaska, USA, *Quaternary Science Reviews*, **87**, 98-113.

Rădan, S.-C., Rădan, S. (2007). A magnetic susceptibility scale for lake sediments; inferences from the Danube Delta and the Razim - Sinoie lagoonal Complex (Romania), *GEO-ECO-MARINA*, **13**, Bucureşti-Constanţa, 61-74.

Rădan, S.-C., Rădan, S. (2011). Recent sediments as enviromagnetic archives. A brief overview, *GEO-ECO-MARINA*, **17**, Bucureşti-Constanţa, 103-122.

Rădan, S.-C., Rădan, S., Catianis, I. (2013). The use of the magnetic susceptibility record as a proxy signature for the lithological composition of lake sediments: Evidences from Danube Delta short cores in the Meşteru – Fortuna Depression (Danube Delta), *GEO-ECO-MARINA*, **19**, Bucureşti-Constanţa, 77-105.

Trodahl M. I. (2010). *Late Holocene Sediment Deposition in Lake Wairarapa*, M. Sc. Thesis, submitted to Victoria University of Wellington, New Zealand, 114 p.